UNIVERSITY OF CALIFORNIA,
IRVINE

Development and Techno-Economic Analysis of SOFC-GT Hybrid Systems Employing Renewable Hydrogen for Stationary Applications and LNG for Mobile Applications

THESIS

submitted in partial satisfaction of the requirements
for the degree of

MASTER OF SCIENCE
in Mechanical and Aerospace Engineering

by
Chun Yin Chan

Thesis Committee:
Professor Scott Samuelsen, Ph.D.
Professor Vincent G. McDonell, Ph.D.
Professor Yoonjin Won, Ph.D.

2021

DEDICATION

To

My family, as their everlasting support for a 1st generation college student and immigrant.

“That's one small step for a man, one giant leap for mankind.”

Neil Armstrong – 1st person to step on the Moon.

Table of Contents

List of Figures

List of Tables

Nomenclature

Roman Symbols

C	Cost, Specific Heat Capacity
Q	Heat Rate
R	Universal Gas Constant
T	Temperature
W	Work
m	Mass Flowrate
p	Pressure, Pressure Ratio
s	entropy

Greek Symbols

$\propto$	Directly Proportional
v	Specific Volume
β	Constants
η	Effectiveness/Efficiency
σ	Entropy Generation

Subscripts

h	Enthalpy, Hot
RH_2	Renewable Hydrogen
w&s	Wind and Solar
GT	Gas Turbine
c	Compressor, Cold
cv	Control Volume
f	Feedstock
i	Inlet
nf	Non-Feedstock
o	Outlet
p	Constant Pressure, Pump
u	scaling exponent
v	Constant Volume

Units

cuf	Cubic feet
h	hour
K	Kelvin (Temperature)
kg	kilograms
kW	kilowatts
kWh	kilowatt Hours
MW	Megawatts

MWh	Megawatt-Hours
psig	Pounds Per Square Inches Gauge
s	seconds
sqm	Square Meters

Abbreviations

APEP	Advanced Power and Energy Program
AC	Alternating Current
AER	Annual Escalation Rate
AFOC	Annual Fixed Operating Cost
AR	Autothermal Reforming
AVOC	Annual Variable Operating Cost
CA-ISO	California Independent System Operator
CCE	Capital Cost Estimator
CCF	Capital Charge Factor
CF	Capacity Factor
CH_4	Methane
CNG	Compressed Natural Gas
CO	Carbon Monoxide
CO_2	Carbon Dioxide
COE	Cost of Electricity
DC	Direct Current
DIR	Direct Internal Reforming
DOE/NETL	Department of Energy/National Energy Technology Laboratory
EDR	Exchanger Design and Rating
EPC	Engineering, Procurement and Construction
GHG	Greenhouse Gases
GHG	Greenhouse Gases
GT	Gas Turbine
H_2	Hydrogen
HC	Hydrocarbons
HHV	Higher Heating Value
HRSG	Heat Recovery Steam Generator
IIR	Indirect Internal Reforming
LC	Land Cost
LCSF	Lanthanum-Strontium Cobaltite Ferrite
LHV	Lower Heating Value
LNG	Liquefied Natural Gas
LSC	Lanthanum-Strontium Cobaltite
LSF	Lanthanum-Strontium Ferrite
LSM	Strontium-Doped Lanthanum Manganite
MIEC	Mixed Ion-Conducting and Electronically Conducting
MWH	Annual Net Megawatt hours
NG	Natural Gas
NOx	Nitric-Oxide Compounds (Emissions)

PEMFC	Proton-Exchange Membrane Fuel Cell
POX	Partial Oxidation
PR	Pressure Ratio
p-v	Pressure-Specific Volume
RC	Reference Cost
RH_2	Renewable Hydrogen
RP	Reference Parameter
RY	Reference Year
SC	Scaled Cost
SCAQMD	South Coast Air Quality Management District
SOFC	Solid Oxide Fuel Cell
SOFC-GT	Solid Oxide Fuel Cell – Gas Turbine
SP	Scaled Parameter
SR	Steam Reforming
SY	Study Year
TIT	Turbine Inlet / Firing Temperature
TPC	Total Plant Cost
TR	Number of Trains/Purchased Amount of Equipment in Reference Case
TS	Number of Trains/Purchased Amount of Equipment in Study Case
T-s	Temperature-Specific Entropy
WGS	Water Gas Shift
YSZ	Yttria-Stabilized Zirconia

Acknowledgments

I would like to give the deepest admiration to Professor Scott Samuelsen, my academic advisor and committee chair. He provided an exceptional support to me not only in technical questions, but also in mental support. His balanced guidance allowed me to understand deeper about the world of power systems and the potential to improve it by advanced power generation methods. Without his guidance and persistence, this thesis would not have been completed successfully.

I would like to give the highest gratitude to Dr. Ashok Rao, my technical advisor. As a Chief Scientist at Advanced Power and Energy Program (APEP), Dr. Rao had over 30 years of technical expertise before taking the position at the University in 2004. Dr. Rao was always available to discuss any research questions I may have, his patience contributed countless hours to my research work. Without his contributions, the completion of this thesis would be infeasible.

I would like to give the greatest appreciation to Fabian Rosner, a PhD student in APEP. He provided many advices and appropriate criticisms to my research. His excellent knowledge on the subject matter, especially the economic analysis, provided a great assistance towards the successful completion of this work.

I would like to thank my committee members, Professor Vincent G. McDonell and Professor Yoonjin Won, for serving as my thesis committee. I admire each of them for their outstanding teaching and research inspiring me to pursue a better academic journey.

I would like to thank South Coast Air Quality Management District (SCAQMD) to fund my thesis work. SCAQMD was a reliable partner for the entire time of this thesis, providing accurate information and reasonable time to complete this project.

Lastly, I would like to thank every faulty members and fellow students in APEP for their great support and constructive conversations regarding to my thesis.

Abstract

Development and Techno-Economic Analysis of SOFC-GT Hybrid Systems Employing Renewable Hydrogen for Stationary Applications and LNG for Mobile Applications

By

Chun Yin Chan

MASTER OF SCIENCE in Mechanical and Aerospace Engineering

University of California, Irvine, 2020

Distinguished Emeritus Professor Scott Samuelsen, Ph.D.

Solid Oxide Fuel Cell – Gas Turbine (SOFC-GT) technology is known to produce continuous electric power with ultra-high efficiency and virtually zero emission of criteria pollutants. Research to date has focused on operation on compressed natural gas (CNG) and stationary power applications. This thesis addresses operation on renewable hydrogen (RH_2) in mobile as well as stationary applications, and liquified natural gas (LNG) in two mobile applications (locomotive and tugboat). 10 and 50MW plants are adopted for the stationary applications, and a 3.5MW engine is adopted for the two mobile applications.

The results confirm that SOFC-GT hybrids reach high efficiencies even at small scales. Hybrids in the 10 MW class exceed efficiencies of 68%-LHV while hybrids in the 50 MW class can exceed efficiencies of 70%-LHV. Although SOFC-GT hybrids are modular and cost does not scale linearly with plant size, savings in traditional-of-plant equipment and plant operation lead to a substantial cost of electricity reduction when considering future technological advancement. For example, the Cost of Electricity (COE) for the 10 MW hybrid operating on RH_2 is reduced from $197.06/MWh in 2020 to $150.00/MWh in 2030 and $136.79/MWh in 2050. For a 50 MW hybrid operating on RH_2, the COE is reduced from $171.94/MWh in 2020 to $126.04/MWh in

2030 and $113.17/MWh in 2050. The feedstock cost of RH_2 contributes to more than 75% of COE. To lower the feedstock cost, electricity for the electrolysis of water to hydrogen can be sourced from wind and solar plants during curtailment. Under these circumstances, the COE in 2020 can be reduced by 40% for the 10 MW scale and 44% for the 50 MW scale.

Hybrids in the 3.5 MW long-haul locomotive and the tugboat both exceed efficiencies of 68%-LHV. A novel strategy to incorporate into the cycle the “heat sink” associated with the evaporation of the LNG is shown to significantly increase the overall efficiency.

1. Introduction

1.1. Motivation

Energy is essential to societal development. As society grows, the demand for energy grows. Therefore, new power generation methods must be developed not only to satisfy the ever-growing power demand, but also to provide sustainability and to alleviate environmental impact by reducing greenhouse gas (GHG) emissions.

Figure 1-1 [1] below shows the U.S. electricity generation by different energy sources. United States has relied heavily on coals since the 1950s. For example, coal accounted for 1966 billion kWh in 2000, which was around 52% among all the energy sources. However, conventional coal processing power plants have the biggest environmental impact because of their heavy carbon contents per unit of released energy, which lead to greater carbon emissions [2]. Recently, natural gas (NG) starts to get much higher attention because it is relatively clean to process and fast in combustion. For example, natural gas accounted for 1,468 billion kWh in 2018, which was around 35% among all the sources and is expected to increase [1]. The main component of natural gas is methane (CH_4), which has a much lower carbon content compared to coal. Also, the final emissions from natural gas power plants could consist of only carbon dioxide and water through proper management.

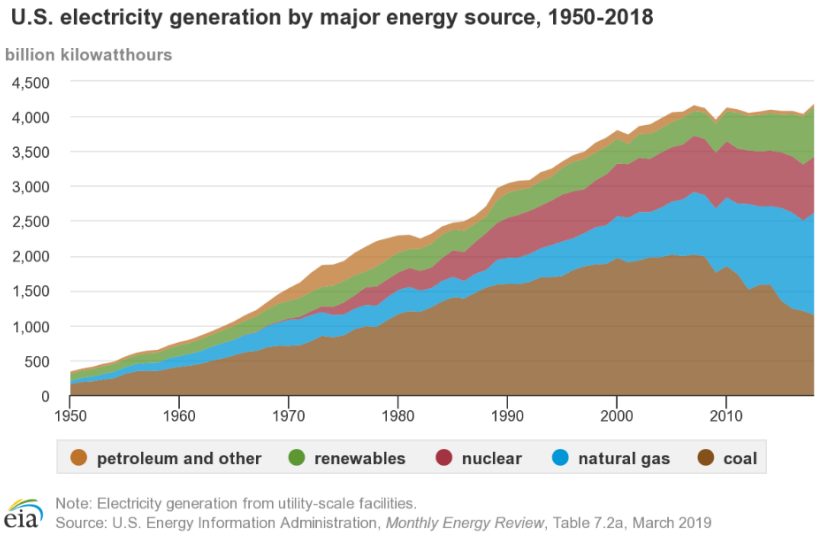

Figure 1-1: Major energy sources from 1950 to 2018

As a result, scholars have investigated into new technologies to utilize NG as a fuel. Solid Oxide Fuel Cell – Gas Turbine (SOFC-GT) hybrid system is one of the best available options. It is currently the only known continuous power generation technology which produces electricity dynamically with ultra-high efficiency while minimizing criteria pollutants and greenhouse gas emissions [3]. Utilizing NG in the SOFC-GT hybrids improves the overall system efficiencies by various reforming reactions, integration schemes and recirculation techniques, which would be discussed in detail in the following sections especially the mobile scale applications which utilize liquefied natural gas (LNG) as a fuel. Although NG is a great fuel, it is non-sustainable like most of the other fossil fuels. Therefore, hydrogen (H_2) is another fuel that has been actively investigated among the research communities. Because H_2 contains no carbon content, it has virtually no criteria pollutant emissions. Although the most economical method of obtaining H_2 is by natural gas reformation, it is non-renewable. One way to produce renewable hydrogen (RH_2) is by taking electricity from wind and solar plants to break down water molecules into hydrogen and oxygen molecules, which is a process known as electrolysis. Stationary power applications would utilize H_2 from electrolysis as a fuel, and detail discussions would be provided in the stationary application sections.

1.2. Goals and Objectives

The thesis composed of two main goals. First, to investigate the feasibility and optimal configuration for stationary SOFC-GT hybrids in the range 10 MW to 50 MW that utilize RH_2 as the fuel. Second, using lessons learned from the first goal, to develop the optimal configuration for a 3.5 MW long-haul locomotive and a 3.5 MW tugboat SOFC-GT hybrid utilizing LNG as the fuel.

A systematic approach is required for successful completion of this thesis. To this end, the following objectives are prescribed, and detailed discussion of which is presented in the Approach section.

1. Conduct a literature search of established SOFC-GT hybrid system configurations in both stationary and mobile applications.
2. Adapt an existing NG-fueled SOFC-GT hybrid system model from NG-Fueled to explore H_2-Fueled systems for stationary applications.

3. For 10 MW stationary applications, analyze three recycle scenarios for the optimal performance: different configurations including anode, cathode, and no recycle .
4. Scale the optimal scenario for the 10 MW stationary power plant application design to 50 MW.
5. Perform cost analyses for both the 10 MW and 50 MW applications.
6. Using lessons learned from the stationary applications, develop a 3.5 MW mobile SOFC-GT for long-haul locomotive SOFC-GT systems utilizing LNG as a fuel.
7. Develop 3.5 MW tugboat applications by incorporating GT suction air desalting system using the best configuration from the locomotive application.

2. Background

Working principles of key components including the SOFC, reformers, GT, compressors and pumps, eductor, as well as recuperators and intercoolers are provided. Detail thermodynamic analyzes would be provided for compressors and pumps because they are used for screening analysis in mobile applications. Then, the status of SOFC-GT hybrids on stationary and mobile applications would be discussed in terms of configurations, efficiencies as well cost based on the published research papers.

2.1. Working Principle of Key Components

2.1.1. Solid Oxide Fuel Cell (SOFC)

Fuel cell is an electrochemical device which converts chemical energy in the fuel into electrical energy without going through the combustion process. Since fuel cell does not operate in a thermodynamic cycle, it is not limited by the Carnot efficiency and can potentially reaches a much higher system efficiency while causing a much lower environmental impact compared to the conventional power plants [4]. Among all the fuel cells, Solid Oxide Fuel Cell (SOFC) and Molten Carbonate Fuel Cell (MCFC) are the most suitable for power generation because they both provide high-quality waste heat for cogeneration applications. Research paper suggested that operating the MCFC alone is around 2% more efficient than operating the SOFC alone in a power size of 20 MW [5]. However, the same paper also proposed that a SOFC operated under pressurized condition produces more exhausted heat than the MCFC, leading to around 1.5% higher efficiency when used in a hybrid system [5]. Therefore, SOFC is more efficient when used in the SOFC-GT hybrids for trigeneration applications when pressurized [5]. Figure 2-1 [7] shows a basic schematic of a SOFC. SOFC usually operates at a high temperature between 600 °C and 1000 °C and at a pressurized condition above the atmospheric pressure. The advantage of operating at high temperature and pressure can provide a higher power output/electrical efficiency to the overall system, as well as providing a high-quality waste heat for cogeneration purposes. The SOFC is made up of three major components, namely anode, cathode, and the electrolyte. The anode is where the fuel comes in and reacts with oxygen ion to produce water and electrons. The cathode is where the air (i.e., oxygen) comes in and reacts with the electrons to produce oxygen ion. The interconnect between anode and cathode is called an electrolyte, in

which only ions can pass through but not electrons. Equation (2.1) and (2.2) below provide the anode and cathode reactions of the SOFC.

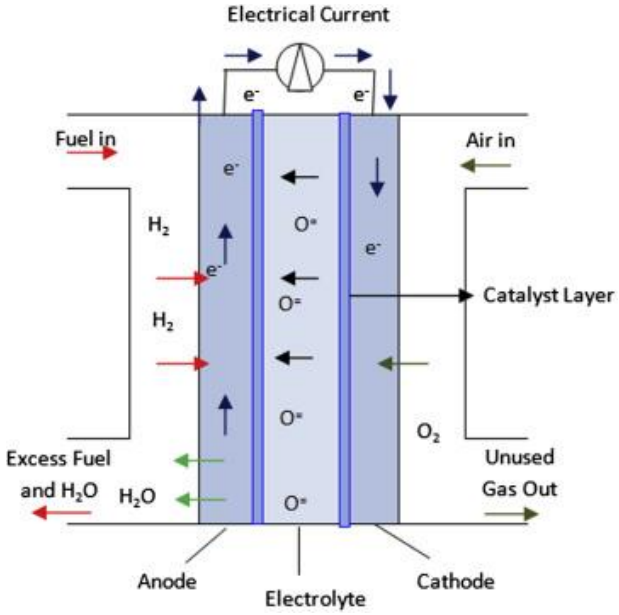

Figure 2-1: SOFC Basic Schematic

$$\text{Anode: } H_2 + O^{2-} \rightarrow H_2O + 2e^- \tag{2.1}$$

$$\text{Cathode: } \frac{1}{2}O_2 + 2e^- \rightarrow O^{2-} \tag{2.2}$$

The anode, cathode and electrolyte all employ different materials due to the different properties and operating conditions. For example, the anode material needs to withstand a highly reducing and a high temperature environment while the cathode material needs to withstand a highly oxidizing and a high temperature environment. On the other hand, the electrolyte material needs to enhance ion conductivity, thermal expansion compatibility, mechanical stability, and to maintain a sufficiently high porosity to the surrounding area. Most importantly, it needs to be sealed perfectly so that no hydrogen molecules are allowed to across the electrolyte because combustion will happen once the hydrogen molecules react with the oxygen molecules, resulting into a permanent damage to the fuel cell stack. Yttria-Stabilized Zirconia (YSZ) is a common material for both the anode and the electrolyte. The YSZ used in the anode adds an additional layer of Nickel cermet to provide enough support to its structure. The cathode usually employs a group of ceramic materials known as the Mixed Ion-Conducting and Electronically Conducting

(MIEC) materials, which include Strontium-Doped Lanthanum Manganite (LSM), Lanthanum-Strontium Ferrite (LSF), Lanthanum-Strontium Cobaltite (LSC), and Lanthanum-Strontium Cobaltite Ferrite (LCSF). MIEC shows good resistance to oxidation and high catalytic activity in the cathode environment [6].

Planar and tubular are two main SOFC types due to their difference in geometric shapes. The planar type is the most popular design in current fuel cell industry because it offers a considerably high-power density and a relatively low manufacturing cost due to its manufacturing simplicity. Figure 2-2 [9] shows the schematic diagram for a planar SOFC, in which the stacks are arranged in series in the pattern of interconnector-air-cathode-electrolyte-anode-fuel-interconnector.

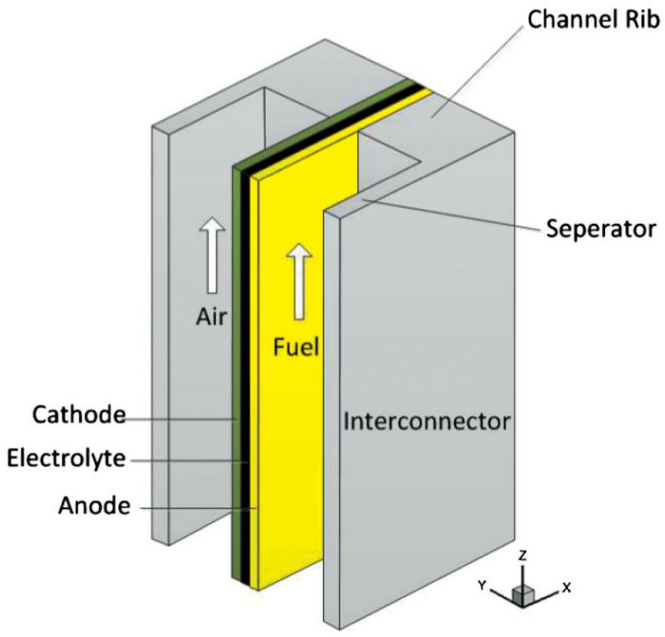

Figure 2-2: Planar SOFC Stack Arrangement Schematic Diagram

The tubular design is constructed like a circular tube, in which the anode is on the inside of each tube and the cathode is on the outside, as shown from Figure 2-3 [9]. The tubular design provides some major advantages over the planar design, including reduction of polarization losses, better fuel and air distribution, better management of thermal stresses, and faster response to dynamic operations [7]. However, the cost of tubular design is much more expensive, and there have been a lot of efforts to lower the manufacturing cost of tubular designs.

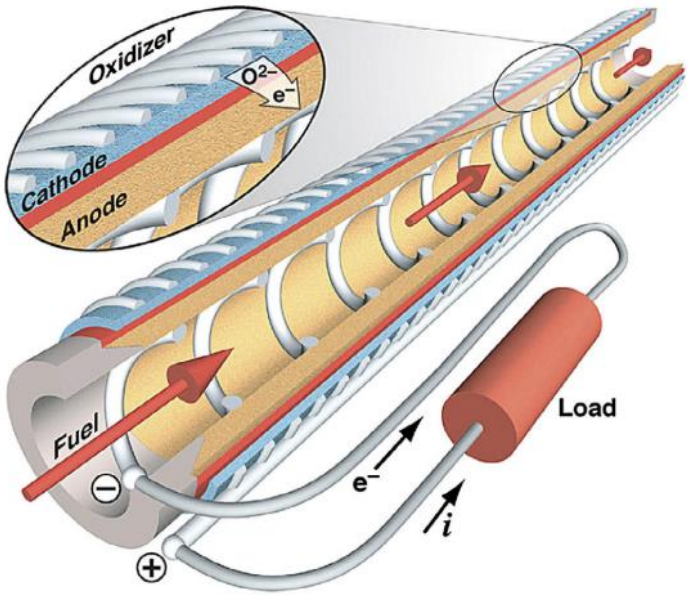

Figure 2-3: Tubular SOFC Stack Arrangement Schematic Diagram

2.1.2. Reformer

Most fuels today are hydrocarbons (HC), and they are required to react with high temperature steam and catalysts before they can be used in the SOFC. The chemical reaction undergoes is known as the reforming reaction and the component for reforming reaction is known as the reformer. In a reforming reaction, HC reacts with high temperature steam to produce hydrogen (H_2) and carbon monoxide (CO). Equation (2.3) gives an example of a reforming reaction given the HC is methane (CH_4), which is a main component of Natural Gas (NG). CO can produce additional hydrogen by another chemical reaction known as the Water-Gas-Shift (WGS) reaction, which is shown by Equation (2.4). Therefore, the hydrogen can then be sent to the SOFC anode and carbon dioxide (CO_2) becomes the final emission product.

$$CH_4 + H_2O(g) \leftrightarrow CO + 3H_2 \qquad \text{(Reforming Reaction)} \qquad (2.3)$$

$$CO + H_2O(g) \leftrightarrow CO_2 + H_2 \qquad \text{(WGS reaction)} \qquad (2.4)$$

The three major reforming reaction types are the steam reforming (SR), partial oxidation (POX) as well as the autothermal reforming (AR). Figure 2-4 [6] below summaries the

characteristics for each of the reforming reaction. SR is an endothermic reaction which operates at a temperature range from 700 °C to 1000 °C. A major advantage of SR is that it produces the highest H_2 yield among three reforming reactions at about 76% given natural gas as the input fuel [6]. However, SR requires a careful thermal management during the start-up and dynamic operations to provide enough system reaction heat, and it only works on a limited number of fuels [6]. POX is an exothermic reaction which operates at a temperature range of over 1000 °C, it allows a quick start and dynamic response for a less careful thermal management and works on many different fuels [6]. However, it yields the lowest amount of H_2 at around 41% and produces the highest amount of pollutants like unused HCs and CO [6]. The AR is a neutral reaction (i.e., not exothermic nor endothermic) which operates at a temperature range from 600 °C to 900 °C. The AR combines the WGS reaction in a single process resulting into a simplification of thermal management, which reduces the size of heat exchangers and allow a quick start [6]. However, it yields a relatively low amount of H_2 at 47% and requires a careful control system design to balance between endothermic and exothermic reactions during start-up and dynamic responses [6]. The advantages and disadvantages of three major reforming reactions are summarized in Figure 2-5 [6] below.

Type	Chemical Reaction	Temperature Range (°C)	Gas Composition of Hydrogen Outlet Stream on a Dry, Molar Basis (with NG Fuel Input)					Exothermic or Endothermic?
			H_2	CO	CO_2	N_2	Other	
Steam Reforming (SR)	$C_xH_y + xH_2O(g) \leftrightarrow xCO + \left(\frac{1}{2}y + x\right)H_2$ $\Rightarrow CO, CO_2, H_2, H_2O$	700 – 1000	76%	9%	15%	0%	Trace NH_3, CH_4, SO_x	Endothermic
Partial Oxidation (POX)	$C_xH_y + \frac{1}{2}xH_2O \leftrightarrow xCO + \frac{1}{2}yH_2$	> 1000	41%	19%	1%	39%	Some NH_3, CH_4, SO_x, HC	Exothermic
Autothermal Reforming (AR)	$C_xH_y + zH_2O(g) + \left(x - \frac{1}{2}z\right)O_2$ $\leftrightarrow xCO_2 + \left(z + \frac{1}{2}y\right)H_2$ $\Rightarrow CO, CO_2, H_2, H_2O$	600 - 900	47%	3%	15%	34%	Trace NH_3, CH_4, SO_x, HC	Neutral

Note: For the three primary fuel reforming reactions, the table shows examples of outlet gas compositions on a dry, molar basis. The steam reforming reaction produces the highest H_2 yield and the cleanest exhaust. The low H_2 yield for the partial oxidation and autothermal reforming reactions is a result of their intake of air; the O_2 in the air partially oxidizes the fuel while the N_2 in air dilutes the H_2 composition in the outlet gas. For all three reactions, the H_2 yield can be increased by downstream use of the water gas shift reaction. In the chemical reaction for steam reforming, the first line shows the typical reactions and products in their correct molar ratios. The second line below this shows the full range of products for an actual reactor, which may include not only CO and H_2 but also CO_2 and H_2O. The chemical reaction for autothermal reforming is shown in a similar manner. Concentrations are noted on a dry, molar basis (i.e., no water vapor in gas stream).

Figure 2-4: Characteristics of Three Primary Reforming Reactions

Type	Advantages	Disadvantages
Steam Reforming (SR)	Highest H_2 yield	- Requires careful thermal management to provide heat for reaction, especially for (a) start-up and (b) dynamic response. - Only works on certain fuels.
Partial Oxidation (POX)	- Quick to start and respond because reaction is exothermic. - Quick dynamic response. - Less careful thermal management required. - Works on many fuels	- Lowest H_2 yield. - Highest pollutant emissions (HCs, CO)
Autothermal Reforming	- Simplification of thermal management by combining exothermic and endothermic reactions in same process. - Compact due to reduction in heat exchangers. - Quick to start.	- Low H_2 yield. - Requires careful control system design to balance exothermic and endothermic processes during load changes and start-up.

Note: Autothermal Reforming combines with Steam Reforming and Partial Oxidation to achieve some of the benefits of both, including simple heat management and quick response. Partial oxidation provides the greatest fuel-type flexibility.

Figure 2-5: Advantages and Disadvantages of Three Primary Reforming Reactions

The types of reforming reactions can also be categorized by the locations of where they occur. If reforming reactions occur inside the SOFC stacks, they are known as internal reforming. There are two major internal reforming arrangements. The Direct Internal Reforming (DIR) is where the hydrocarbons convert directly into hydrogen-rich mixture inside the anode compartment of the SOFC. The advantage of using DIR is to improve system simplicity as well as reducing capital costs [7]. The disadvantages of using DIR include: (i) the need to employ a proper catalyst for the SMR reaction; (ii) a higher risk for carbon deposition due to high concentration of CH_4; (iii) a higher complexity in thermal management because the endothermic SMR reaction has a fast kinetics resulting in a large thermal gradients [7][8][9][10]. All the issues from DIR can be solved by an Indirect Internal Reforming (IIR) arrangement, where the SMR reactions occur away from the anode compartment of the SOFC, receives the heat from the SOFC to support the endothermic SMR reactions. However, the IIR has a higher system complexity and thus more expensive to build than the DIR arrangement [7].

If the reforming reactions occur outside the SOFC stacks, they are known as external reforming. Most research papers that utilize NG as a fuel on the designs focus on internal reforming because of the expected higher efficiency and lower capital costs [7][8][9][10][11]. However, using both internal and external reforming sometimes can improve the efficiency. For example, employing external reforming using a pre-reformer can break down higher hydrocarbons and produce a small amount of hydrogen, so electrochemical reactions can start immediately and thus enhancing power output [12][13][14]. If no pre-reformer is added, the electrochemical reaction kinetics is very slow, which results into a low system efficiency due to a low hydrogen concentration [15]. Also, a pre-reformer is required for higher complexity fuels such as biogas, syngas and liquids, in which they cannot be directly supplied to the SOFC anode [16][17].

Since reforming is a relatively complex process with high thermal inertia, eliminating a reformer by using hydrogen can portends simplification, improved reaction dynamics and lower cost.

2.1.3. Gas Turbine (GT)

When operating in a steady state condition, the SOFC should be able to provide most of the power. However, since the SOFC does not have a good dynamic (i.e., ramping on/off)

capability compared to fuel cells like Proton Exchange Membrane Fuel Cell (PEMFC), adding a GT can help providing transient powers during start-up and dynamic operations. Also, adding a GT would be beneficial for cogeneration purposes since the SOFC can provide a good quality waste heat. The SOFC-GT hybrid technology is currently the only known continuous power generation technology that can dynamically produce electricity with ultra-high efficiency but ultra-low emissions for criteria pollutants and greenhouse gases (GHG) [3].

Like some of the gas power systems, the GT operates in a simple Brayton Cycle. Figure 2-6 [18] shows a simple schematic of air-standard gas turbine cycle.

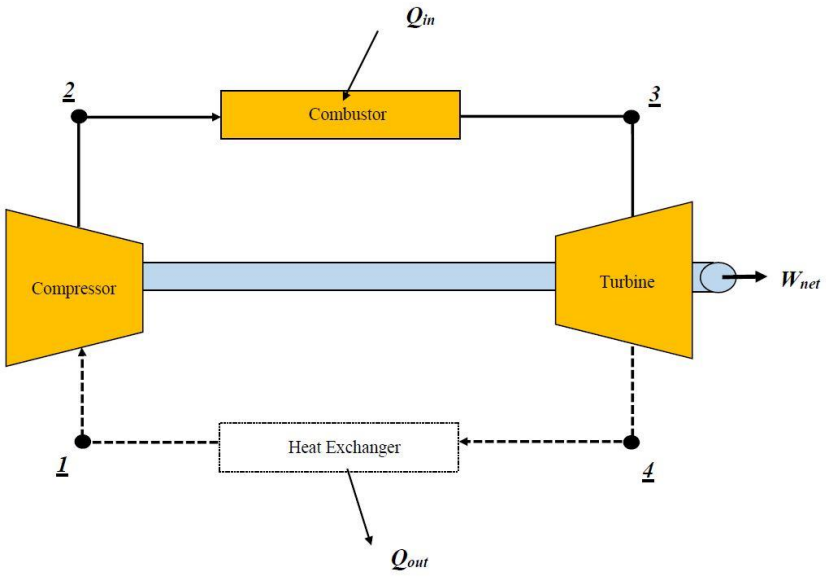

Figure 2-6: Air-Standard Gas Turbine Cycle Schematic

An idealized air-standard Brayton cycle operates in four main steps, namely:

1) Isentropic Compression
2) Isobaric Heat Addition
3) Isentropic Expansion
4) Isobaric Heat Rejection

The pressure-specific volume (p-v) and the temperature-specific entropy (T-s) diagrams are shown below in Figure 2-7 [18]. Step 1-2 represents the isentropic compression by the compressor, in which the pressure and temperature increases with constant entropy. Step 2-3 represents the isobaric heat addition by a combustor, in which the temperature and entropy

increases at constant pressure. Step 3-4 represents the isentropic expansion by the turbine, in which the work is produced by lowering the temperature and pressure at constant entropy. Step 4 to 1 represents the isobaric heat rejection, in which the temperature and entropy decreases at constant pressure. On the p-v diagram, the area enclosed by "1-2-a-b-1" represents the amount of compression work by the compressor and the area enclosed by "3-4-b-a-3" represents the amount of work produced by the turbine. Therefore, the enclosed area "1-2-3-4-1" by the curve represents the amount of net work produced by the cycle. On the T-s diagram, the area enclosed by "a-b-2-3-a" represents the amount of heat addition and the area enclosed by "a-b-1-4-a" represents the amount of heat rejection. Therefore, the area enclosed by "1-2-3-4-1" represents the amount of net heat addition, which is equivalent to the amount of net work production. Notice on the T-s diagram, if the compressor can compress until it reaches point 2' instead of point 2, or if the turbine can expand from point 3' instead of point 3, net work production increases and improves the overall cycle performance.

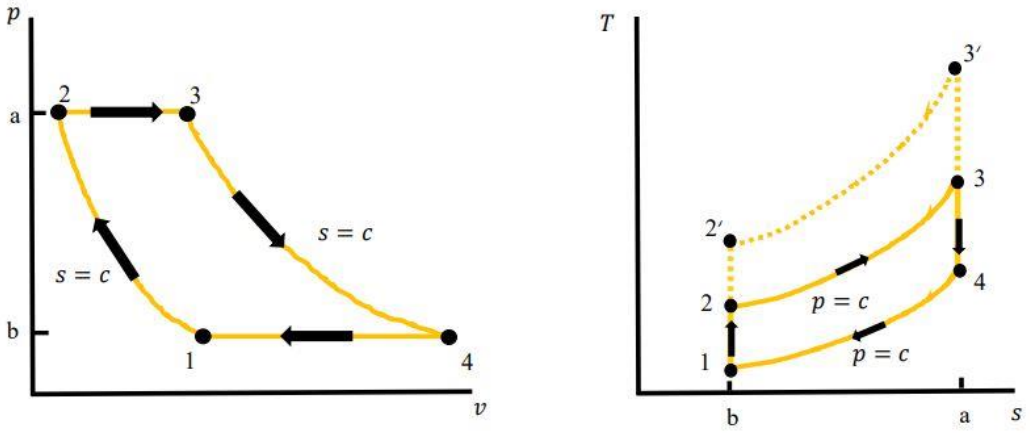

Figure 2-7: P-v and T-s Diagram for Air-Standard Ideal Brayton Cycle

In the SOFC-GT hybrid, a heat exchanger for heat addition from Figure 2-6 (i.e., state 2 – 3) is replaced by the SOFC, as shown below from Figure 2-8 [18]. If enough fuel is supplied, the SOFC can continuously producing electricity while increasing the Turbine Inlet Temperature (TIT), or the SOFC exhaust temperature. Note that only the air side operates close to a simple Brayton Cycle, the SOFC-GT hybrid is more complicated than what is shown from Figure 2-8. Instead of a conventional vapor gas turbine, a customized GT is needed because the GT in the

hybrid is responsible for the SOFC's thermal management rather than a large amount of power output, which is achieved by the SOFC.

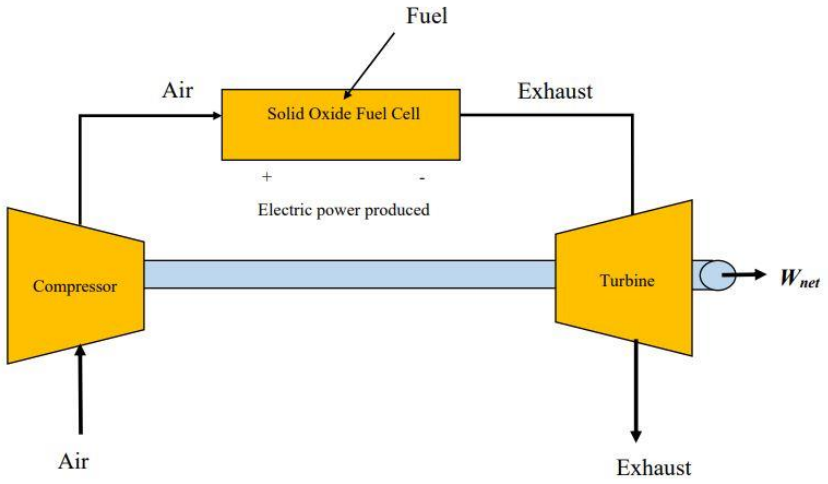

Figure 2-8: Solid Oxide Fuel Cell – Microturbine Hybrid Schematic

2.1.4. Compressor and Pump

The purpose of a compressor and a pump is to pressurize the working fluid. An idealized compressor or a pump should be isentropic, meaning pressurization occurs with constant entropy. A compressor should be used only for vapor and a pump should be used only for liquid. Liquid should not go into a compressor because they will corrode the compressor blades, hurting its aerodynamic efficiency and resulting into permanent damages. Similarly, vapor should not go into a pump because it cannot do any useful work to pressurize the gases. Major types of compressors include reciprocating, axial, centrifugal and rotary, each with its own advantages and applications. For example, reciprocating compressors typically produce a relatively high pressure and power while keeping low installation and maintenance costs, but the compressor itself is very expensive and its large size and volume makes it unattractive for mobile and lightweight applications [19]. The typical types of pumps are the same as those of the compressors.

From a thermodynamic perspective, putting in work for a gas results in a heat addition, and gas temperature increases with pressure increases. On the other hand, putting in work for a liquid results in a change in volume, but temperature stays constant with pressure increases. Applying the first law of thermodynamics for a steady state control volume enclosing a

compressor or a pump assuming adiabatic condition and negligible change in kinetic and potential energy, the required power can be obtained as shown from Equation (2.5) and (2.6).

$$\underbrace{\Delta E}_{=0} = \underbrace{\dot{Q}_{cv}}_{=0} - \dot{W}_{cv} + \dot{m}_{cv}(h_i - h_o) \tag{2.5}$$

$$\dot{W}_{cv} = \dot{m}_{cv}(h_o - h_i) \tag{2.6}$$

where

- ΔE is the change of total energy ($\Delta E = 0$ for control volume analysis).
- $\dot{Q}_{cv}$ is the heat flowrate under control volume ($\dot{Q}_{cv} = 0$ for adiabatic condition).
- $\dot{W}_{cv}$ is the power under control volume.
- $\dot{m}_{cv}$ is the mass flowrate under control volume.
- h_o is the outlet enthalpy and h_i is the inlet enthalpy, which can be expanded from the differential form of the first law, as shown in Equation (2.7).

$$dh = du + d(pv) \tag{2.7}$$

where

- p is the pressure.
- v is the specific volume.
- du is the change of internal energy per mass, which can be further expanded as shown from Equation (2.8).

$$du = \underbrace{T ds}_{=0} + \underbrace{\sigma_{cv}}_{=0} = 0 \tag{2.8}$$

where

- T is the temperature.
- ds is the change in entropy ($ds = 0$ in isentropic condition).
- σ_{cv} is the entropy generation ($\sigma_{cv} = 0$ for no entropy generation).

By substituting the result from Equation (2.8) into Equation (2.7) and expanding the terms using chain rule, Equation (2.9) is obtained.

$$dh = \underbrace{du}_{=0} + p\,\underbrace{dv}_{=0} + vdp = vdp \tag{2.9}$$

Assume $dv = 0$ (for a control volume analysis), the difference in enthalpy can be obtained by taking the integral of Equation (2.9), as shown in Equation (2.10).

$$h_o - h_i = \int_i^o vdp \tag{2.10}$$

Here comes to the difference between a pump and a compressor. For a pump, the change in specific volume between inlet and outlet is near zero because liquids are incompressible. Therefore, v can be treated as a constant and the enthalpy difference is directly proportional to the pressure difference. Since the specific volume is usually small for a liquid, the work of a pump is usually small as shown in Equation (2.11) and (2.12).

$$h_o - h_i = v(p_o - p_i) \tag{2.11}$$

$$\dot{W}_p = \dot{m}_{cv} v(p_o - p_i) \tag{2.12}$$

In a compressor, the change of specific volume can no longer be assumed constant because gases are compressible. Therefore, specific volume needs to be integrated in terms of pressure, as shown from Equation (2.13).

$$P_i v_i^n = P v^n = constant \tag{2.13}$$

where

- P_i is the inlet pressure.
- v_i is the inlet specific volume.
- n is the ratio between C_p and C_v, as defined by Equation (2.14).

$$n = \frac{C_p}{C_v} \tag{2.14}$$

where

- C_p is the specific heat capacity under constant pressure.
- C_v is the specific heat capacity under constant volume.

Substitute Equation (2.14) into Equation (2.13) in terms of specific volume gives Equation (2.15).

$$v = v_i \left(\frac{P_i}{P}\right)^{\frac{1}{n}} \tag{2.15}$$

Substitute Equation (2.15) into Equation (2.10) and evaluate the integral gives the enthalpy difference for a compressor, as shown in Equation (2.16) and (2.17).

$$h_o - h_i = \int_i^o \left[v_i \left(\frac{P_i}{P}\right)^{\frac{1}{n}} \right] dp \tag{2.16}$$

$$h_o - h_i = v_i P_i \left[\frac{n}{n-1}\right] \left[\left(\frac{P_o}{P_i}\right)^{\frac{n-1}{n}} - 1 \right] \tag{2.17}$$

Substitute the value of n from Equation (2.14) into (2.17) gives:

$$h_o - h_i = v_i P_i \left[\frac{C_p}{C_p - C_v}\right] \left[\left(\frac{P_o}{P_i}\right)^{\frac{C_p - C_v}{C_p}} - 1 \right] \tag{2.18}$$

Note that:

$$R = C_p - C_v \tag{2.19}$$

where

- R is the universal gas constant, which is always positive (i.e., $C_p > C_v$)

Substituting Equation (2.19) and (2.18) into (2.6), the compressor work then becomes:

$$\dot{W}_{cv} = \dot{m}_{cv} v_i P_i \left[\frac{C_p}{R}\right] \left[\left(\frac{P_o}{P_i}\right)^{\frac{R}{C_p}} - 1 \right] \tag{2.20}$$

From Equation (2.20), note that the exponent $\frac{R}{C_p}$ in this study is between 0 and 1, which does not increase exponentially. However, the specific volume is much greater in gases than in liquids because the volumetric flowrate for a gas is much higher than that of a liquid for a given mass flowrate. Therefore, using a compressor requires significantly higher amount of work and thus using a pump should always be more efficient. This hypothesis/observation is justified in the Section "Development of Mobile Scale Applications", where a screening analysis is first applied for a 3.5 MW long-haul locomotive to determine whether a fuel pump is more efficient than a fuel compressor.

2.1.5. Eductor

An eductor is a special type of pump which takes both liquids and gases. However, unlike a pump, an eductor is not used to pressurize a fluid. Rather, it is used to transfer energy from a higher-pressure fluid to a lower-pressure fluid and then reaches a final pressure between them. In the SOFC-GT hybrids, using an eductor can help recycling some of the unused fuel from the SOFC anode since the SOFC is limited by a fuel utilization. The recycled fuel is mixed with the compressed fresh fuel until it reaches the SOFC operating pressure. Power is not required to operate an eductor, thus increasing the efficiency of the plant. Also, an eductor is not an expensive component in a plant, it can help reducing the system initial and operating cost. Figure 2-9 [20] below shows the basic schematic of an eductor model. The pressurized fresh fuel comes from point g and the SOFC anode recycled fuel comes from point e. The fresh fuel enters the nozzle with converging-diverging structure that axially points towards the eductor exhaust. After the recycled fuel enters the eductor, it circulates around the outside area of the nozzle and then starts converging and mixing with the fresh fuel at the nozzle outlet, as shown from section line y-y to m-m. There happens to be a suction effect due to an increase in velocity but a decrease in pressure at the nozzle. The pressure difference thus causing the working fluid sucked into the eductor and mixing the flow stream to be guided out of the eductor by a diffuser at the end.

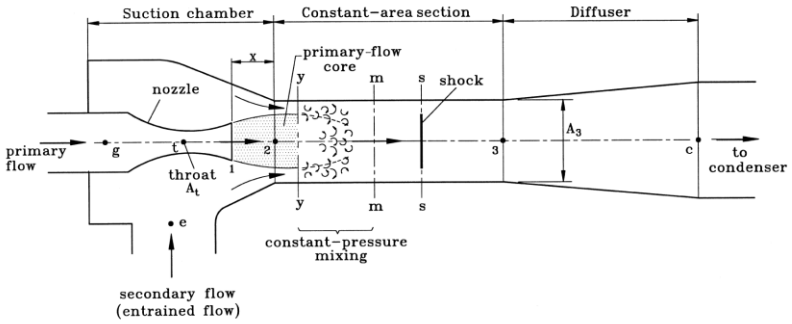

Figure 2-9: Eductor Schematic

Similarly, an eductor can also be placed in the SOFC cathode exhaust to recycle the air. A main goal of this thesis is to perform a screening analysis by placing an eductor in the anode exhaust and the cathode exhaust, compare with placing no eductor in the system for an optimal efficiency. For details regarding the configurations, please refer to the Stationary Applications section.

2.1.6. Recuperator and Intercooler

A recuperator, which is also known as a regenerator, is a heat exchanger which aims at reducing the exhaust temperature of the system by recovering the exhaust heat and exchange those with the lower temperature incoming air or fuel. The gas exhaust temperature from the GT in the hybrid system is usually high enough to provide thermodynamic utility, known as exergy, before it is emitted directly to the atmosphere. Therefore, placing a recuperator at the exhaust stream of the system allows the incoming fuel or air to be preheated, thus reducing the exhaust temperature and improves the efficiency. For a typical SOFC-GT hybrid designs that would be discussed in the following section, two recuperators are often needed. One recuperator that is used to pre-heat the fuel is known as the fuel pre-heater, and one recuperator that is used to pre-heat the air is known as the air-preheater. Equation (2.21) provides the definition for recuperator effectiveness. In practice, recuperator gets very expensive for over 90% effective. Therefore, recuperators in the hybrids are limited to 90% effective.

$$\eta_{re} = \frac{T_{c,o} - T_{c,i}}{T_{h,i} - T_{c,i}} \tag{2.21}$$

where

- η_{re} is the recuperator effectiveness.
- $T_{c,o}$ is the cold stream outlet temperature.
- $T_{c,i}$ is the cold stream inlet temperature.
- $T_{h,i}$ is the hot stream inlet temperature.

An intercooler is another type of heat exchanger which works to reduce the compression power of multi-stages compression. It is installed at the location between two compressors and this explains its name intercooler. If the cooler is installed after the compressors, it is known as the aftercooler. As the compression power gets reduced, the net power output of a GT is increased, thus increasing the overall efficiency. Figure 2-10 [18] shows the P-v and T-s diagrams for a two-stage compression with intercooling. On the p-v diagram, Area enclosed by "a-b-1-2'-a" is the required work for a single stage compression without an intercooler. By adding an extra intercooler between two compressors, it becomes a two-stage compression and thus the work is the area enclosed by "a-b-1-c-d-2-a". The overlapped shaded area enclosed by "c-d-2-2'-c" represents the reduction of compression work. The same area on the T-s diagram represents the equivalent amount of heat reduction. Therefore, instead of compressing the gas at a single stage, multiple compressors can be used with an intercooler when the goal is to compress the gas under a considerably high pressure. In theory, the more compression stages, the higher the efficiency would be as suggested by the Ericsson Cycle. However, normally there should be no more than three compression stages before the costs become too high [18].

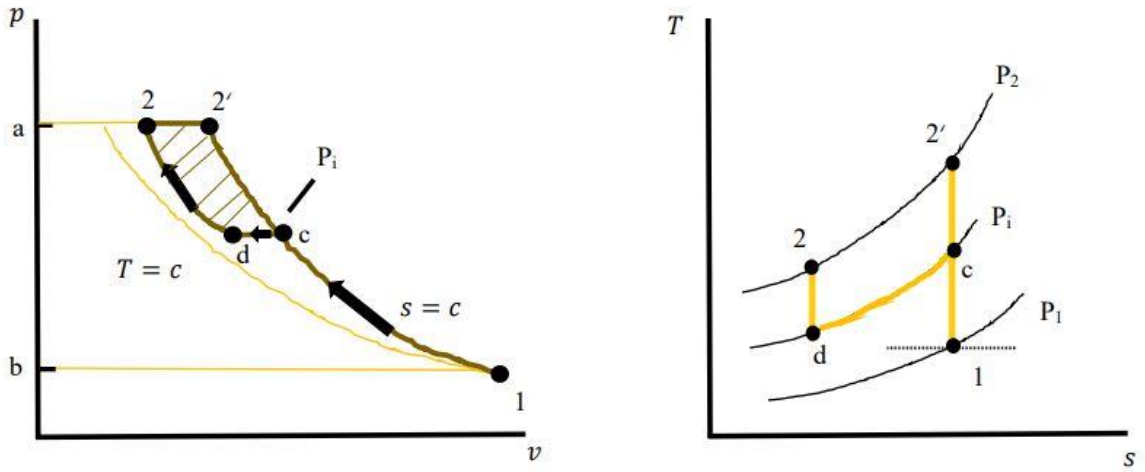

Figure 2-10: P-v and T-s Diagram for Two-Stage Compression with Intercooling

2.2. SOFC-GT Technology Status and Literature Review

2.2.1. Stationary Applications

Siemens Westinghouse was one of the earliest pioneers to look at stationary power applications using a SOFC [7]. Its idea of recycling the fuel at the SOFC anode to replace a traditional Heat Recovery Steam Generator (HRSG) driven by system exhaust gases allows a higher system efficiency and a reduction of capital costs [21][12]. Most SOFC-GT hybrid designs are fueled with NG because it is relatively easy to access, economical and provide an extra efficiency bonus due to reforming reactions [12][22][23][24]. Figure 2-11 [7] shows a NG-fueled SOFC-GT with an anode recirculation and internally reforming scheme. The design is based on a Brayton Cycle with recuperation, using the Siemens Westinghouse anode recirculation technique as well as an internally reformed SOFC. Note that the NG is also pre-reformed before entering the SOFC, so to increase the efficiency as mentioned before in the Reformer section. Recuperators are used to preheat the fuel and the air from the GT exhaust heat. This design produces a total of 1.5 MW net power at 67.9%-Lower Heating Value (LHV) electrical efficiency and a SOFC fuel utilization factor of 85% [7].

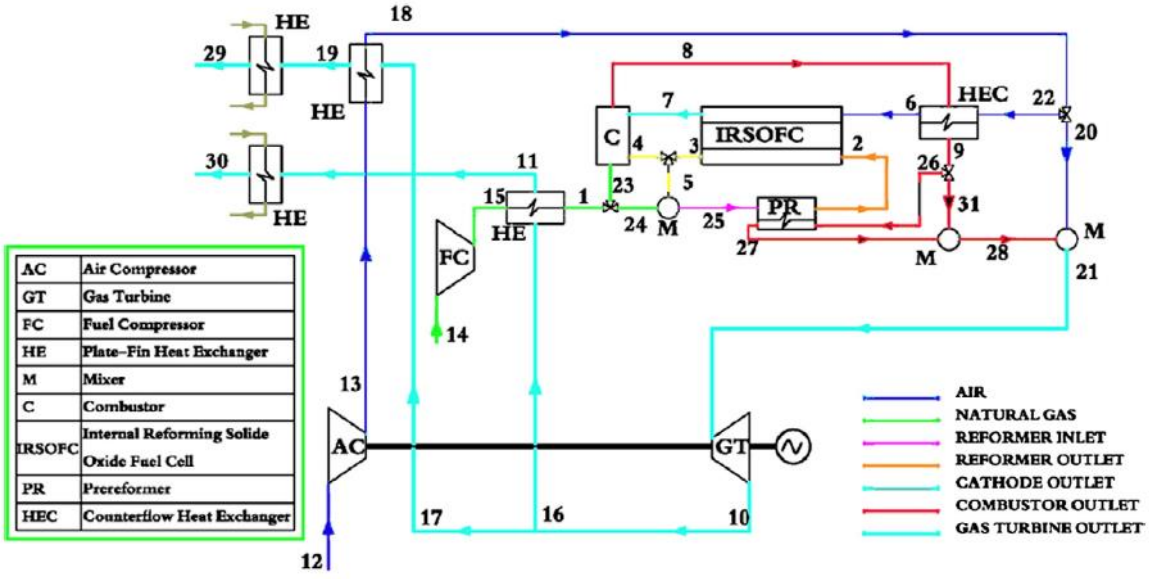

Figure 2-11: Novel 1.5 MW SOFC-GT NG-Fueled Hybrid with Anode Recirculation and Internal Reforming

Figure 2-12 [25] shows another SOFC-GT NG-fueled hybrid with higher power output. The configuration also utilizes the anode recirculation and internal reforming scheme with a net power output of 37 MW at 66.2% thermodynamic efficiency. An optimization from the study shows the larger the SOFC stack area, the higher the thermodynamic efficiency ranging from around 55% at a cell area of around 1,000 sqm to almost 70% at 16,000 sqm [25]. Table 2-1 [25] shows the economic summary of this power plant, the costs are shown in millions $USD.

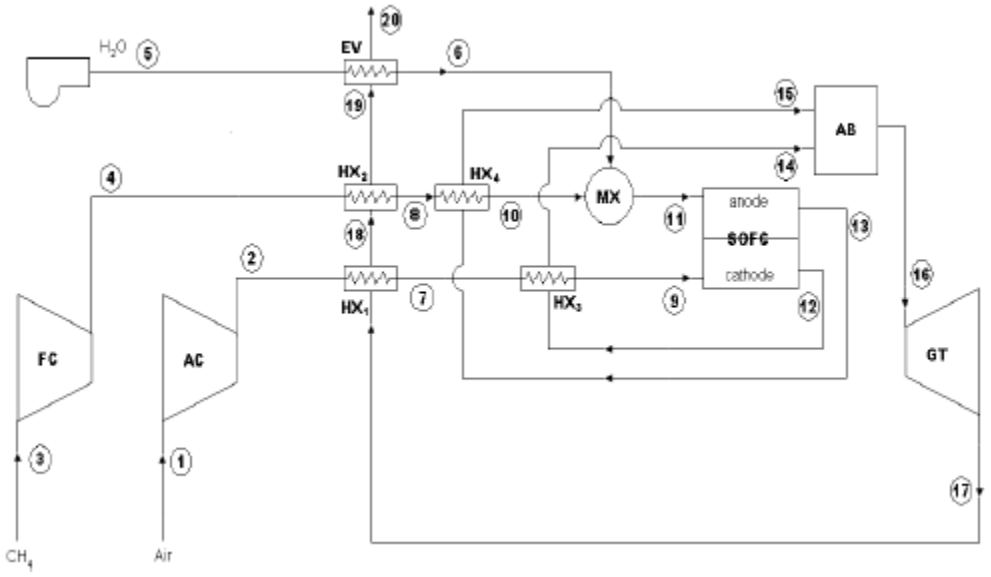

Figure 2-12: Novel 37 MW SOFC-GT NG-Fueled Hybrid

Table 2-1: Cost Breakdown for a Novel 37 MW SOFC-GT NG-Fueled Hybrid

Component	Capital Cost	Annual Gain (Cost)
SOFC Stack	20.1	
Inverter	1.5	
Pre-reformer	0.2	
SOFC Auxiliary	2.0	
SOFC TOTAL	23.8	
Heat Exchangers	2.3	
Fuel Costs		(2.3)
Power Gains		11.9
NPV	34.9	
Payback Period	3.3 years	

Figure 2-13 [26] shows a comparison between an internal and external reforming on the SOFC-GT hybrids using anode recirculation. The configuration on the top (case a) shows an IIR arrangement and the configuration at the bottom (case b) shows an external reformer before the fuel goes into the SOFC anode. By varying the SOFC operating temperature between 700 °C and 1000 °C with TIT varying between 750 °C to 1050 °C [26], case a (i.e., internally reformed SOFC-GT hybrid) gives about 10% better in thermodynamic efficiency than case b (i.e., externally reformed) [26]. External reforming alone has a more complex thermal management, requiring additional fuels to achieve the SOFC operating temperatures and TIT, thus affecting the overall performance [7][26].

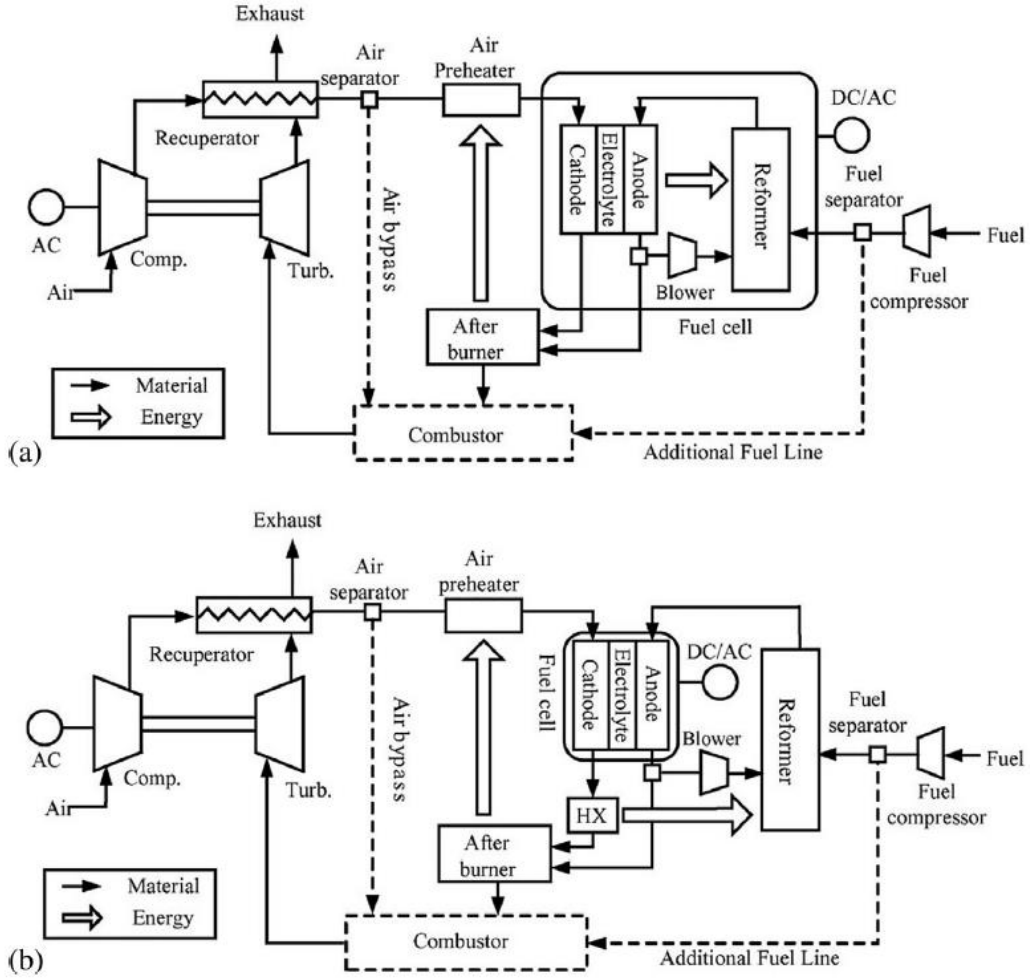

Figure 2-13: Novel (a) Internal vs (b) External Reforming SOFC-GT NG-Fueled Hybrids with Anode Recirculation

The SOFC-GT hybrids are usually under a pressurized condition rather than an atmospheric condition because the pressurized condition is typically more efficient and less expensive than the atmospheric condition [7][8][10][11]. The atmospheric configuration may be attractive for special types of fuels which cannot be tolerated by the SOFC [10][27][28], but the pressurized condition should be considered for fuels like NG and H_2.

Although NG provides a good system efficiency while maintaining a relatively low GHG emissions in the SOFC-GT hybrids, it is non-renewable. Therefore, the stationary applications in this thesis utilizes RH_2 as a fuel, which is sustainable and is relatively new in the research community. Instead of looking at only the anode recirculation, two other configurations including the cathode recirculation and the no recirculation are also analyzed. The SOFC is pressurized at 5 bars as recommended by the above-mentioned papers.

2.2.2. Mobile Applications

Around 75% of worldwide railroads and almost all of the U.S. freight rails are hauled by diesel fuels [29]. The extremely high dependence of diesel fuel is mainly due to its high accessibility, high energy density and low cost. According to Figure 2-14 [30], Diesel No. 2 contains the highest energy density compared with LNG and Compressed Natural Gas (CNG). For instance, Diesel No. 2 provides about 1.75 times the range compared with LNG and provides 4.3 times the range compared with CNG given the same fuel storage volume. In other words, LNG provides about 2.4 times the range compared with CNG given the same fuel storage volume.

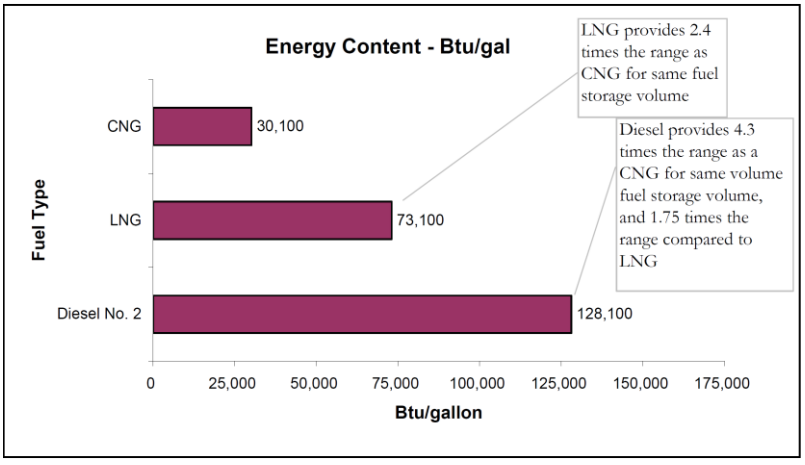

Figure 2-14: Energy Content by Fuel Type

However, the heavy dependence of diesel and other forms of petroleum since the last century has significantly increased its rate of extinction. They also caused many environmental concerns like GHG emissions and global warming. For instance, the South Coast Basin in California is known to have one of the worst air qualities in the U.S. due to a large amount of GHG emissions as many long-haul locomotives utilize diesel fuel in the region [31]. Besides the long-haul locomotives, ships are also accounted for a large percentage of GHG emissions [32][33]. Therefore, an eventual goal is to replace non-renewable fuels like petroleum to renewable fuels like hydrogen. Nonetheless, there needs to be a transitional fuel considering the current insufficient infrastructure and relatively high cost for dispensed hydrogen. LNG is a good transitional fuel not only because of its relatively high energy density compared with CNG, but also because it is cleaner to process for near zero GHG emissions when utilized in the SOFC-GT hybrids. Also, the recent increasing activity for hydraulic fracturing of shale deposits in the U.S. has greatly increased the amount of NG exploitation, which makes it a more economical fuel. Figure 2-15 [34] shows the amount of LNG imports and exports between 1985 and 2019, which shows the amount of LNG exports since 2015 has increased significantly. Therefore, the price of exporting LNG from U.S. drops from $16.67 per thousand cuf in November 2015 to $5.5 per thousand cuf in August 2020, which is around 66% cheaper [35]. Therefore, LNG is used in the mobile scale applications in this thesis.

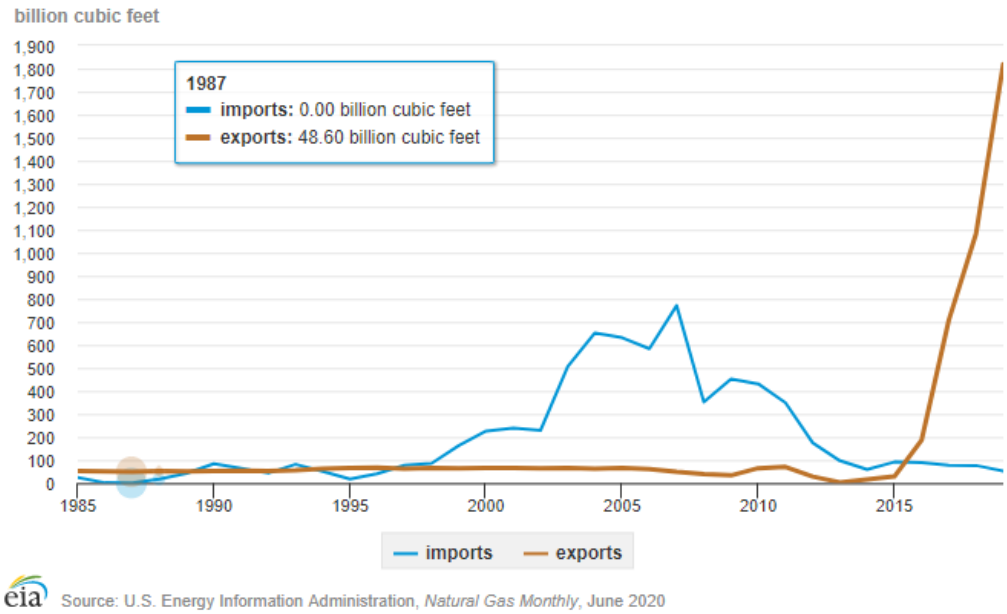

Figure 2-15: U.S. LNG imports and Exports from 1985 to 2019

A major challenge for the SOFC is its use in mobile applications. Since the SOFC is mainly made up of ceramic materials and operated under very high temperatures, it requires a slow and careful operational procedure for load following to protect the SOFC from degradation. It may not have a good start-stop capability compared to some of the other fuel cell technologies like the Proton Exchange Membrane Fuel Cell (PEMFC). Typically, a SOFC would be more ideal for operating at constant or near constant load, making them more suitable to applications such as locomotives and ships that operate in a steady-state mode. The SOFC-GT hybrid technology in addition to its very high thermal efficiency has the advantage of alleviating the GHG emissions associated with the traditional diesel engines, which have been typically used in these applications for over a century.

Figure 2-16 [36] below shows a novel 3.5 MW SOFC-GT hybrid in long-haul locomotive applications fueled by hydrogen, natural gas reformate as well as diesel reformate. The configuration employs a cathode recirculation for improved SOFC thermal management. Also, only an air-preheater is employed as it is expected that the simplification can reduce the complexity and cost, while it does not impact the system's overall performance significantly [36]. On an overall dynamical response, both the natural gas reformate and hydrogen cases reach above 70%-LHV system efficiency at the start-up while maintaining around 68% efficiency when approaching the steady state condition [36]. Hydrogen has around 1% less in system efficiency compared to natural gas reformate at the start-up due to the lack of endothermic reformation steps, which acts as a heat sink to improve the system efficiency [36]. The diesel reformate has only 65%-LHV efficiency at the start-up and approaches around 64%-LHV efficiency in a steady-state condition due a large amount of nitrogen is introduced into the stream under the AR reaction, which acts as a huge diluent and interfere the system's efficiency [36]. Also, this system provides an acceptable dynamic performance in which the desired steady state values are settled within 500 seconds even in the toughest route simulation [37]. Similar research has been done to propose that the risk of surge in hybrid SOFC-GT system due to sudden power demand perturbations can be reduced significantly through the proper design of control systems that maintains the compressor mass flowrate [38]. Therefore, it is expected that a 3.5 MW SOFC-GT hybrid system would provide enough steady-state as well as dynamic power to the long-haul locomotives.

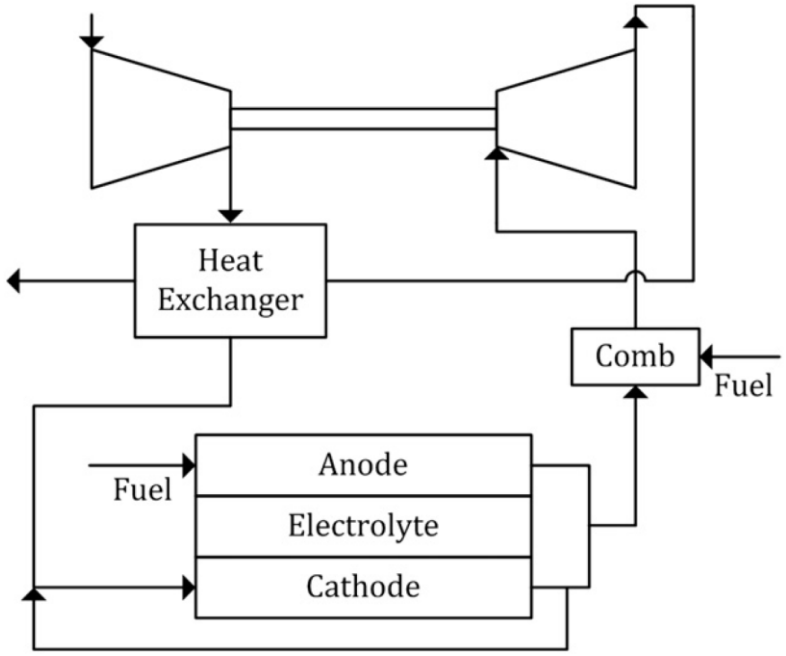

Figure 2-16: Novel 3.5 MW SOFC-GT Hybrid in Long-Haul Locomotives with Cathode Recirculation and Air-Preheating

Figure 2-17 [39] below shows another SOFC-GT configuration employed on the long-haul locomotives. This configuration also employs the cathode recirculation and produces around 3.3 MW of power between 25%-LHV efficiency and 81%-LHV efficiency, with an average of 57%-LHV efficiency at the start-up operation [39]. The significant reduction of an average LHV efficiency in this case compared to the previous one is due to the highly dynamic nature of the route from Bakersfield to Mojave in California [39]. Different than the previous configuration, this configuration is more complex by adding back a fuel pre-heater and a lithium-ion battery to provide more tractive forces for an extended period of time in more demanding situations [39]. The battery is charged when the SOFC operates in a less dynamic environment and provides the necessary power in demanding situations. Adding a battery can also provide regenerative braking and thus giving a better performance.

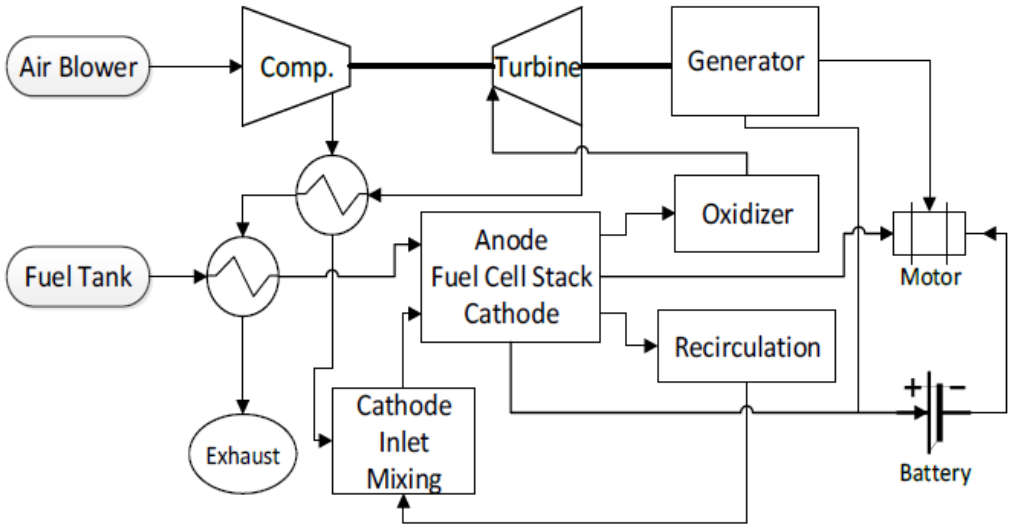

Figure 2-17: Novel 3.3 MW SOFC-GT-Battery Hybrid in Long-Haul Locomotives with Fuel and Air Preheating

On marine applications, a Finland power source and marine manufacturing company Wärtsilä manufactured a LNG-powered tugboat [40]. The tugboat consists of 2 main engines at 1,665 kW each, which provides a total of 3.33 MW of power. Therefore, it is reasonable to assume that tugboat application also has a total of 3.5 MW power demand by adding a small GT, in which the transient power may be met. The presence of salt in the ambient air for marine applications can be trapped in the compressor blades and reduce the aerodynamic efficiency in addition to causing corrosion [41]. Therefore, tugboat applications require removal of salts from the ambient air which is accomplished by a commercially available filter that requires a higher pressure drop compared to that for a conventional (i.e., non-marine application) air filter. The higher pressure drop across the GT air filter results into a lower GT compressor inlet pressure, which increases the amount of compression work and thus may affect the overall system efficiency. As a result, it is important to balance the air filter pressure drop to account for a sufficient level of blocking the containment while minimizing the amount of GT compression work. In tugboat applications, a pressure drop of 0.06 bar is assumed for simulation, which has twice the value of that of conventional air filter in locomotive applications.

Both the locomotive and ship applications are assumed to utilize Alternating-Current (AC) motors rather than Direct-Current (DC) motors. Even though the DC motors can reduce

inverter losses and free from harmonics, they do not offer the same number of benefits as provided by the AC motors. For example, AC motors can operate under high temperature and flammable environment while DC motors cannot [42][43]. This would be beneficial since the SOFC operates at 700 °C. AC motor also provides a better speed and acceleration control, easier to maintain and thus less maintenance cost, lighter in size for equivalent power, and more effective regenerative braking for higher efficiency [42][43]. Since the GT produces AC power, an inverter is required to convert the SOFC power output from DC power to AC power.

Both locomotive and tugboat applications in the thesis have the same power output of 3.5 MW and thus the same configuration is applied to both applications. The presented data have already shown that the SOFC-GT can handle dynamic operating environments encountered in the above applications. Therefore, the focus of this current investigation is on evaluating the integration aspects of the SOFC with the GT in LNG-fueled applications, of special interest is the use of the low temperature heat sink associated with the evaporation of the LNG prior to its use in the SOFC.

2.3. Summary

The SOFC-GT is currently the only known power generation method which can continuously and dynamically produce clean electric power with ultra-high efficiency and ultra-low emission of criteria pollutants [3]. Most of the SOFC-GT hybrid research literature addresses systems operated on NG with pressurized anode recirculation, and internal reforming plus an external pre-reformer. In this thesis, hydrogen produced from renewable sources is considered for stationary applications and LNG for mobile applications. Given that the literature for stationary applications focuses on anode recirculation and, for mobile applications, focuses on cathode recirculation, this thesis undertakes a screening analysis on both the anode and cathode recirculation compared with the no recirculation configuration for a 10 MW stationary application, and utilizes the result to (1) scale the 10MW to a 50MW NG-fueled stationary application, and (2) to design a 3.5 MW locomotive and tugboat mobile application. The innovative parts of this thesis are (1) utilize renewable hydrogen as a fuel for stationary power plant and provide techno-economic analyzes, and (2) utilize LNG as a fuel for mobile scale applications which serves as a heat sink associated with the evaporation of the LNG prior to its use in the SOFC, which believes to improve the electrical efficiency of the system.

3. Approach

The following tasks would be achieved for the outcome of this study.

Task 1. Conduct a literature search of established SOFC-GT hybrid system configurations in both stationary and mobile applications.

- Comparison between recirculation schemes (i.e., anode, cathode, and no recirculation).
- Comparison between pressurized and atmospheric SOFC operating pressure and temperature.
- Comparison between internal and external reforming reactions, which is only needed for mobile applications that utilize LNG.
- Investigate the LNG container pressures between minimum and maximum condition.
- Investigate the cost of renewable hydrogen in 2020, 2030 and 2050.

Task 2. Adapt an existing NG-fueled SOFC-GT hybrid system model from NG-Fueled to explore H2-Fueled systems for stationary applications.

- Remove desulfurizer (since NG has sulfur compounds added but not H_2, which a leakage sensor is used instead of an odorant).
- Remove pre-reformer.
- Remove one of the fuel compressors and intercooler if necessary.
- Add or remove recuperators if necessary.

Task 3. For 10MW stationary applications, analyze three recycle scenarios for the optimal performance: different configurations including anode, cathode, and no recycle.

- First configuration is to recycle anode exhaust stream to increase fuel utilization and preheat the fuel. Eductor is used to mix fresh fuel with recycled stream.
- Second configuration is to recycle cathode stream to increase air utilization and preheat the air. Eductor is used to mix fresh air with recycled stream.
- Final configuration has no recycle and thus no educator is utilized. Heating of the fuel and air will be accomplished in heat exchangers alone.

- Scale the above three configurations to produce roughly 10 MW of power. Choose the configuration with the highest power output/efficiency.
- There are several constraints to be satisfied including the SOFC thermal gradients and recuperator effectiveness.

Task 4. Scale the optimal scenario for the 10MW stationary power plant application design to 50 MW.

- Again, from the best configuration selected from Task 4, the power output is adjusted to be around 50 MW while satisfying all other constraints.
- Component efficiencies is adjusted to reflect the higher efficiencies of larger equipment.

Task 5. Perform cost analyses for both the 10 MW and 50 MW applications.

- Perform cost analysis for two best cases including the 10 MW and the 50 MW stationary applications varying the cost of renewable hydrogen in the year of 2020, 2030 and 2050.

Task 6. Using lessons learned from the stationary applications, develop a 3.5 MW mobile SOFC-GT for long-haul locomotive SOFC-GT systems utilizing LNG as a fuel.

- Modify the anode recycle configuration developed in Task 3 from hydrogen fuel to LNG. A pre-reformer is needed and thus put back to the configuration. Desulfurizer is not added since the leakage sensor is used instead of sulfur compounds for enhanced safety. Make necessary changes to the equipment operating conditions.
- There are two screening configurations to determine which one has the best LHV efficiency. One configuration is to vaporize the LNG first from heat provided by the turbine exhaust gases, then pressurize the NG using a fuel compressor. The other configuration is to pressurize the LNG first using a fuel pump, then vaporize the LNG from heat provided by the turbine exhaust gases.
- Choose the configuration with the highest power output/efficiency, then develop three cases based on different LNG container storage pressures at 20 psig, 85 psig and 150 psig.

Task 7. Develop 3.5 MW tugboat applications by incorporating GT suction air desalting system using the best configuration from the locomotive application.

- Modify the best locomotive configuration (i.e., fuel compressor vs. fuel pump) from Task 6 by incorporating the GT suction air desalting system.
- Generate 3 different cases based on the fuel tank conditions.
- Conclude if there is a difference in efficiency for three different cases.

4. Design and Results

The simulations performed in this study utilize ASPEN Plus® V10, which is a well-established and commercially available chemical processing design software. The software allows complicated process design and provides an appropriate selection of thermodynamic models. The software also allows the design specifications and calculator blocks to minimize errors, and automatically obtain certain performance variables such as electrical efficiency, heat exchanger effectiveness as well as heating values of the fuel. More importantly, it allows a custom-built model like the SOFC model to be incorporated into the software. ASPEN Plus® also has built-in products including the Exchanger Design and Rating (EDR) and the Capital Cost Estimator (CCE), which provide an accurate estimation for the cost of the stationary power plants. In the following sections, the design basis for each application, simulation results, as well as the cost for stationary applications would be addressed.

4.1. Establish Design Basis and Calibrate Key Models

10 MW and 50 MW are selected to be the power sizes for the SOFC-GT hybrid systems for stationary applications. Hydrogen produced from electrolysis supplied by renewable electricity is chosen to be the fuel for stationary power plants. 3.5 MW is chosen to be the power size for the SOFC-GT hybrid systems for mobile applications, including the land-based long-haul locomotives and marine-based tugboats, in which both utilize LNG as their fuels. The reason of choosing LNG instead of H_2 in mobile applications is because LNG is currently more accessible than hydrogen, and accessibility is important for mobile applications in practice. Also, LNG can potentially give a higher system efficiency given the necessity of reforming reaction as discussed in the Background. Therefore, it is beneficial to investigate both LNG and hydrogen in this thesis.

4.1.1. Stationary Applications

Site Characteristics

Applications of the SOFC-GT systems in the United States are considered while minimizing water usage. As summarized in Table 4-1, ISO ambient conditions consisting of 15°C, 60% relative humidity and 1 atm pressure are assumed. Table 4-2 summarizes the ambient

air composition. A level power stationary plant site is considered and accessible to road transportation of all equipment but constrained by overhead highway bridges.

Table 4-1: Stationary Plant Site Characteristics

Parameter	Value	Unit
Elevation	0	m
Barometric Pressure	1.015	bar
Design Ambient Temperature, Dry Bulb	15.0	°C
Design Ambient Temperature, Wet Bulb	10.8	°C
Design Ambient Relative Humidity	60	%

Table 4-2: Stationary Plant Air Composition

Component	Volume %
N_2	77.315
O_2	20.741
H_2O	0.987
Ar	0.924
CO_2	0.033

Renewable Hydrogen Characteristics

Stationary power plants will be fueled by hydrogen derived from electrolyzers supplied by renewable electricity. Therefore, it is assumed that the only "impurity" present in the fuel will be moisture. Table 4-3 shows the composition of hydrogen. The pressure of the fuel at plant battery limits for each size plant are shown in Table 4-4 while its temperature is assumed to be 15°C. It is also assumed that an odorant will not be added to the hydrogen based on the recommendations provided by Kopasz [44] that available hydrogen detectors can increase safety compared to addition of an odorant. Therefore, component like the desulfurizer can be eliminated from the plant. Along with the detectors, features like automatic shut-off valves and startup of ventilation fans can provide increased level of safety over that provided with an odorant strategy by removing the reliance on a person to take the appropriate actions.

Table 4-3: Hydrogen Composition

Component	Mole %
Hydrogen	99.9861
Water	0.0139

Table 4-4: Hydrogen Supply Pressure

Plant Size	10 MW	50 MW
Pressure	0.41 MPa	0.41 MPa

The higher heating value (HHV) of renewable hydrogen is 141.78 $\frac{\text{MJ}}{\text{kg}}$ and the lower heating value (LHV) is 119.76 $\frac{\text{MJ}}{\text{kg}}$. The electrical efficiency is calculated based on the LHV basis.

Liquefied Natural Gas Characteristics

The long-haul locomotives and tugboats would utilize LNG and Table 4-5 [45] provides compositions for various locations. Values shown for San Diego Gas and Electric are chosen for this study. The LNG is assumed to be stored as a saturated liquid at atmospheric pressure and the corresponding temperature is calculated. It is fed to a heat exchanger after being pumped up to the pressure required by the SOFC-GT system and then vaporized. Taking advantage of this low temperature heat sink is investigated in configuring the overall power system. As in the hydrogen fuel, it is again assumed that an odorant would not be added to the LNG nor after vaporization as multiple detectors for methane would be placed to detect leakages [46]. Again, as in the case of hydrogen, automatic shut-off valves and startup of ventilation fans would be prudent design feature to be incorporated along with the detectors.

Table 4-5: LNG Composition

Component, Mole %	Alaska	Algeria	Baltimore Gas and Electric	New York City	San Diego Gas and Electric
Methane	99.72	86.98	93.32	98.00	92.00
Ethane	0.06	9.35	4.65	1.40	6.00

Propane	0.0005	2.33	0.84	0.40	1.00
Butanes	0.0005	0.63	0.18	0.10	-
Nitrogen	0.20	0.71	1.01	0.10	1.00

The HHV of LNG in this case study is 52.34 $\frac{\text{MJ}}{\text{kg}}$ and the LHV is 47.20 $\frac{\text{MJ}}{\text{kg}}$.

4.1.2. Marine Based Applications

Ambient Air

Ambient air composition on a dry salt-free basis is assumed to be the same as that in the land-based applications while the relative humidity of 100% is assumed. An average ambient temperature of 21°C is used based on the range of 2°C to 40°C considered in a Sandia National Laboratory study [47] evaluating fuel cells in marine applications. The maximum salt content of 50 ppm is used in treating the incoming ambient air [48].

Liquefied Natural Gas

The marine applications would utilize LNG and its composition and temperature are assumed the same as those in the land-based applications.

4.1.3. Techno-Economic Analysis Basis

Mobile scale applications are typically pre-assembled inside a factory and then transport to the destination. The stationary power plants, however, are typically assembled after all the equipment and raw materials are sent to the destination. Therefore, the economic analysis for the current investigation can only be applied to the stationary applications. The mobile applications would be addressed for their potentials to operate instead of the cost.

The 10 MW stationary plant utilizes a single train design while the 50 MW stationary plant composes of five trains of the 10 MW design. Redundancies are not considered in the techno-economic analysis. The basis for analysis is provided by the U.S. Department of Energy/National Energy Technology Laboratory (DOE/NETL) and the related scholars [2][49][50].

Total Plant Cost Basis

The Total Plant Cost (TPC) includes the costs of process equipment, supporting facilities, direct and indirect labor, as well as engineering procurement and construction (EPC) services. To obtain costs best estimate for the stationary applications, Equation (4.1) is used to scale to the required capacity [2].

$$\mathrm{SC} = \mathrm{RC} \cdot \left(\frac{\mathrm{SP}}{\mathrm{RP}}\right)^{u} \cdot (1 + \mathrm{AER})^{\mathrm{SY}-\mathrm{RY}} \cdot \left(\frac{\mathrm{TS}}{\mathrm{TR}}\right)^{0.9} \tag{4.1}$$

where

- SC represents the scaled cost ($).
- RC represents the reference cost ($).
- SP represents the scaled parameter.
- RP represents reference parameter.
- u represents the scaling exponent.
- AER represents the annual escalation rate, which is 3% in this case study.
- SY represents the study year.
- RY represents the reference year.
- TS represents the number of trains or purchased amount of equipment in the scaled case.
- TR represents the number of trains or purchased amount of equipment in the reference case.

The accuracy of this methodology is expected to have an error within -15% to +30% [2].

Solid Oxide Fuel Cell. The high operating temperature and the limited moisture tolerance provides a major challenge to the fabrication technology of the SOFC [51]. The challenges with stack hardware, sealing and cell interconnect issues all contribute to a high cost of manufacturing the SOFC [6]. To reduce the high cost of SOFC is another major challenge to this technology. The detailed breakdown for the cost of SOFC include ceramic cell, interconnect, testing and conditioning, end plates, stack assembly, ceramic-glass sealing, anode frame, cathode mesh, anode mesh, stack brazing, picture frame, cathode frame, and laser welding [52]. Figure 4-1 [53] shows the major components of SOFC which contribute to the costs.

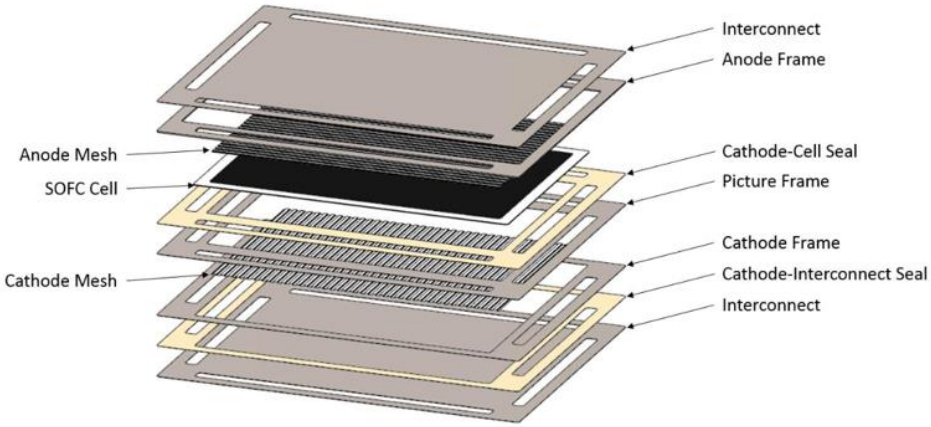

Figure 4-1: SOFC Major Components

Figure 4-2 [53] shows the detailed assembly and size specification for the SOFC cell. Notice that the figure is not drawn to scale, parts are shown for clarity.

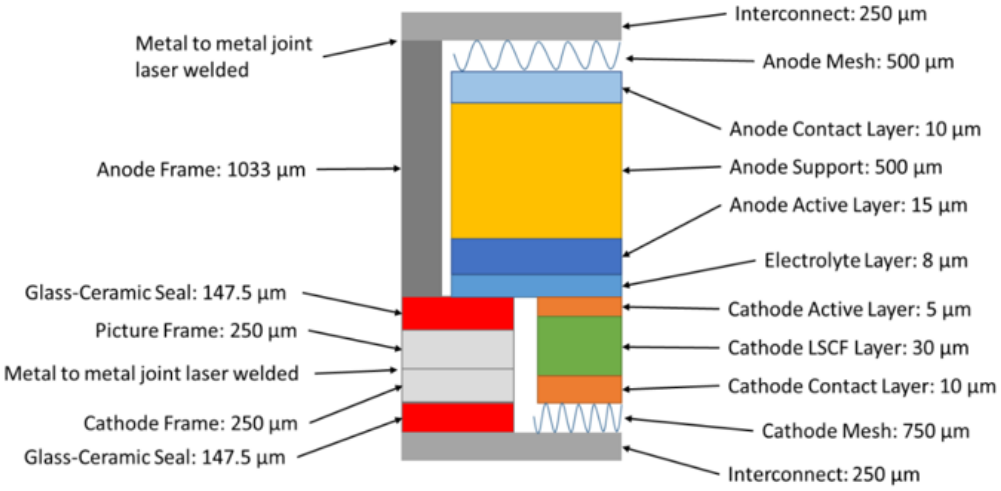

Figure 4-2: Detail Assembly and Specification of SOFC Cell

In this case study, the SOFC production is assumed to be at a moderate scale, which has 1,000 modules per year, and each module is capable of producing more than 300 kW of power [53]. The higher the production volume, the cheaper the SOFC cost due to economics of scale. The SOFCs are sold per stack, and each stack is expected to have 10 years of lifetime. The cost of SOFC is $16,000 per stack, which is rounded to the nearest thousands. Figure 4-3 [53] shows the stock cost distribution.

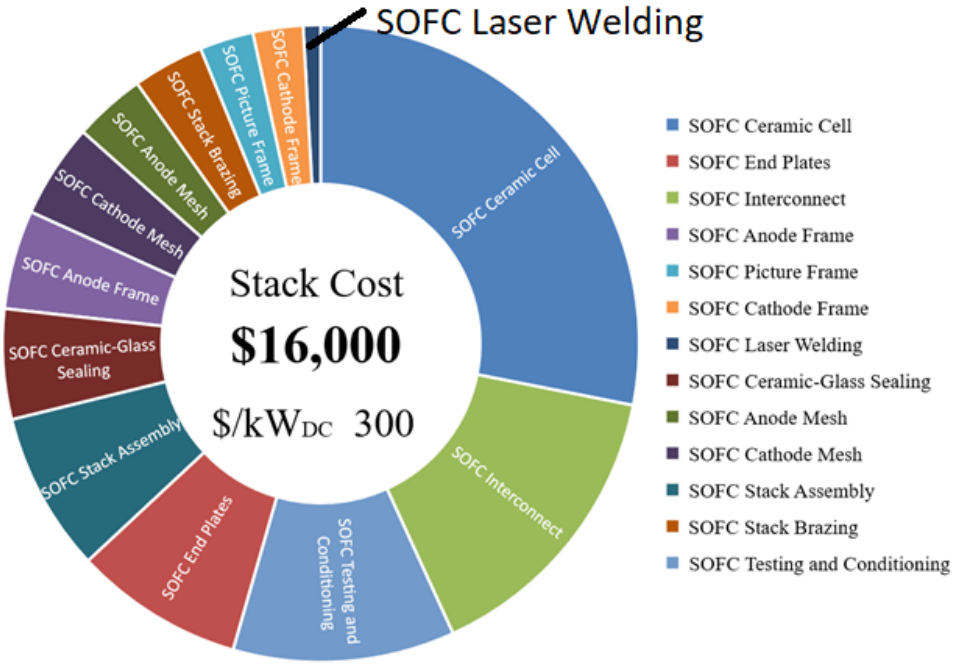

Figure 4-3: SOFC Stack Cost Distribution

Gas Turbine. Since a GT is usually the most expensive component in a conventional power plant, it is usually purchased from what is available on the market, or "off-the-shelf". However, the available GT models in the current market do not fit perfectly into this hydrogen-fueled SOFC-GT hybrid. A suitable GT for this application needs to have a high TIT but a relatively low air flowrate and thus a lower amount of work output. The GT in this hybrid is mainly used for cooling the SOFC while providing an auxiliary and dynamic power output, and the SOFC provides most of the power output. For a conventional GT, the TIT tends to be directly proportional to the air flowrate as well as the work output. A high TIT indicates a high air flowrate and work output, vice versa. However, the time frame for introducing these hydrogen-fueled hybrids will occur after the 10 MW natural gas-fueled hybrids, which is currently the most popular fuel selection, have been successfully deployed in numerous applications and for a number of years. Thus, it may be expected that the GT manufacturers will have gained confidence in their commercial viability to invest the capital in designing a customized GT for hydrogen-fueled applications. Consequently, the GT for this 10 MW and 50 MW power plant are assumed to be custom-built, unlike the natural gas-fueled hybrids may utilize "off-the-shelf" GTs.

For a customized GT, Equation (4.2) is used to estimate the cost [54].

$$C_{GT} = 0.1391(m_{air})^{0.73} + 0.0474(m_{air})^{0.73}p_c^{0.55} + 8.8221(10^{-13})\left(m_{air}^{0.73}\right)(\mathrm{TIT}^{3.5}) + 0.0356 \qquad (4.2)$$

where

- C_{GT} represents the cost of the GT (Millions $USD).
- m_{air} represents the GT compressor air flowrate (kg/s).
- p_c represents the GT compressor pressure ratio (PR).
- TIT is the turbine inlet temperature (K).

Heat Exchangers. There are two types of heat exchangers in this stationary power plant, which are heat recuperators and intercoolers. All shell and tube heat exchanger pinch temperature would be limited to 11°C while air-cooled exchanger pinch temperature would be limited to 25°C. However, for services with poor heat transfer coefficients and/or exotic metallurgical requirements, higher pinch temperatures may be warranted. The two heat recuperators used to preheat the air and the fuel from the GT exhaust are made up of stainless steel while the intercooler is made up of carbon steel. Stainless steel is more expensive than carbon steel but it can avoid corrosion from acids. In the GT exhaust stream, there would be condensing water that contains dissolved carbon dioxide and forms carbonic acid. Using stainless steel in the heat recuperators can avoid carbonic acid from corroding the tubes and thus making them more durable. The intercooler can use cheaper carbon steel since there is no such concern. The costs of the two recuperators involve equipment and setting, piping, civil, as well as instrumentation. The cost of the intercooler involves equipment and setting, piping, instrumentation, electrical, insulation, as well as paint.

Annual Fixed Operating Cost Basis

There are two types of annual expenses in implementing the stationary plants, the annual fixed operating cost (AFOC) and the annual variable operating cost (AVOC). The AFOC includes expenses such as operating labor, maintenance labor, administrative and support labor, as well as property tax and insurance. In the reference case, the plant employs two skilled operators, ten regular operators, one foreman as well as three lab technicians, and the average hourly wage is $40.85 [2]. However, the stationary plants in this thesis only need to employ two

skilled operators considering the smaller plant size compared to the reference case. Table 4-6 shows the AFOC basis [50].

Table 4-6: Annual Fixed Operating Cost Basis

Operating Labor Cost Rates	Value
Operating Labor Rate	$40.85/hour
Operating Labor Burden	30% of Base
Labor Overhead Charge Rate	25% of Labor
Workers/Employees	
Skilled Operator	2
Fixed Operating Costs	
Maintenance Labor	35% of Total Maintenance Cost
Administrative and Support Labor	25% of Operating and Maintenance Labor
Property Tax and Insurance	2% of TPC

Annual Variable Operating Cost Basis

The other annual expenses are the AVOC, which includes the fuel cost for hydrogen, fuel cell stack replacement and the maintenance cost. Since hydrogen infrastructure has not been developed to a sophisticated level, the cost of hydrogen accounts for the biggest portion of the AVOC as well as the operation costs. Currently, the cheapest and the most common way of producing hydrogen is by steam-reforming of natural gas. However, this method is not considered because the current investigation focuses on evaluating the potential of utilizing hydrogen produced by renewable sources.

As shown by Figure 4-4 [55] below, main ways of producing renewable hydrogen include electrolyzers, thermochemical as well anerobic digestion. The error bar subjects to a +/- 25% error [55]. Although thermochemical has the cheapest non-feedstock cost, it is not commercially available due to its large scale deployment and challenges related to the concentrated mirror systems [47]. Instead, production by electrolyzer, which is splitting water molecules into hydrogen and oxygen molecules by electricity, is promising because large scale production (i.e., 20,000 kg of hydrogen per day) has the second cheapest non-feedstock cost and

the cost is going to reduce in future years as would be explained below. The current non-feedstock cost is $1.45 per kg, and it is projected to reduce to $0.80/kg in 2030 and $0.50/kg is 2050.

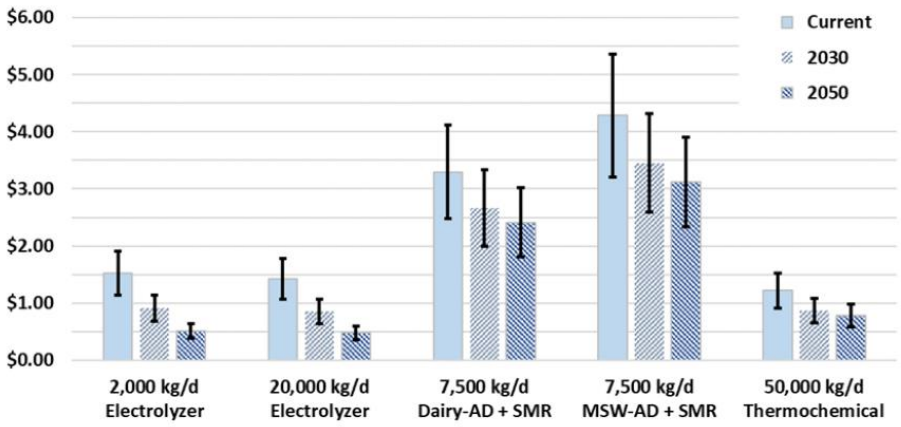

Figure 4-4: Non-Feedstock Renewable Hydrogen Production Costs

Note that Figure 4-4 only provides the non-feedstock cost, which is considered as the "conversion cost" to produce H_2 without accounting for the feedstock cost. The feedstock cost for electrolyzer is the Cost of Electricity (COE), and about 0.05 MWh of electricity is required to generate 1 kg of H_2 [55]. To obtain 100% RH_2, the electricity can only be obtained from renewable sources like solar panels and wind turbines. Considering the wind and solar potentials in California, electolyzers would be a very promising way in the future to supply sustainable H_2. Figure 4-5 [55] and Figure 4-6 [55] below show the levelized COE from wind and solar forecast scenarios in California.

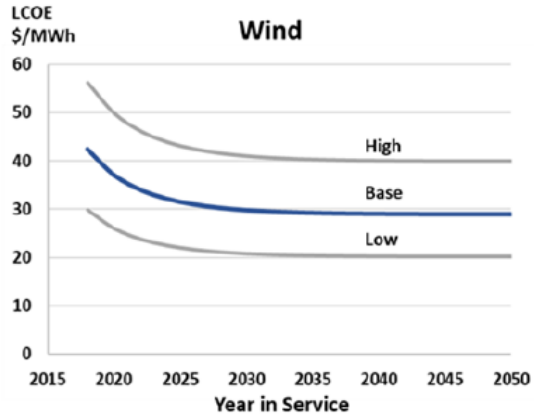

Figure 4-5: Levelized COE from Wind Forecast Scenarios

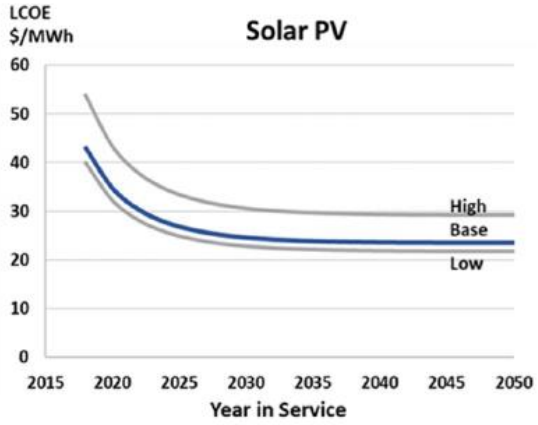

Figure 4-6: Levelized COE from Solar Forecast Scenarios

Consider the base case line in blue, the current levelized COE from wind turbines is $37/MWh and from solar panels is $35/MWh [55]. Based on the weighted average, California currently has 34.3% of wind production and 65.7% of solar production [56][57]. Multiply the levelized COE by their corresponding weights and sum the total, the current COE from wind and solar ($\mathrm{COE}_{\mathrm{w\&s}}$) is then estimated to be $35.69/MWh. Similarity, the levelized COE in 2030 is $30/MWh from wind and $25/MWh from solar [55]. By then, California is expected to have 44.8% of wind production and 55.2% of solar production [58][59]. The $\mathrm{COE}_{\mathrm{w\&s}}$ is then estimated to be $27.24/MWh in 2030. In 2050, the levelized COE is $29/MWh from wind and $24/MWh from solar [55]. By then, California is expected to have 62.5% wind production and 37.5% solar production [60]. The $\mathrm{COE}_{\mathrm{w\&s}}$ is then estimated to be $27.13/MWh in 2050. Therefore, the feedstock cost can be calculated by Equation (4.3).

$$C_f = 0.05(\mathrm{COE}_{\mathrm{w\&s}}) \tag{4.3}$$

where

- C_f is the feedstock cost per kg H_2 for electrolyzer ($).
- 0.05 represents the amount of electricity needed for 1 kg of H_2 produced (MWh).
- $\mathrm{COE}_{\mathrm{w\&s}}$ is the cost of electricity produced by wind and solar ($/MWh).

The feedstock cost is $1.78/kg in 2020, $1.36/kg in both 2030 and 2050, as summarized by Table 4-7 below.

Table 4-7: Summary of Feedstock Cost Basis

Year		2020	2030	2050
Levelized COE ($/MWh)	Wind	37	30	29
	Solar	35	25	24
Weighted Percentage (%)	Wind	34.3	44.8	62.5
	Solar	65.7	55.2	37.5
$\mathrm{COE_{w\&s}}$ ($/MWh)		35.69	27.24	27.13
C_f ($/kg H_2)		1.78	1.36	1.36

The total cost for producing RH_2 from electrolyzers would then be the summation of feedstock cost and the non-feedstock cost, as depicted by Equation (4.4).

$$\mathrm{C_{RH2}} = C_{nf} + \mathrm{C}_f \tag{4.4}$$

where

- $\mathrm{C_{RH2}}$ is the total cost of renewable hydrogen ($/kg).
- C_{nf} is the non-feedstock cost ($/kg).
- C_f is the feedstock cost ($/kg).

Then, the total cost for producing RH_2 is $3.23/kg in 2020, $2.16/kg in 2030 and $1.86/kg in 2050. The cost of transporting the RH_2 by pipelines has been included. The uncertainty in cost is in the range of -25% to + 25%. Table 4-8 shows the summary for the cost of RH_2.

Table 4-8: Summary for the Cost of Renewable Hydrogen

Year	Current (2020)	2030	2050
Non-feedstock cost (C_{nf}), $/kg	1.45	0.80	0.50
Feedstock cost (C_f), $/kg	1.78	1.36	1.36
Total Cost, $/kg	3.23	2.16	1.86

Note that the current tariff structure does not allow electrolyzers to receive electricity without paying a significant transmission and distribution charges even if they are direct access

customers. However, the regulatory agencies are working on this matter and the goal is to provide wholesale access to electrolytic fuel producers. If they can own power from others or on the wholesale market, they would only need to pay the transmission cost which would be around $0.02 [61]. Even though the feedstock cost should not be expected to be free, it would be beneficial to investigate the extreme points to cover the entire range, especially during curtailment. Curtailment happens when there is more electricity supply than demand from solar and wind production. To prevent damaging the electric grid, the excess generated electricity would not go into the grid but simply be "curtailed" and those energy would be wasted. In 2019, the average curtailment from solar PV and wind is around 321 MW [62], which can produce around 6,420 kg/h of RH_2. Therefore, purchasing electricity during curtailment is expected to be beneficial not only to lower the cost of RH_2, but also provides a good way to save the curtailed electricity from wind and solar to an energy storage medium in RH_2. When the weather is not ideal for wind and solar to produce sufficient electricity, the RH_2-fueled SOFC-GT stationary hybrids can produce electricity to supply the local needs. Figure 4-7 below shows the cost comparison per kg of RH_2 for 3 cases:

- Total cost when there is no curtailment (i.e., full feedstock and non-feedstock cost).
- Midpoint cost between no curtailment and curtailment (i.e., half feedstock cost and full non-feedstock cost).
- Non-feedstock cost only when there is curtailment (i.e., assume free COE from wind and solar).

Note that only the current year (i.e., 2020) is considered based on the curtailment information available in 2019. Prediction in 2030 and 2050 is difficult or inaccurate for curtailment.

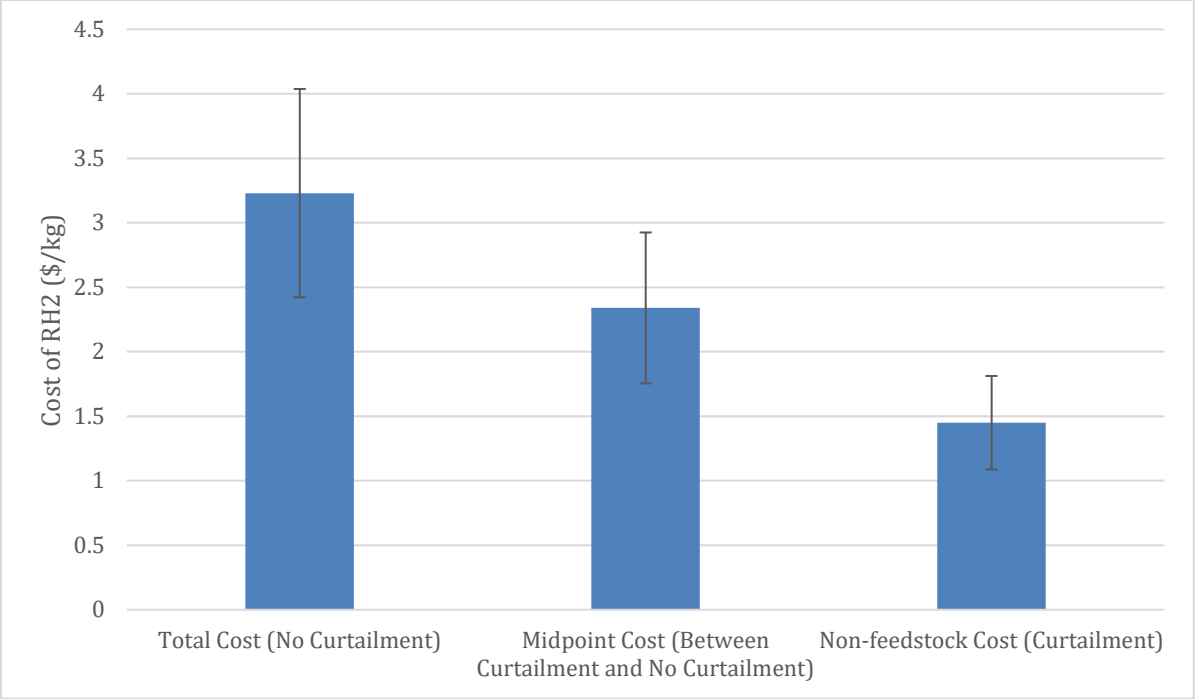

Figure 4-7: Cost of Renewable Hydrogen in 2020 Considering Curtailment

Land Cost Basis

The space required to build the stationary power plant includes the SOFC-GT power island and auxiliary plant area. The reference case requires 4,047 sqm total process unit area for the SOFC-GT power island [63], and requires 1,108 sqm for the auxiliary plant equipment [64]. The land cost is estimated to be $30.89/sqm [65]. Both the 10 MW and 50 MW stationary power plants utilize the same standard for the land cost. Table 4-9 below summaries the basis of land cost.

Table 4-9: Summary of Land Cost Basis

		Total Process Unit Area (sqm)
SOFC-GT Power Island		4,047
Auxiliary Plant Area		1,108
	Switch Yard	800
	Control Building	308
Cost per sqm: $30.89		

Cost of Electricity Basis

The first year COE is based on Equation (4.5) [2].

$$\mathrm{COE} = \frac{(\mathrm{CCF})(\mathrm{TPC} + \mathrm{LC}) + \mathrm{AFOC} + (\mathrm{CF})(\mathrm{AVOC})}{(\mathrm{CF})(\mathrm{MWH})} \tag{4.5}$$

where

- COE represents the cost of electricity in the first year ($/MWh).
- CCF represents the capital charge factor.
- TPC represents the Total Plant Cost ($).
- LC represents the land cost ($).
- AFOC represents the Annual Fixed Operating Cost ($).
- AVOC represents the annual variable operating cost ($).
- CF represents the capacity factor of the plant.
- MWH represents the annual net megawatt hours assuming the 100% capacity factor.

4.2. Development of Stationary Power Plant Applications

A screening analysis was first conducted in 10 MW for three different configurations, include anode eductor, cathode eductor, and no eductor. After determining the best configuration, the 50 MW plant would be built for the same configuration. The criterion for best configuration depends on the power output for a given fuel (i.e., RH_2) flowrate or electrical efficiency. The SOFC is subjected to a local and global thermal gradient before it degrades. To maximize the power output, the best case needs to satisfy the constraints listed: (1) the global thermal gradient ≤ 150 K and (2) local thermal gradient ≤ 15 K/cm. The recuperator effectiveness is another important parameter to check. Recuperator gets very expensive when effectiveness is over 90%. (3) Therefore, all recuperators in each case are constrained to have a maximum of 90% effectiveness to keep this plant economical. It should be noted that the electrical efficiency is calculated based on the LHV of RH_2.

4.2.1. 10 MW SOFC-GT Hybrid Systems for Stationary Applications

The 10 MW plant would be simulated by ASPEN Plus® V10, which has been mentioned at the beginning paragraph of Section 4. It would be based on three different configurations,

which are anode eductor, cathode eductor, and no eductor. The corresponding net power output was > 10 MW for the fuel flow rate initially selected, and then fine-tuned to have a power output close to 10 MW. For a given fuel flowrate, adjusting the GT air flowrate as well as the SOFC stack number (i.e., size of the SOFC) determine how much power the plant can produce. The case which gives the highest electrical efficiency/power output is determined to be the best configuration as mentioned at the beginning of the section.

Configurations and Results

Anode Eductor Configuration. This case is configurated by placing an eductor on the anode (i.e., fuel side) recycle stream, mixing the fresh fuel with the recycled stream from the SOFC anode and supplying the mixture to the SOFC operating at a pressure of 5 bar. This case utilizes two compressors with intercooling between them since the inlet fuel needs to be compressed to a sufficiently high pressure for the lower pressure recycled anode gas. An intercooler not only reduces the amount of compression work but also limits the operating temperature of the compressor to stay within its design constraints. Two recuperators are utilized to preheat the incoming air and fuel by exchanging heat with the GT exhaust. Figure 4-8 below illustrates the anode eductor case configuration.

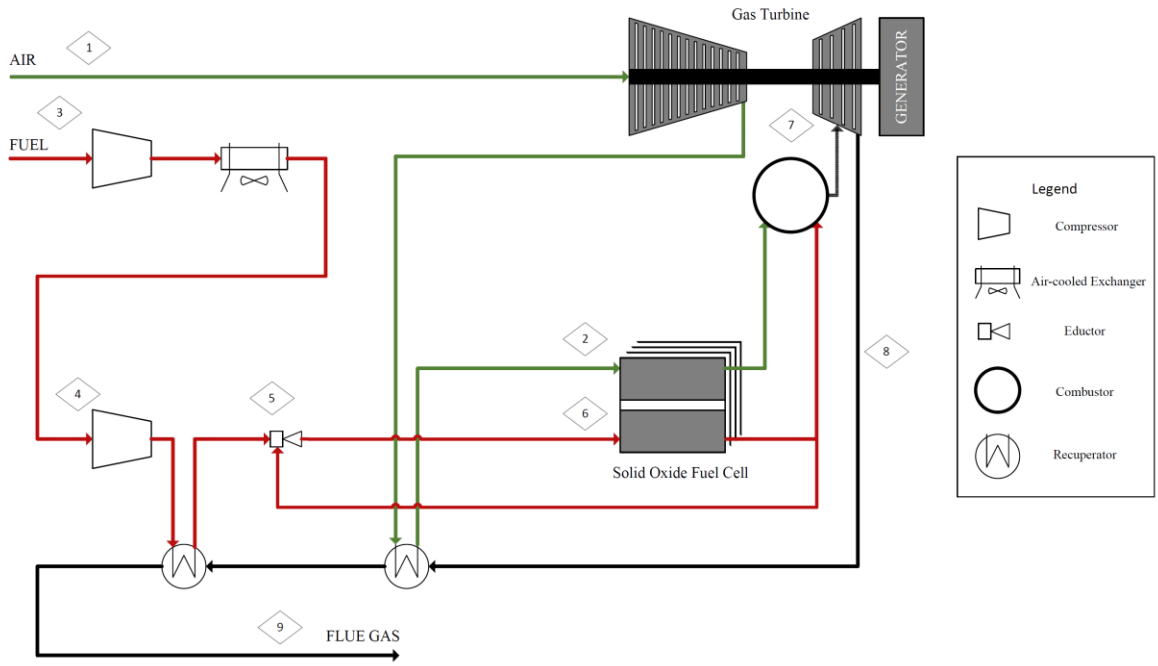

Figure 4-8: Anode Eductor Case Configuration for 10 MW RH_2-Fueled SOFC-GT Hybrid

The anode eductor case produces 10.00 MW of AC power and has a 68.50%-LHV efficiency. Table 4-10 below summarizes the results for this case.

Table 4-10: Anode Eductor Case Results for 10 MW RH_2-Fueled SOFC-GT Hybrid

Overall Performance		
	AC Power Output (MW_{AC})	10.00
	LHV Electrical Efficiency (%)	68.50
SOFC		
	DC Power Output (MW_{DC})	7.94
	AC Power Output (MW_{AC})	7.78
	Inverter Losses (%)	2
	Number of Stacks	150
	Fuel Flowrate (kg/h)	439
	Operating Voltage (V)	0.82
	Operating Temperature (°C)	700
	Operating Pressure (bar)	5.00
	Overall Fuel Utilization (%)	82.92
	Single Pass Fuel Utilization (%)	69.11
	Air Utilization (%)	29.52
	Local Temperature Gradient (K/cm)	14.10
	Maximum Local Temperature Gradient (K)	15.00
	Global Temperature Gradient (K)	149.44
	Maximum Global Temperature Gradient (K)	150.00
GT		
	AC Power Output (MW_{AC})	2.62
	Air Flowrate (kg/h)	42,500
	Compressor Pressure Ratio	5.30
	Turbine Inlet Temperature (°C)	1,103
	Compressor Polytropic Efficiency (%)	84.85
	Compressor Mechanical Efficiency (%)	98.04

	Expander Polytropic Efficiency (%)	83.31
	Expander Mechanical Efficiency (%)	98.04
Fuel Compressors		
	Compressor I AC power consumed (MW_{AC})	0.16
	Compressor I Polytropic Efficiency (%)	70.00
	Compressor I Mechanical Efficiency (%)	89.00
	Compressor II AC power consumed (MW_{AC})	0.19
	Compressor II Polytropic Efficiency (%)	67.00
	Compressor II Mechanical Efficiency (%)	89.00
Heat Recuperators		
	Air-Preheater Effectiveness (%)	89.68
	Fuel-Preheater Effectiveness (%)	90.32
Exhaust		
	Flue Gas Temperature (°C)	312
	Flue Gas Flowrate (kg/h)	42,939

Cathode Eductor Configuration. This case is configurated by placing an eductor on the cathode (i.e., air side) recycle stream, mixing the fresh air with the recycled stream from the SOFC cathode and supplying the mixture to the SOFC operating at a pressure of 5 bar. This case utilizes only one fuel compressor since the eductor is not placed in the anode side, and there is no need to compress the fuel pressure to as high as the previous case. Since there is only one compressor, there is no need for an intercooler. Three recuperators are utilized in this case. On the other hand, the GT compressor has to now operate at a higher-pressure ratio (PR) to provide the air at a sufficiently high pressure for the lower pressure recycled cathode gas. Same as the previous case, one recuperator is used to preheat the fuel and one recuperator is used to preheat the air. An additional recuperator is used replace the eductor at the location from the previous case to the SOFC operating temperature and pressure. Figure 4-9 below illustrates the cathode eductor case configuration.

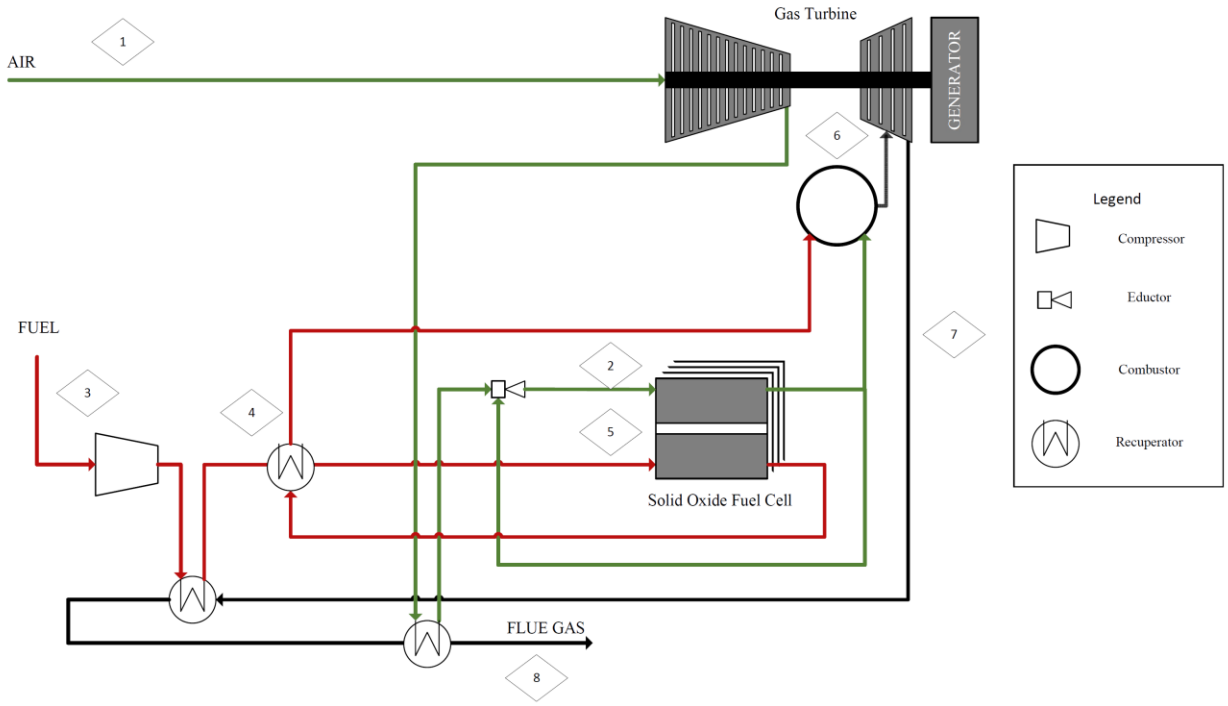

Figure 4-9: Cathode Eductor Case Configuration for 10 MW RH_2-Fueled SOFC-GT Hybrid

The cathode eductor case produces 9.91 MW of AC power and has a 66.80%-LHV efficiency. Table 4-11 below summarizes the results for this case.

Table 4-11: Cathode Eductor Case Results for RH_2-Fueled SOFC-GT Hybrid

Overall Performance		
	AC Power Output (MW_{AC})	9.91
	LHV Electrical Efficiency (%)	66.80
SOFC		
	DC Power Output (MW_{DC})	8.49
	AC Power Output (MW_{AC})	8.32
	Inverter Losses (%)	2
	Number of Stacks	138
	Fuel Flowrate (kg/h)	446
	Operating Voltage (V)	0.82
	Operating Temperature (°C)	700

	Operating Pressure (bar)	5.00
	Overall Fuel Utilization (%)	87.27
	Single Pass Fuel Utilization (%)	87.27
	Air Utilization (%)	23.89
	Local Temperature Gradient (K/cm)	14.94
	Maximum Local Temperature Gradient (K)	15.00
	Global Temperature Gradient (K)	138.28
	Maximum Global Temperature Gradient (K)	150.00
GT		
	AC Power Output (MW_{AC})	1.91
	Air Flowrate (kg/h)	44,000
	Compressor Pressure Ratio	5.30
	Turbine Inlet Temperature (°C)	1,037
	Compressor Polytropic Efficiency (%)	84.85
	Compressor Mechanical Efficiency (%)	98.04
	Expander Polytropic Efficiency (%)	83.31
	Expander Mechanical Efficiency (%)	98.04
Fuel Compressor		
	AC Power Consumed (MW_{AC})	0.27
	Polytropic Efficiency (%)	67.00
	Mechanical Efficiency (%)	89.00
Heat Recuperators		
	Air-Preheater Effectiveness (%)	89.97
	Fuel-Preheater Effectiveness (%)	89.93
	Anode-off Gas Effectiveness (%)	15.91
Exhaust		
	Flue Gas Temperature (°C)	332
	Flue Gas Flowrate (kg/h)	44,446

No Eductor Configuration. The last case is the simplest configuration, which has no eductor. The case utilizes four recuperators in total. Three of the recuperators are at the same location as in the

previous cases being placed in the anode outlet stream as well as the GT exhaust flue gas stream. The fourth recuperator is placed in the cathode outlet stream, which is used to exchange heat between cathode outlet with the incoming warmed air. Figure 4-10 below illustrates the no eductor case configuration.

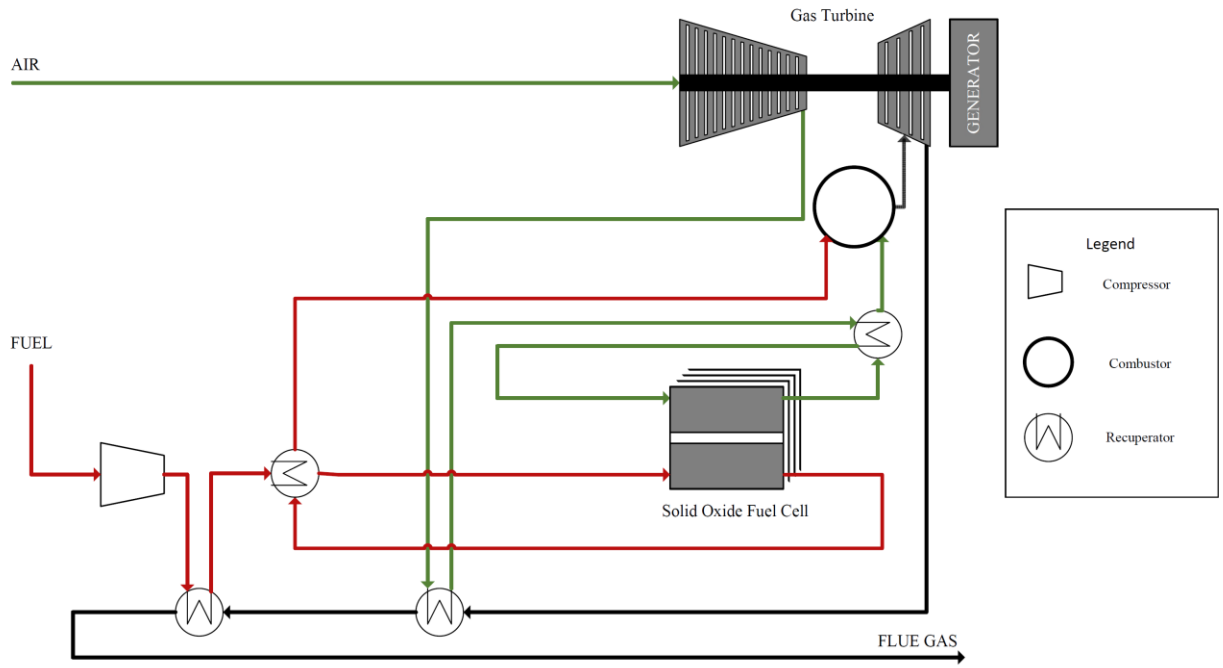

Figure 4-10: No Eductor Case Configuration for 10 MW RH_2-Fueled SOFC-GT Hybrid

The no eductor case produces 9.97 MW of AC power and has a LHV electrical efficiency of 63.38%. Table 4-12 below summarizes the results for this case.

Table 4-12: No Eductor Case Results for 10 MW RH_2-Fueled SOFC-GT Hybrid

Overall Performance		
	AC Power Output (MW_{AC})	9.97
	LHV Electrical Efficiency (%)	63.38
SOFC		
	DC Power Output (MW_{DC})	8.55
	AC Power Output (MW_{AC})	8.38

	Inverter Losses (%)	2
	Number of Stacks	121
	Fuel Flowrate (kg/hr)	473
	Operating Voltage (V)	0.82
	Operating Temperature (°C)	700
	Operating Pressure (bar)	5.00
	Overall Fuel Utilization (%)	82.83
	Single Pass Fuel Utilization (%)	82.83
	Air Utilization (%)	21.56
	Local Temperature Gradient (K/cm)	12.51
	Maximum Local Temperature Gradient (K)	15.00
	Global Temperature Gradient (K)	149.72
	Maximum Global Temperature Gradient (K)	150.00
GT		
	AC Power Output (MW_{AC})	1.93
	Air Flowrate (kg/hr)	62,630
	Compressor Pressure Ratio	5.60
	Turbine Inlet Temperature (°C)	860
	Compressor Polytropic Efficiency (%)	84.85
	Compressor Mechanical Efficiency (%)	98.04
	Expander Polytropic Efficiency (%)	83.31
	Expander Mechanical Efficiency (%)	98.04
Fuel Compressor		
	AC Power Consumed (MW_{AC})	0.28
	Polytropic Efficiency (%)	67.0
	Mechanical Efficiency (%)	89.0
Heat Recuperators		
	Air-Preheater Effectiveness (%)	89.58
	Fuel-Preheater Effectiveness (%)	89.80
	Anode-off Gas Effectiveness (%)	66.19
	Cathode-off Gas Effectiveness (%)	42.82

Exhaust		
	Flue Gas Temperature (°C)	283
	Flue Gas Flowrate (kg/hr)	63,103

Summary of Configurations and Results

Table 4-13 shows the summary of results. Anode Eductor has the best electrical efficiency among three configurations, which produces 10.00 MW power at 68.50% LHV electrical efficiency. This indicates that recycling anode exhaust gas is more effective than recycling cathode exhaust gas or no recycling. The higher the efficiency, the lower is the amount of heat rejected to the atmosphere. In this case, heat is primarily carried away with the flue gas. Anode recycle case has the lowest amount of exhaust flue gas flowrate and no eductor case has the highest amount of exhaust flue gas flowrate. The anode recycle case has the lowest air flowrate while no recycle has the highest. Recycle helps cooling the SOFC and thus less excess air is required for cooling the SOFC. Therefore, lower air flowrate to the GT indicates higher power output/efficiency. Furthermore, the anode recycle case has a lower exhaust temperature compared to the cathode recycle case which explains the higher efficiency for the anode recycle case. The exhaust temperature for the anode recycle case is higher than that for the no recycle case but its lower flowrate more than offsets the higher temperature. Although the number of SOFC stacks is the highest for the anode recycle case which would increase the plant cost, it is expected that this increase would be more than offset by the reduction in plant cost due to fewer recuperators used and the lower airflow rate, and lower operating costs due to the higher plant efficiency. Since the anode eductor case gives the highest power output and efficiency, it would be recommended to build a power plant based on this configuration.

Table 4-13: Comparison of Results for 10 MW RH_2-Fueled SOFC-GT Hybrid

Overall Performance	Anode Eductor	Cathode Eductor	No Eductor
AC Power Output (MW_{AC})	10.00	9.91	9.97
LHV Electrical Efficiency (%)	68.50	66.80	63.38
SOFC			

DC Power Output (MW_{DC})	7.94	8.49	8.55
AC Power Output (MW_{AC})	7.78	8.32	8.38
Inverter Losses (%)	2		
Number of Stacks	150	138	121
Fuel Flowrate (kg/hr)	439	446	473
Operating Voltage (V)	0.82		
Operating Temperature (°C)	700		
Operating Pressure (bar)	5.00		
Overall Fuel Utilization (%)	82.92	87.27	82.83
Single Pass Fuel Utilization (%)	69.11		
Air Utilization (%)	29.52	23.89	21.56
Local Temperature Gradient (K/cm)	14.10	14.94	12.51
Maximum Local Temperature Gradient (K/cm)	15.00		
Global Temperature Gradient (K)	149.44	138.28	149.72
Maximum Global Temperature Gradient (K)	150.00		

GT

AC Power Output (MW_{AC})	2.62	1.91	1.93
Air Flowrate (kg/h)	42,500	44,000	62,630
Compressor Pressure Ratio	5.30		5.60
Turbine Inlet Temperature (°C)	1,103	1,037	860
Compressor Polytropic Efficiency (%)	84.85		
Compressor Mechanical Efficiency (%)	98.04		
Expander Polytropic Efficiency (%)	83.31		
Expander Mechanical Efficiency (%)	98.04		

Fuel Compressors

AC Power Consumed (MW_{AC})	0.35	0.27	0.28
Compressor I Polytropic Efficiency (%)	70.00	N/A	
Compressor I Mechanical Efficiency (%)	89.00	N/A	
Compressor II Polytropic Efficiency (%)	67.00		
Compressor II Mechanical Efficiency (%)	89.00		

Heat Recuperators

Air-Preheater Effectiveness (%)	89.68	89.97	89.58
Fuel-Preheater Effectiveness (%)	90.32	89.93	89.80
Anode-off Gas Effectiveness (%)	N/A	15.91	66.19
Cathode-off Gas Effectiveness (%)	N/A		42.82

Exhaust

Flue Gas Temperature (°C)	312	332	283
Flue Gas Flowrate (kg/h)	42,939	44,446	63,103

Techno-Economic Analysis

Only the anode eductor configuration is used for the cost analysis because it gives the highest efficiency. The basis for cost estimates is in the year of 2020, and the overall plant annual escalation rate is at 3.00%. The case study presented assumes no water recovery as well as no carbon capture and storage.

Total Plant Cost (TPC). The TPC for the 10 MW stationary power plant is estimated to be $19,671,000, with a specific plant cost of $1,966 per kW ($/kW). Table 4-14 and Figure 4-11 show the summary and distribution of the TPC for the 10 MW stationary power plant. All the costs are rounded to the nearest thousands.

Table 4-14: Summary of TPC for 10 MW RH_2-Fueled SOFC-GT Hybrid

Total Plant Cost		$19,671,000
Specific Plant Cost		$1,966/kW
Total SOFC Cost	$10,651,000	
SOFC Stack Cost		$3,836,000
Power Conditioning Systems		$4,788,000
Housing & Final Assembly		$1,642,000
System Installation Cost		$385,000
Total GT Cost	$4,195,000	
Generator Set		$3,536,000

Foundation		$51,000
Piping & Insulation		$298,000
Instrumentation & Electrical Equipment		$310,000
Gas Processing Equipment Cost	$732,000	
Fuel Screw Compressor I		$236,000
Fuel Screw Compressor II		$184,000
Air-cooled Fuel Intercooler		$157,000
Flue Gas Stack		$155,000
Heat Recuperation Cost	$1,496,000	
Air Preheater		$1,246,000
Fuel Preheater		$250,000
Auxiliary Plant Equipment Cost	$2,597,000	
Accessory Electric Plant		$985,000
Instrumentation & Controls		$722,000
Improvement to Site		$188,000
Buildings & Structures		$702,000

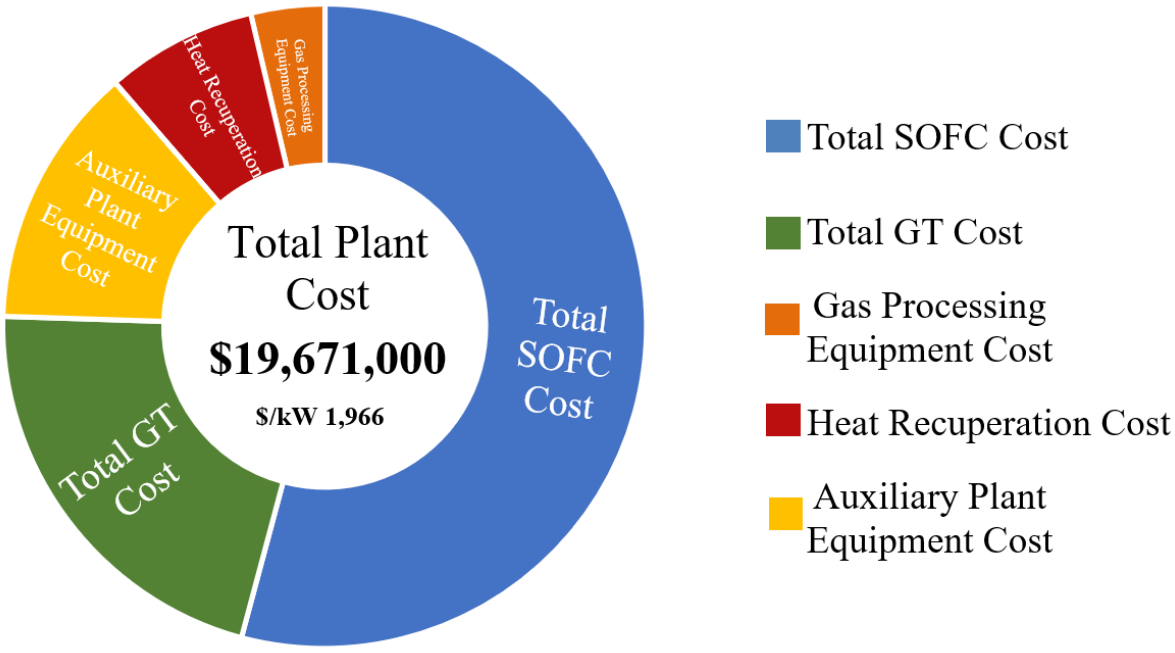

Figure 4-11: Distribution of TPC for 10 MW RH_2-Fueled SOFC-GT Hybrid

Annual Fixed Operating Cost (AFOC). The AFOC includes the costs of operating labor, maintenance labor, administrative and support labor, as well as property tax and insurance. The AFOC is estimated to be $2,063,000 per year, rounded to the nearest thousands. Table 4-15 and Figure 4-12 show the summary and distribution of AFOC for the 10 MW stationary power plant.

Table 4-15: Summary of AFOC for 10 MW RH_2-Fueled SOFC-GT Hybrid

Operating Labor	$1,163,000/year
Maintenance Labor	$173,000/year
Administrative & Support Labor	$334,000/year
Property Tax and Insurance	$393,000/year
Total AFOC	$2,063,000/year

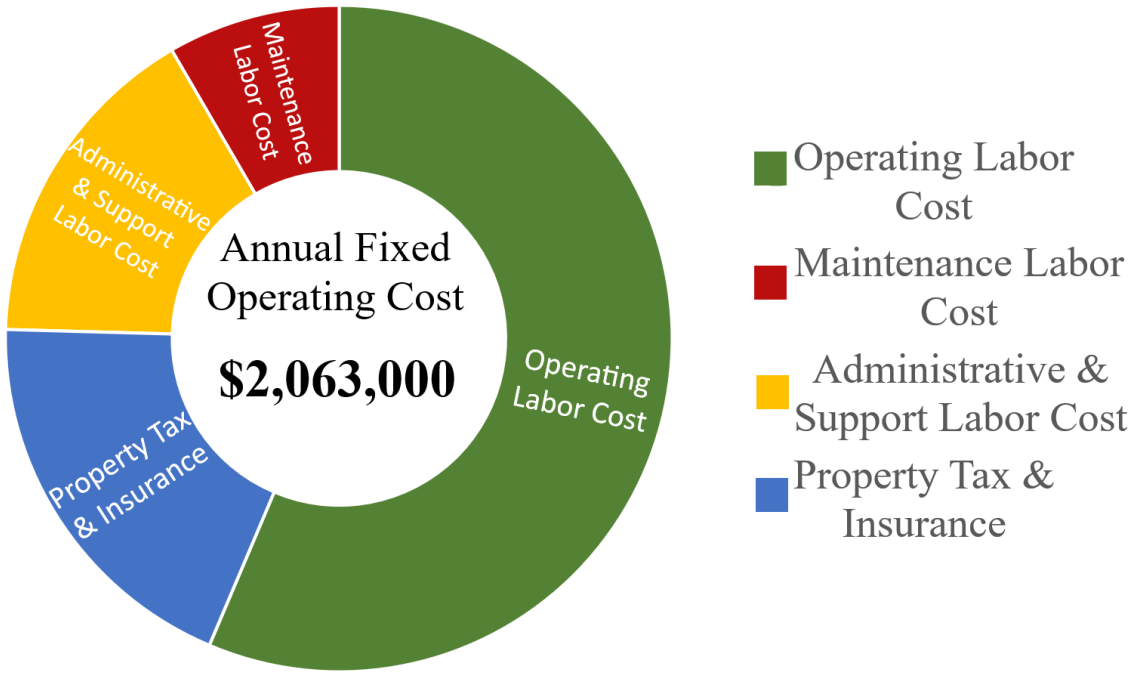

Figure 4-12: Distribution of AFOC for 10 MW RH_2-Fueled SOFC-GT Hybrid

Annual Variable Operating Cost (AVOC). The AVOC includes the cost of maintenance material, fuel cell stack replacement, as well as the fuel cost for renewable hydrogen.

Table 4-16 and Figure 4-13 show the summary and distribution of AVOC for the 10 MW stationary power plant. The annual variable operating cost is estimated to be $11,637,000 per

year, and the RH_2 fuel cost is estimated to be $11,187,000 per year, which accounts for more than 90% of the AVOC and is more than 70% of the COE, a more detailed analysis for the cost of RH_2 has been done at different periods to demonstrate the effect of fuel costs. For details, please refer to the Cost Basis for Renewable Hydrogen. In 2030, the fuel cost is projected to decrease to $7,481,000, which is around a 36% reduction compared to the current year. In 2050, the fuel cost is projected to decrease to $6,442,000, which is around a 14% reduction compared to 2030 and around a 42% reduction compared to the current cost. Figure 4-14 below shows the fuel cost of renewable hydrogen in different years. The fuel cost is subjected to an error between -25% to 25%.

Table 4-16: Summary of AVOC for 10 MW RH_2-Fueled SOFC-GT Hybrid

	Maintenance Material Cost	$289,000/year
	Fuel Cell Replacement Cost	$161,000/year
	Renewable Hydrogen Fuel Cost	$11,187,000/year
Annual Variable Operating Cost		$11,637,000/year

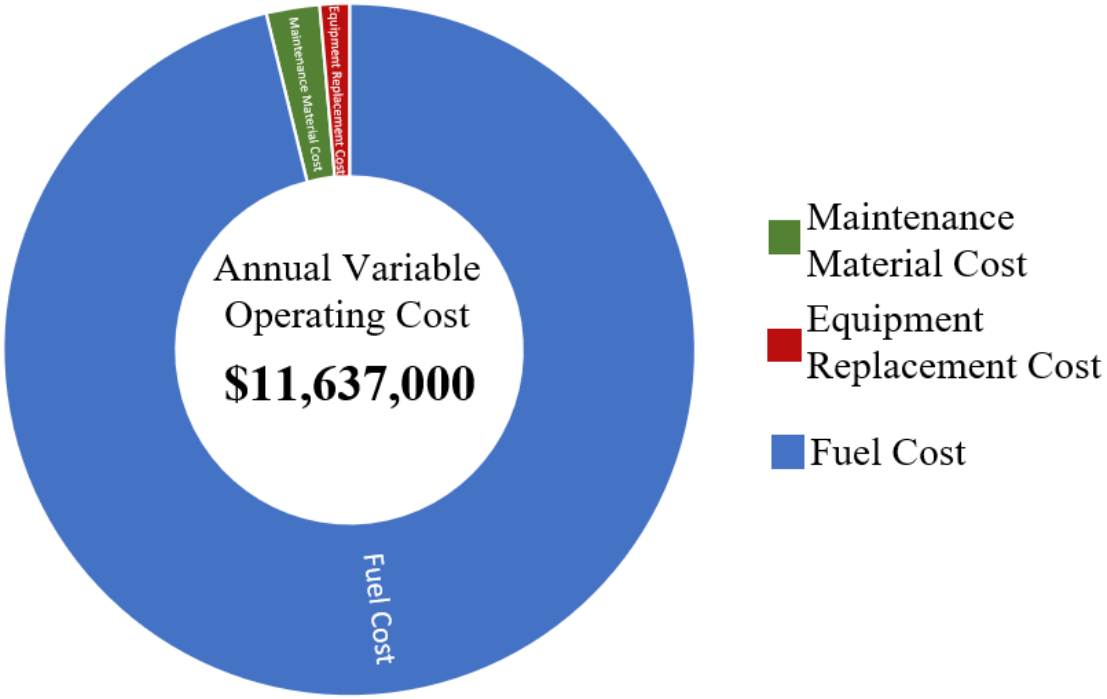

Figure 4-13: Distribution of AVOC for 10 MW RH_2-Fueled SOFC-GT Hybrid

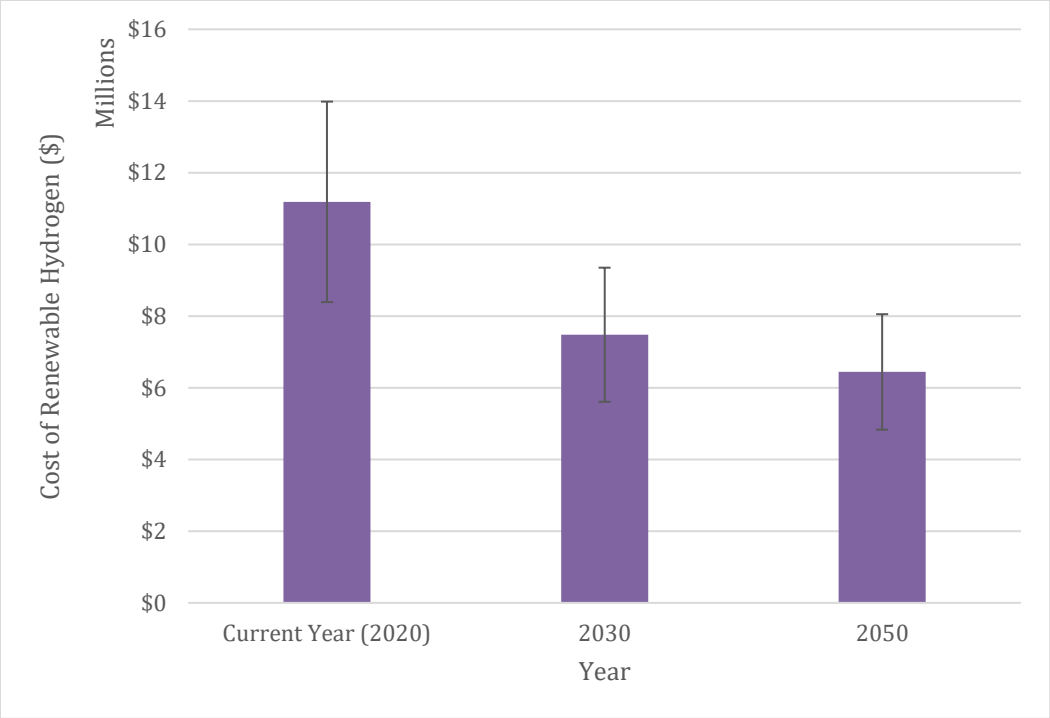

Figure 4-14: RH_2 Cost for 10 MW SOFC-GT Hybrid in Different Years

Land Cost (LC). The total land area for the 10 MW stationary power plant includes the SOFC-GT hybrid power island as well as the auxiliary plant area. The total required land area is 4,022 sqm and each sqm costs $30.89. Therefore, the total land cost is $124,000, rounded to the nearest thousands. Table 4-17 shows the land cost summary.

Table 4-17: Summary of Land Cost for 10 MW RH_2-Fueled SOFC-GT Hybrid

Total Land Area (sqm)		4,022
	SOFC/GT Hybrid Power Island (sqm)	3,607
	Auxiliary Plant Area	415
Land Costs	$30.89/sqm	$124,000

Cost of Electricity (COE). Figure 4-15 summarizes the COE distribution in the current year, which is $197.06/MWh. Since the fuel cost accounts for more than 70% of the COE, a possible way to lower the fuel cost is to consider purchasing electricity from wind and solar during curtailment, which has been mentioned in Cost Basis for Renewable Hydrogen.

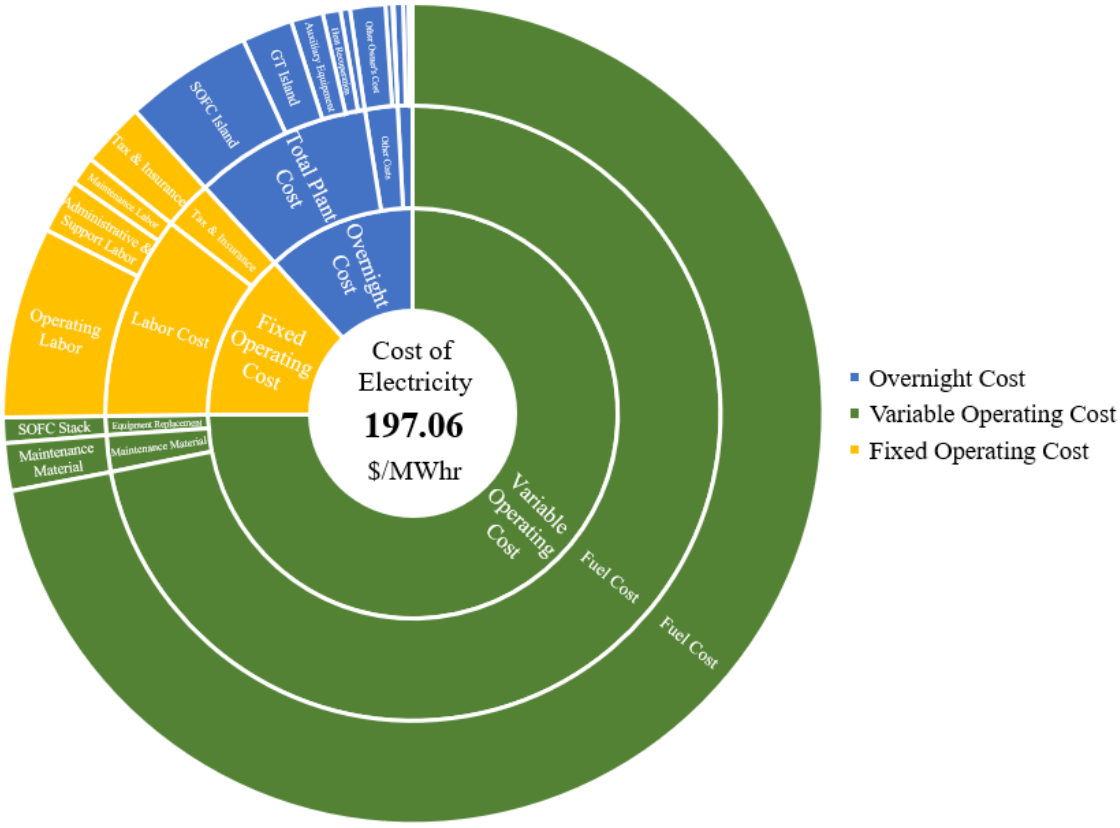

Figure 4-15: Distribution of COE in 2020 for 10 MW RH_2-Fueled SOFC-GT Hybrid

Figure 4-16 below compares the COE in 2020 between different curtailment levels. The left column shows the COE based on regular RH_2 cost when there has no curtailment. The middle column shows the COE based on the midpoint case when there is a 50% reduction in the feedstock cost. The right column shows the COE based on 100% reduction in feedstock cost when there is curtailment occurs, in which the COE from wind and solar is negligible. The curtailment information is based on the available information from California Independent System Operator (CA-ISO) in 2019 [62].

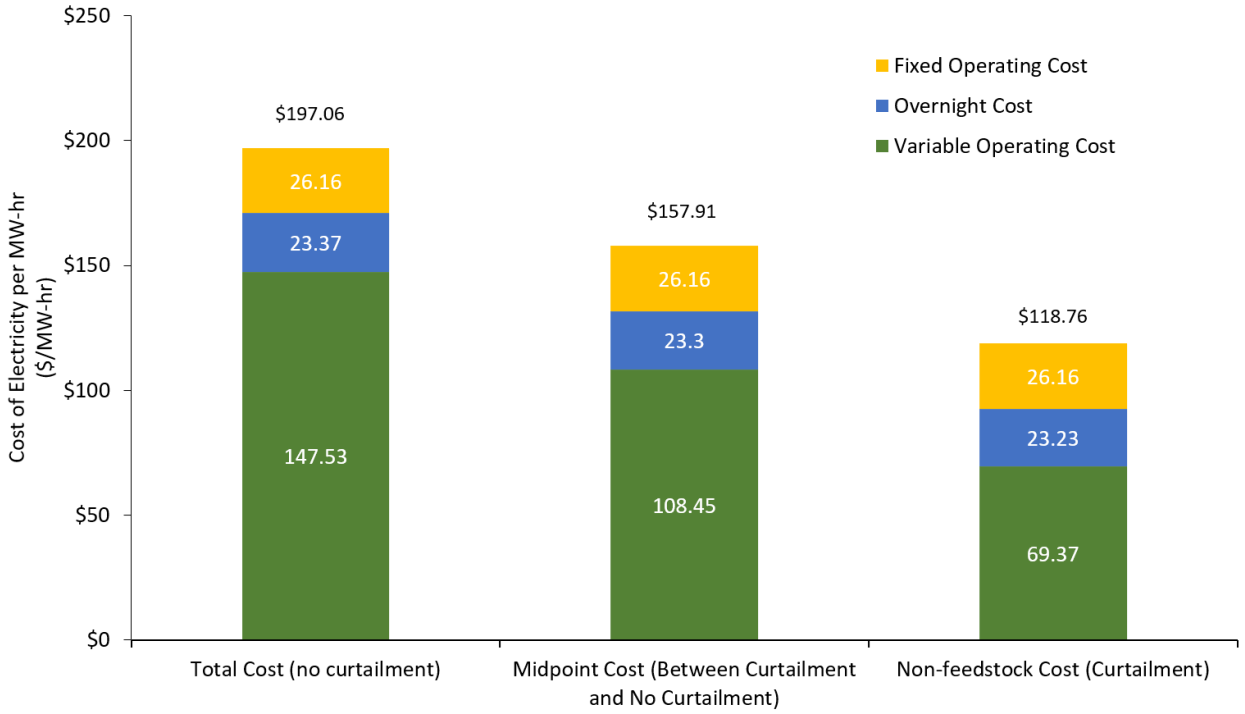

Figure 4-16: COE Comparison in 2020 for 10 MW RH_2-Fueled SOFC-GT Hybrid Varying Curtailment Levels

Figure 4-17 shows a different COE comparison varying the cost of RH_2 in the future. Due to the expectation of cheaper fuel cost as mentioned in Cost Basis for Renewable Hydrogen, the COE is estimated to decrease by about 24% to $150.00/MWh in 2030 and decrease by about 31% to $136.79/MWh in 2050. All costs presented from Figure 4-17 assumed no curtailment and is based on the regular cost of RH_2 because it is hard to predict the level of curtailments in the future.

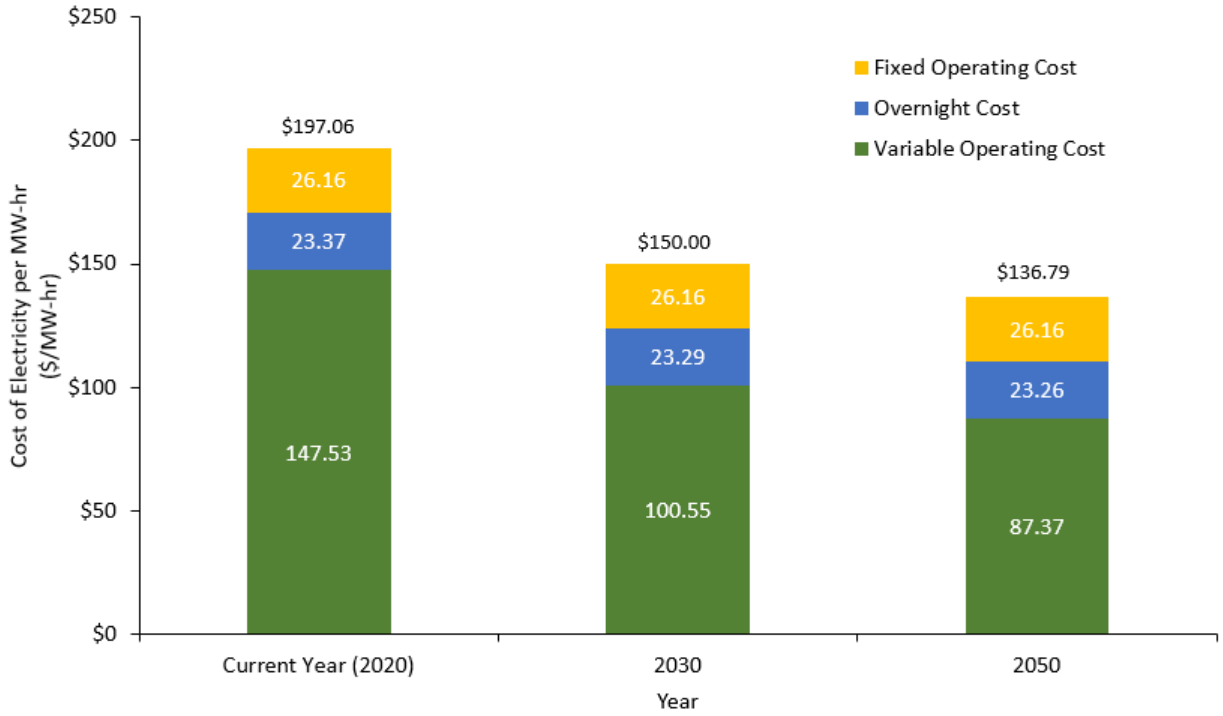

Figure 4-17: Comparison of COE for 10 MW RH_2-Fueled SOFC-GT Hybrid in Different Years

Based on the results presented from Figure 4-16 and Figure 4-17, it is important to emphasize the impact based on the levels of curtailment. The levels of curtailment are proportional to the feedstock cost, which reflects that the feedstock cost has a strong impact for the COE. If the electrolytic fuel producers can receive electricity from wind and solar at free or near free cost during curtailment, then the COE in 2020 can potentially be cheaper than the COE in 2030 and even in 2050 when there is no curtailment. More practically speaking, the COE from wind and solar should decrease as more renewable infrastructures are deployed and cost should reduce with increasing demand in renewable electricity. Table 4-18 summarizes the techno-economic analysis results for the 10 MW stationary power plant.

Table 4-18: Summary of Techno-Economic Analysis for 10 MW RH_2-Fueled SOFC-GT Hybrid

Total Plant Cost		$19,671,000
	Specific Plant Cost	$1,966/kW
	Total SOFC Cost	$10,651,000
	Total GT Cost	$4,195,000
	Gas Processing Equipment Cost	$732,000

	Heat Recuperation Cost	$1,496,000
	Auxiliary Plant Equipment Cost	$2,597,000
Annual Fixed Operating Cost		$2,063,000/year
	Operating Labor Cost	$1,163,000/year
	Maintenance Labor Cost	$173,000/year
	Administrative & Support Labor Cost	$334,000/year
	Property Tax & Insurance	$393,000/year
Annual Variable Operating Cost		$11,637,000/year
	Maintenance Material Cost	$289,000/year
	Fuel Cell Replacement Cost	$161,000/year
	Renewable Hydrogen Fuel Cost	$11,187,000/year
Land Cost		$124,000
COE		
	2020	
	no curtailment	$197.06/MWh
	Between curtailment and no curtailment	$157.91/MWh
	curtailment	$118.76/MWh
	Future Years	
	2030 (no curtailment)	$150.00/MWh
	2050 (no curtailment)	$136.79/MWh

Summary of 10 MW Stationary Applications

The 10 MW anode eductor configuration gives the highest LHV-efficiency at 68.50%. The specific plant cost is $1,966/kWh with a COE at $197.06/MWh without any curtailment. The COE in midpoint case between curtailment and no curtailment is $157.91/MWh, and the COE for curtailment is $118.76/MWh. The COE is expected to decrease to $150.00/MWh in 2030 and $136.79/MWh in 2050 for advanced technologies and more deployments of renewable solar and wind plants.

Table 4-19 shows the summary of key results and economic performance for the 10 MW stationary power plant.

Table 4-19: Summary of 10 MW RH_2-Fueled SOFC-GT Hybrid

Thermodynamic Performance	
Configuration	Anode Supported
AC Power Output (MW_{AC})	10.00
Plant Efficiency, % LHV	68.50
SOFC	
AC Power Output (MW_{AC})	7.78
Operating Voltage (V)	0.82
Operating Temperature (°C)	700
Overall Fuel Utilization (%)	82.92
Single Pass Fuel Utilization (%)	69.11
Air Utilization (%)	29.52
Maximum Local Temperature Gradient (K/cm)	15.00
Maximum Global Temperature Difference (K)	150.00
GT (Custom Built)	
AC Power Output (MW_{AC})	2.62
Compressor Pressure Ratio (bar/bar)	5.30
Turbine Inlet Temperature (°C)	1,103
Economic Performance	
Specific Plant Cost ($/kW)	1,966
Total Plant Cost ($)	19,671,000
Fixed Operating and Maintenance Cost ($/year)	2,063,000
Annual Variable Operating Cost ($/year)	11,637,000
Land Cost ($)	124,000
COE in 2020, no curtailment ($/MWh)	197.06
COE in 2020, midpoint ($/MWh)	157.91
COE in 2020, curtailment ($/MWh)	118.76

COE in 2030, no curtailment ($/MWh)	150.00
COE in 2050, no curtailment ($/MWh)	136.79

4.2.2. 50 MW SOFC-GT Hybrid Systems for Stationary Applications

The 50 MW system is configured with five trains of the corresponding 10 MW plants described in the above section. Anode eductor configuration will be employed based on the simulation results of the 10 MW power plant.

Configuration and Results

The 50 MW anode eductor plant has the same configuration as the 10 MW anode eductor plant, except the fuel compressors, GT compressor and GT expander have slightly higher efficiencies than those of the 10 MW plant. The components in a plant with higher power output usually have higher efficiencies because larger components are designed to be more efficient and better matches the economics of scale. Figure 4-18 shows the configuration for 50 MW by recycling the anode gas.

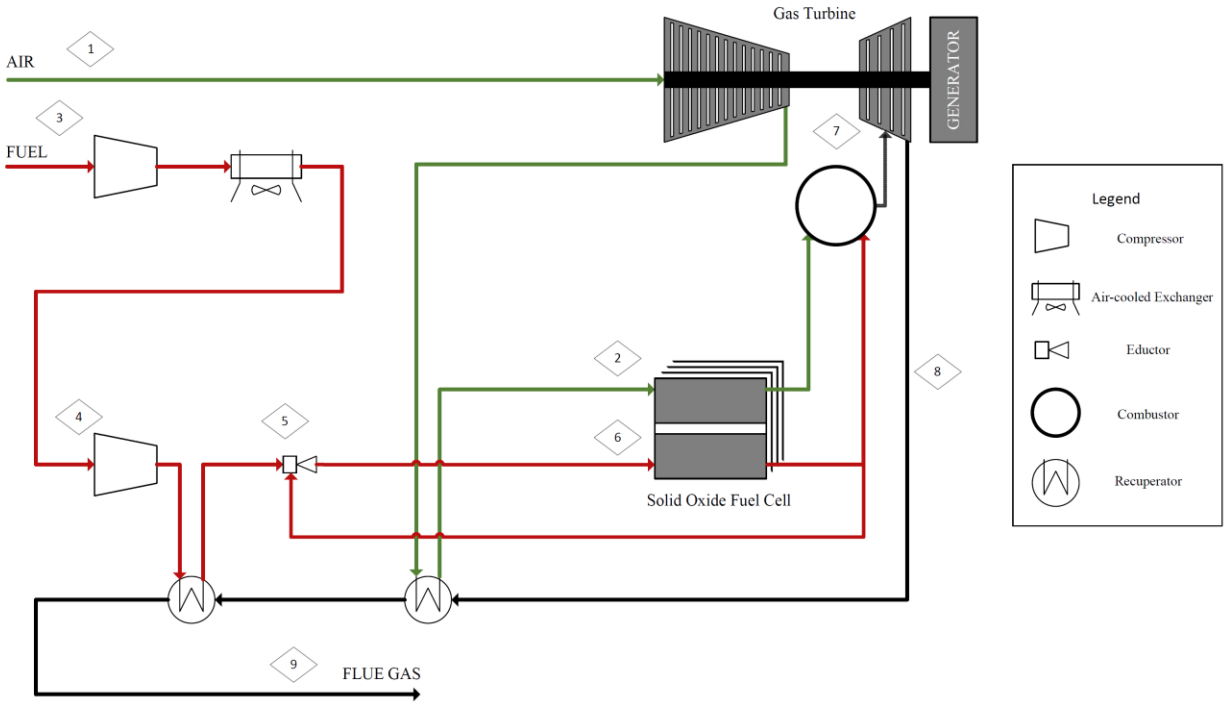

Figure 4-18: Anode Eductor Case Configuration for 50 MW RH_2-Fueled SOFC-GT Hybrid

The 50 MW anode eductor case produces 50.42 MW of AC power at 70.22%-LHV efficiency. Table 4-20 summarizes the results for this case.

Table 4-20: Anode Eductor Case Results for 50 MW RH_2-Fueled SOFC-GT Hybrid

Overall Performance		
	AC Power Output (MW_{AC})	50.42
	LHV Electrical Efficiency (%)	70.22
SOFC		
	DC Power Output (MW_{DC})	38.99
	AC Power Output (MW_{AC})	38.21
	Inverter Loss (%)	2
	Number of Stacks	736
	Fuel Flowrate (kg/h)	2,158
	Operating Voltage (V)	0.82
	Operating Temperature (°C)	700
	Operating Pressure (bar)	5.00
	Overall Fuel Utilization (%)	82.87
	Single Pass Fuel Utilization (%)	68.94
	Air Utilization (%)	29.92
	Local Temperature Gradient (K/cm)	14.28
	Maximum Local Temperature Gradient (K)	15.00
	Global Temperature Gradient (K)	149.86
	Maximum Global Temperature Gradient (K)	150.00
GT		
	AC Power Output (MW_{AC})	13.90
	Air Flowrate (kg/h)	206,019
	Compressor Pressure Ratio	5.30
	Turbine Inlet Temperature (°C)	1,109
	Compressor Polytropic Efficiency (%)	85.60
	Compressor Mechanical Efficiency (%)	98.15

	Expander Polytropic Efficiency (%)	85.70
	Expander Mechanical Efficiency (%)	99.00
Fuel Compressors		
	Compressor I AC Power Consumed (MW_{AC})	0.75
	Compressor I Polytropic Efficiency (%)	72.00
	Compressor I Mechanical Efficiency (%)	90.00
	Compressor II AC Power Consumed (MW_{AC})	0.89
	Compressor II Polytropic Efficiency (%)	71.00
	Compressor II Mechanical Efficiency (%)	89.50
Heat Recuperators		
	Air-Preheater Effectiveness (%)	90.44
	Fuel-Preheater Effectiveness (%)	90.27
Exhaust		
	Flue Gas Temperature (°C)	306
	Flue Gas Flowrate (kg/h)	208,175

Techno-Economic Analysis

The basis for cost estimates is the same as the 10 MW case.

Total Plant Cost (TPC). The TPC for the 50 MW stationary power plant is estimated to be $80,626,000, with a specific plant cost of $1,600 per kW. All the costs presented are rounded to the nearest thousands. Table 4-21 and Figure 4-19 show the summary of TPC and distribution for the 50 MW stationary power plant.

Table 4-21: Summary of TPC for 50 MW RH_2-Fueled SOFC-GT Hybrid

Total Plant Cost		$80,626,000
Specific Plant Cost		$1,600/kW
Total SOFC Cost	$52,346,000	
SOFC Stack Cost		$18,700,000
Power Conditioning Systems		$23,550,000

Housing & Final Assembly		$8,457,000
System Installation Cost		$1,639,000
Total GT Cost	$13,176,000	
Generator Set		$11,107,000
Foundation		$161,000
Piping & Insulation		$935,000
Instrumentation & Electrical Equipment		$973,000
Gas Processing Equipment Cost	$5,943,000	
Fuel Screw Compressor I		$3,027,000
Fuel Screw Compressor II		$2,309,000
Air-cooled Fuel Intercooler		$208,000
Flue Gas Stack		$399,000
Heat Recuperation Cost	$1,568,000	
Air Pre-Heater		$1,225,000
Fuel Pre-Heater		$343,000
Auxiliary Plant Equipment Cost	$7,593,000	
Accessory Electric Plant		$985,000
Instrumentation & Controls		$2,961,000
Improvement to Site		$770,000
Buildings & Structures		$2,877,000

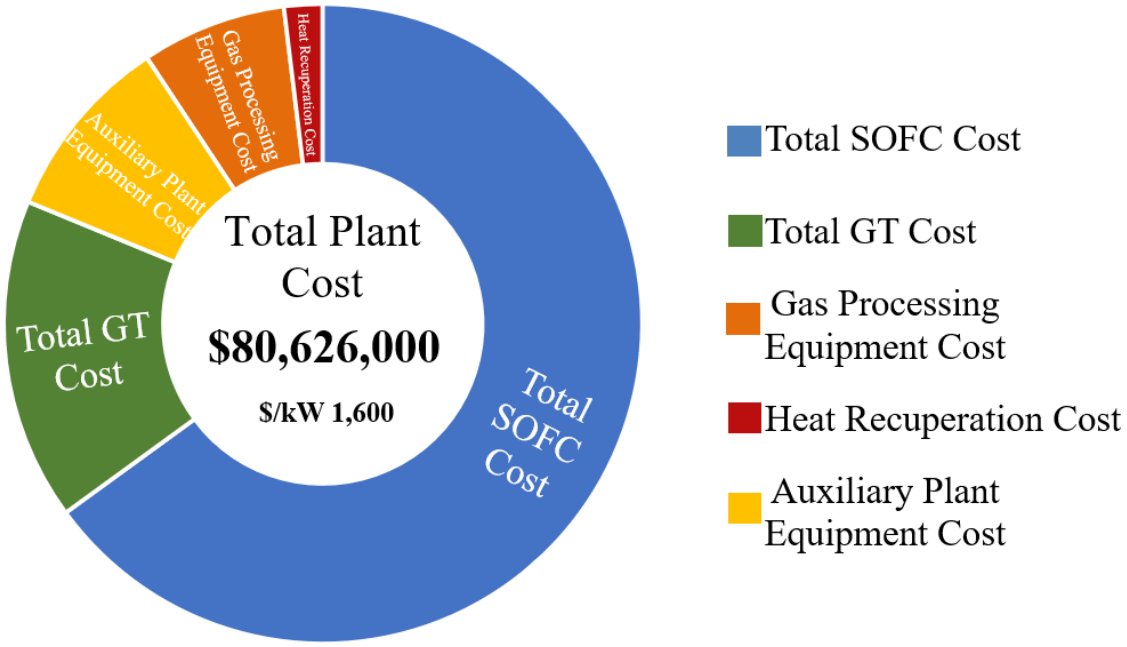

Figure 4-19: Distribution of TPC for 50 MW RH_2-Fueled SOFC-GT Hybrid

Annual Fixed Operating Cost (AFOC). The AFOC for the 50 MW plant is estimated to be $3,962,000 per year. Table 4-22 and Figure 4-20 shows the summary and distribution of AFOC for the 50 MW stationary power plant.

Table 4-22: Summary of AFOC for 50 MW RH_2-Fueled SOFC-GT Hybrid

Operating Labor	$1,163,000/year
Maintenance Labor	$716,000/year
Administrative & Support Labor	$470,000/year
Property Tax and Insurance	$1,613,000/year
Total AFOC	$3,962,000/year

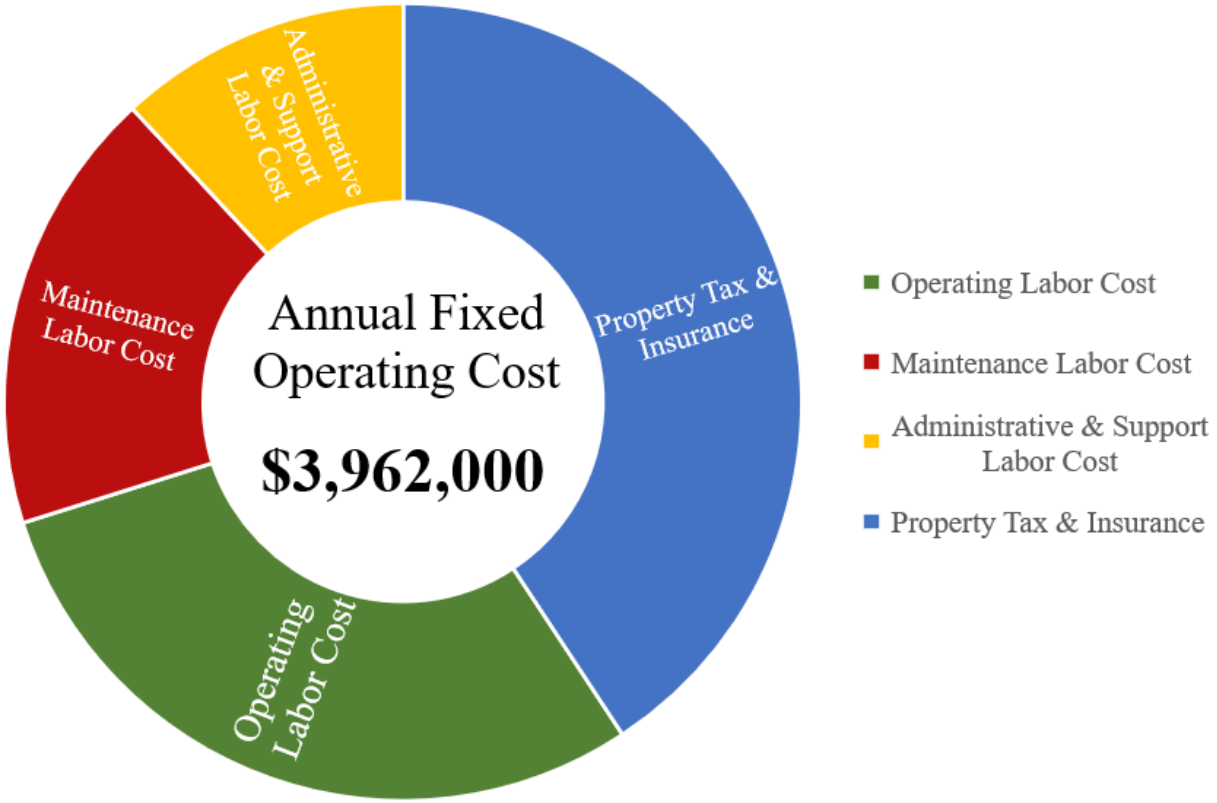

Figure 4-20: Distribution of AFOC for 50 MW RH_2-Fueled SOFC-GT Hybrid

Annual Variable Operating Cost (AVOC). The AVOC is estimated to be $56,977,000. Table 4-23 and Figure 4-21 show the summary and distribution of AVOC for 50 MW power plant. The fuel cost in 2030 is expected to decrease to $38,760,000, which is more than 30% decrease compared to 2020. In 2050, the fuel cost is expected to decrease to $33,652,000, which is more than 40% decrease compared to 2020. Figure 4-22 shows the feedstock cost of renewable hydrogen in different years.

Table 4-23: Summary of AVOC for 50 MW RH_2-Fueled SOFC-GT Hybrid

	Maintenance Material Cost	$1,197,000/year
	Fuel Cell Replacement Cost	$788,000/year
	Renewable Hydrogen Fuel Cost	$54,992,000/year
Total AVOC		$56,977,000/year

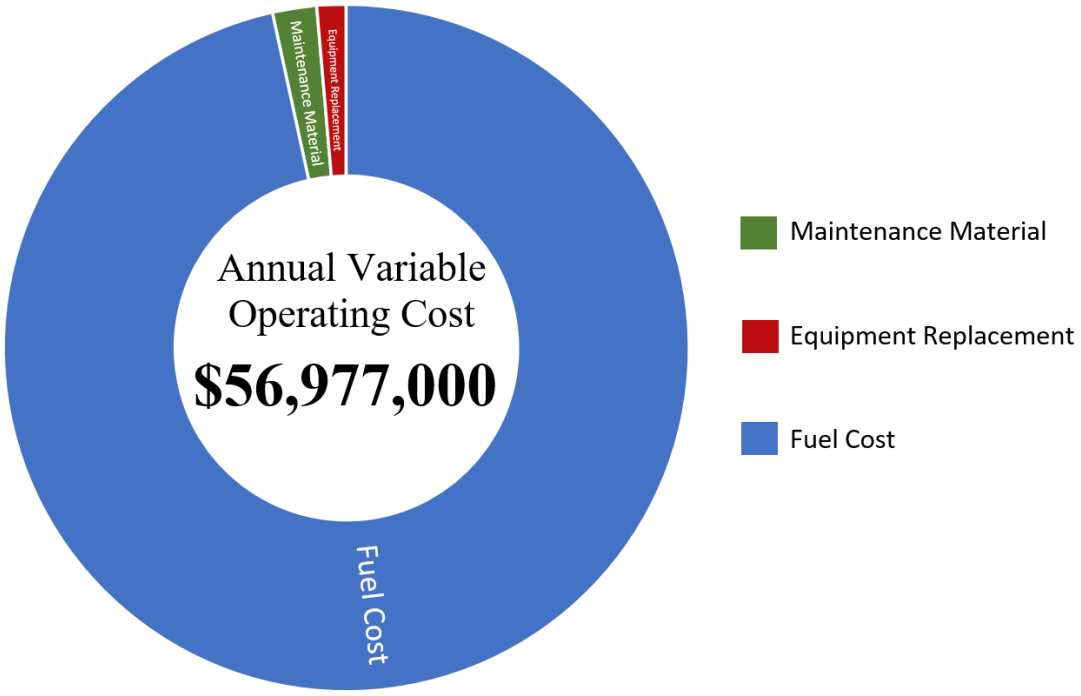

Figure 4-21: Distribution of AVOC for 50 MW RH_2-Fueled SOFC-GT Hybrid

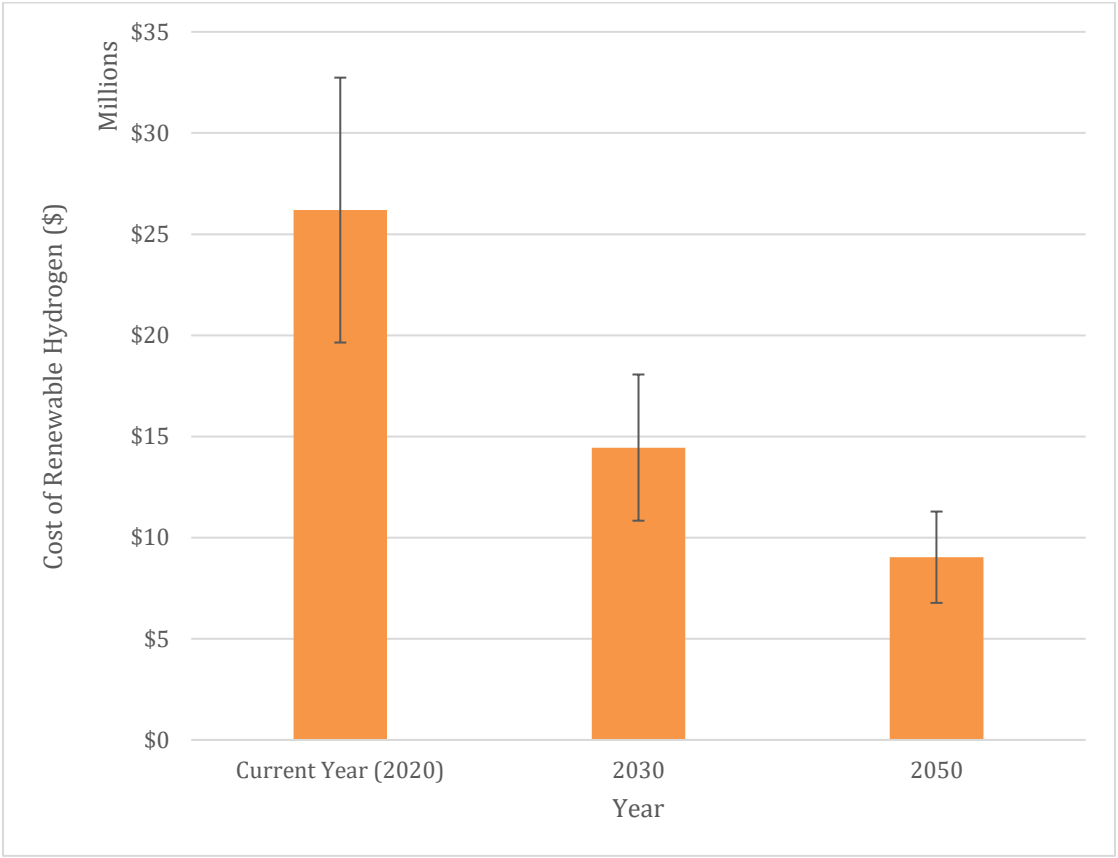

Figure 4-22: RH_2 Cost for 50 MW SOFC-GT Hybrid in Different Years

Land Cost. The total land area for the 50 MW stationary power plant includes the SOFC-GT hybrid power island as well as the auxiliary plant area. The total required land area is 18,728 sqm and each sqm costs $30.89. Therefore, the total land cost is $579,000, rounded to the nearest thousands. Table 4-24 shows the land cost summary.

Table 4-24: Summary of Land Cost for 50 MW RH_2-Fueled SOFC-GT Hybrid

Total Land Area (sqm)		18,728
SOFC/GT Hybrid Power Island (sqm)		17,721
Auxiliary Plant Area		1,007
Land Costs	$30.89/sqm	$579,000

Cost of Electricity (COE). Figure 4-23 summarizes the COE distribution in the current year, which is $171.94/MWh. Since the fuel cost accounts for more than 80% of the COE, Figure 4-24 below shows the COE comparing different levels of curtailment. The midpoint cost between curtailment and no curtailment is $133.76/MWh, and the cost for curtailment is $95.58/MWh. Figure 4-25 shows another analyzes by comparing the COE in future years. The COE is estimated to decrease by about 27% to $126.04/MWh in 2030 and decrease by about 34% to $113.17/MWh in 2050, both assuming no curtailment. Table 4-25 summarizes the techno-economic analysis results for the 50 MW stationary power plant.

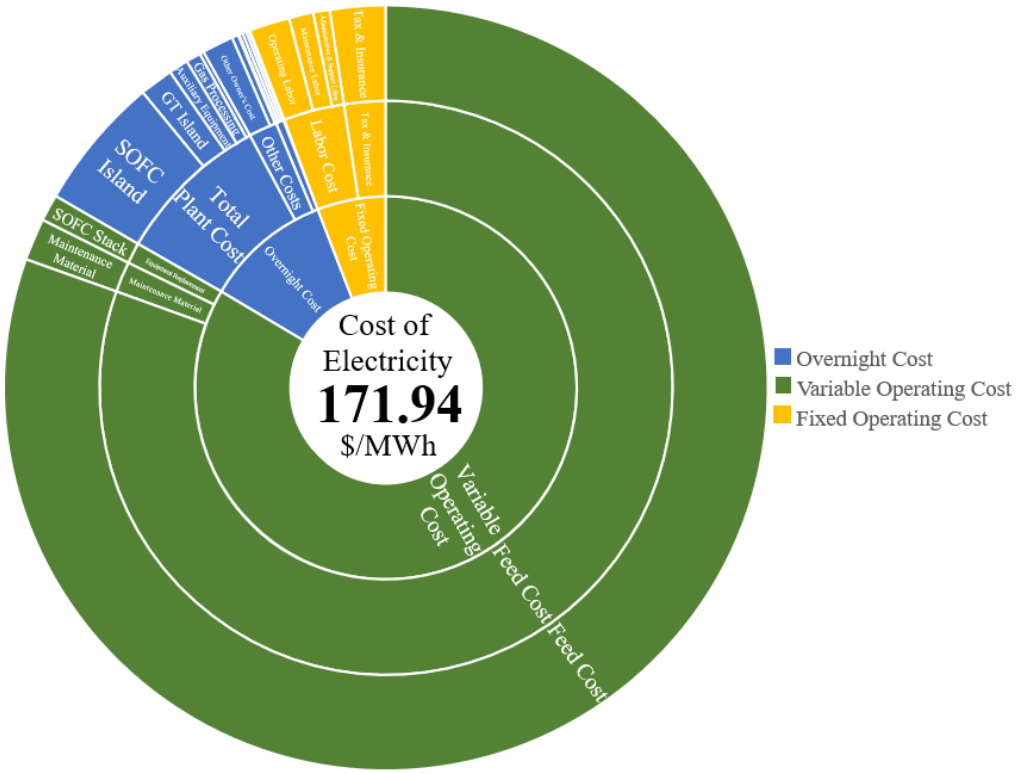

Figure 4-23: Distribution of COE in 2020 for 50 MW RH_2-Fueled SOFC-GT Hybrid

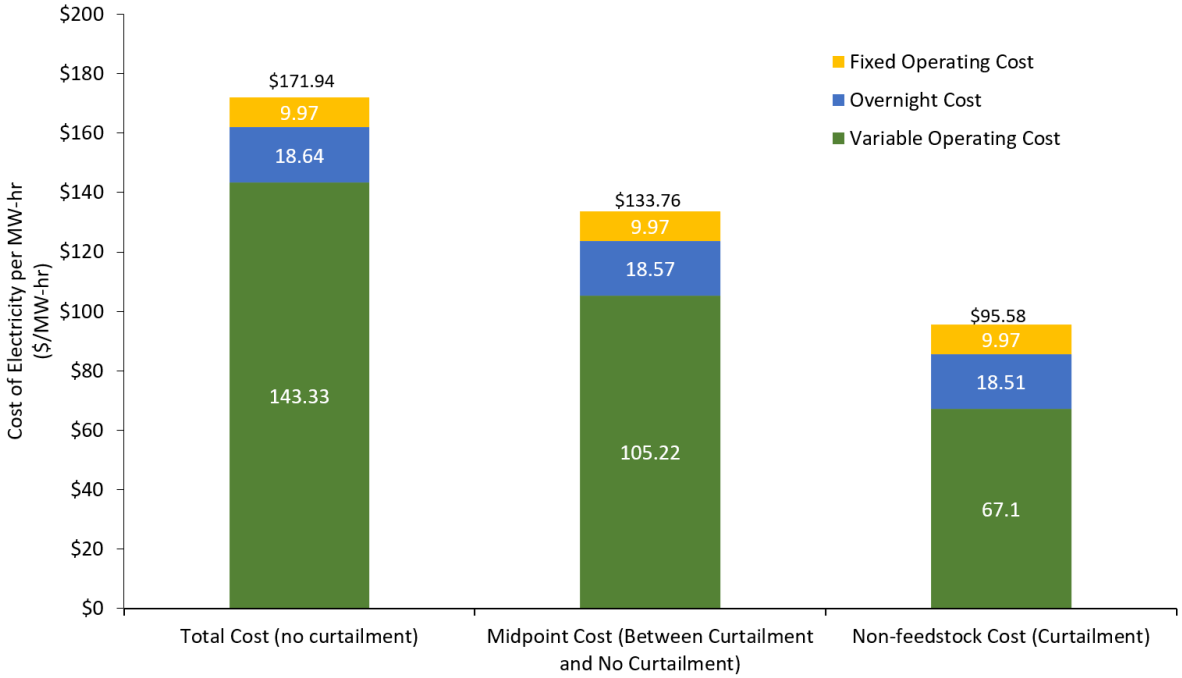

Figure 4-24: COE Comparison in 2020 for 50 MW RH_2-Fueled SOFC-GT Hybrid Varying Curtailment Levels

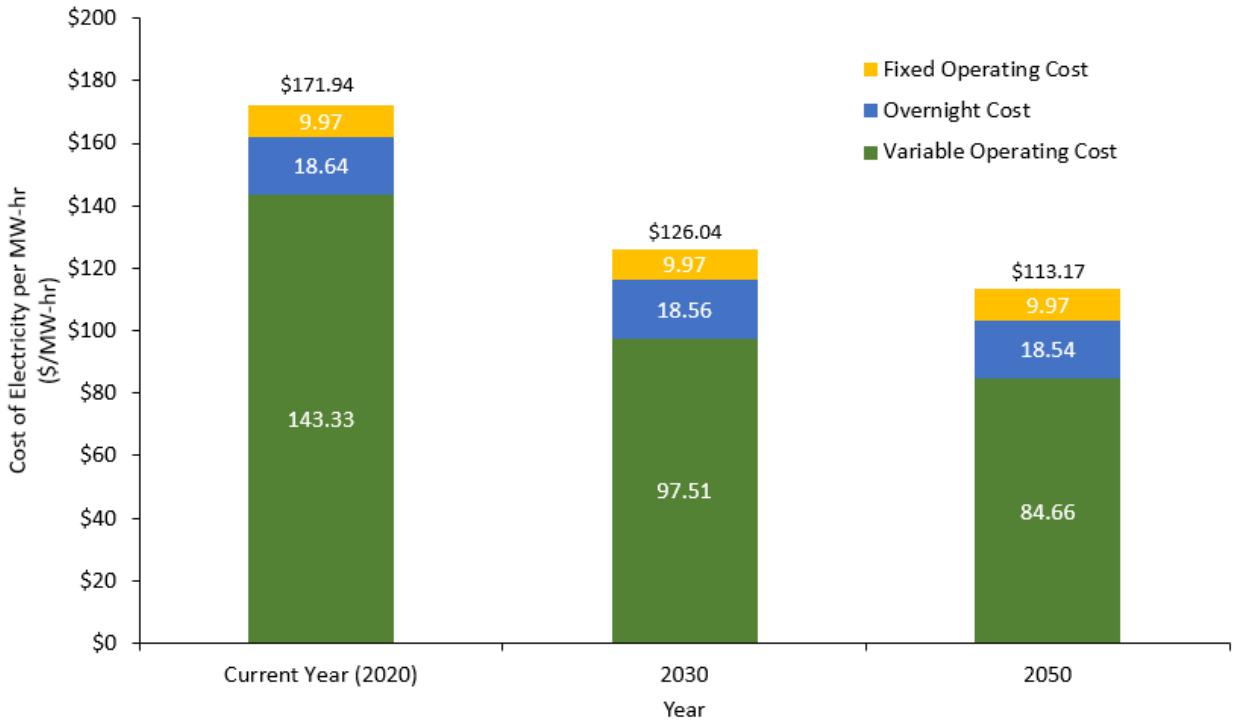

Figure 4-25: Comparison of COE for 50 MW RH_2-Fueled SOFC-GT Hybrid in Different Years

Table 4-25: Summary of Economic Analysis for 50 MW RH_2-Fueled SOFC-GT Hybrid

Total Plant Cost		$80,626,000
	Specific Plant Cost	$1,600/kW
	Total SOFC Cost	$52,346,000
	Total GT Cost	$13,176,000
	Gas Processing Equipment Cost	$5,943,000
	Heat Recuperation Cost	$1,568,000
	Auxiliary Plant Equipment Cost	$7,593,000
Annual Fixed Operating Cost		$3,962,000/year
	Operating Labor Cost	$1,163,000/year
	Maintenance Labor Cost	$716,000/year
	Administrative & Support Labor Cost	$470,000/year
	Property Tax & Insurance	$1,613,000/year
Annual Variable Operating Cost		$56,977,000/year

	Maintenance Material Cost	$1,197,000/year
	Fuel Cell Replacement Cost	$788,000/year
	Renewable Hydrogen Feedstock Cost	$54,992,000/year
Land Cost		$579,000
COE		
	2020	
	No curtailment	$171.94/MWh
	Between curtailment and no curtailment	$133.76/MWh
	Curtailment	$95.58/MWh
	Future Years	
	2030	$126.04/MWh
	2050	$113.17/MWh

Summary of 50 MW Stationary Applications

The 50 MW stationary power plant utilizes the anode eductor configuration based on the analysis of 10 MW plant. The power output is 50.42 MW at 70.22%-LHV efficiency. The specific plant cost is $1,600/kWh with a COE at $171.94/MWh without any curtailment. The COE in midpoint case between curtailment and no curtailment is $133.76/MWh, and the COE for curtailment is $95.58/MWh. The COE is expected to decrease to $126.04/MWh in 2030 and $113.17/MWh in 2050, both assuming no curtailment. Table 4-26 shows the summary of results and economic performance for the 50 MW stationary power plant.

Table 4-26: Summary of 50 MW RH_2-Fueled SOFC-GT Hybrid

Thermodynamic Performance		
	Configuration	Anode Supported
	AC Power Output (MW_{AC})	50.42
	Plant Efficiency, % LHV	70.22
SOFC		
	AC Power Output (MW_{AC})	38.21
	Operating Voltage (V)	0.82

Operating Temperature (°C)	700
Overall Fuel Utilization (%)	82.87
Single Pass Fuel Utilization (%)	68.94
Air Utilization (%)	29.92
Max. Local Temperature Gradient (K/cm)	15.00
Maximum Inlet-Outlet Temperature Difference (K)	150.00
GT (Custom Built)	
AC Power Output (MW_{AC})	13.90
Compressor Pressure Ratio (bar/bar)	5.30
Turbine Inlet Temperature (°C)	1109
Economic Performance	
Specific Plant Cost ($/kW)	1,600
Total Plant Cost ($)	80,626,000
Fixed Operating and Maintenance Cost ($/year)	3,962,000
Annual Variable Operating Cost ($/year)	56,977,000
Land Cost ($)	579,000
COE in 2020, no curtailment ($/MWh)	171.94
COE in 2020, midpoint ($/MWh)	133.76
COE in 2020, curtailment ($/MWh)	95.58
COE in 2030, no curtailment ($/MWh)	126.04
COE in 2050, no curtailment ($/MWh)	113.17

4.2.3. Comparison and Summary of Stationary Applications

Anode eductor is the best configuration to build the 10 MW and 50 MW power plant. Note that the 50 MW has slightly higher LHV-efficiency because of the higher efficiency of the components including the fuel compressors and the GT. The SOFC in both cases are operated under the same temperature and pressure, and the maximum temperature gradients are the same for both cases. Table 4-27 below shows the simulation results for 10 MW and 50 MW stationary power plant based on anode eductor configuration.

Table 4-27: Configuration Summary in 10 MW and 50 MW RH_2-Fueled SOFC-GT Hybrids

Overall Performance		10 MW	50 MW
	AC Power Output (MW_{AC})	10.00	50.42
	LHV Electrical Efficiency (%)	68.50	70.22
	Structure	Anode Recycle	
SOFC			
	AC Power Output (MW_{AC})	7.78	38.21
	Number of Stacks	150	736
	Fuel Flowrate (kg/hr)	439	2,158
	Operating Voltage (V)	0.82	
	Operating Temperature (°C)	700	
	Operating Pressure (bar)	5.00	
	Overall Fuel Utilization (%)	82.92	82.87
	Single Pass Fuel Utilization (%)	69.11	68.94
	Air Utilization (%)	29.52	29.92
	Local Temperature Gradient (K/cm)	14.10	14.28
	Maximum Local Temperature Gradient (K/cm)	15.00	
	Global Temperature Gradient (K)	149.44	149.86
	Maximum Global Temperature Gradient (K)	150.00	
GT			
	AC Power Output (MW_{AC})	2.62	13.90
	Air Flowrate (kg/hr)	42,500	206,019
	Compressor Pressure Ratio	5.30	
	Turbine Inlet Temperature (°C)	1,103	1,109
	Compressor Polytropic Efficiency (%)	84.85	85.60
	Compressor Mechanical Efficiency (%)	98.04	98.15
	Expander Polytropic Efficiency (%)	83.31	85.70
	Expander Mechanical Efficiency (%)	98.04	99.00
Fuel Compressors			
	Compressor I Polytropic Efficiency (%)	70.00	72.00

	Compressor I Mechanical Efficiency (%)	89.00	90.00
	Compressor II Polytropic Efficiency (%)	67.00	71.00
	Compressor II Mechanical Efficiency (%)	89.00	89.50
Heat Recuperators			
	Air-Preheater Effectiveness (%)	89.68	90.44
	Fuel-Preheater Effectiveness (%)	90.32	90.27
Exhaust			
	Flue Gas Temperature (°C)	312	306
	Flue Gas Flowrate (kg/hr)	42,939	208,175

The COE in 2020 for 50 MW scale has around 20% reduction compared to the 10 MW scale. Due to expectation of cheaper RH_2 cost in the future, the COE for a 50 MW scale is expected to be around 25% cheaper than the 10 MW scale in 2030. In 2050, the difference between them would be around 30%. Even though the TPC in 50 MW scale is more than four times higher than the 10 MW scale, the specific plant cost comes out to be around 20% cheaper in the 50 MW compared to the 10 MW scale due to economics of scale. The AFOC in 50 MW scale is around double than that of the 10 MW scale due to higher maintenance cost, support and property taxes. However, both plants have the same operating labor cost. The AVOC is more than four times higher in the 50 MW scale due to the significantly higher amount of fuel flowrate and thus more expensive fuel cost. The land cost in 50 MW scale is almost five times higher than 10 MW scale. Table 4-28 summaries the economic performance for 10 MW and 50 MW. Figure 4-26 shows the COE comparison in 2020 by varying levels of curtailment. Figure 4-27 show the COE comparison in future years considering no curtailment.

Table 4-28: Economic Performance in 10 MW and 50 MW RH_2-Fueled SOFC-GT Hybrids

	10 MW	50 MW
Total Plant Cost	$19,671,000	$80,626,000
Specific Plant Cost	$1,966/kW	$1,600/kW
Total SOFC Cost	$10,651,000	$52,346,000
Total GT Cost	$4,195,000	$13,176,000
Gas Processing Equipment Cost	$732,000	$5,943,000

	Heat Recuperation Cost	$1,496,000	$1,568,000
	Auxiliary Plant Equipment Cost	$2,597,000	$7,593,000
Annual Fixed Operating Cost		$2,063,000/year	$3,962,000/year
	Operating Labor Cost	$1,163,000/year	
	Maintenance Labor Cost	$173,000	$716,000
	Administrative & Support Labor Cost	$334,000	$470,000
	Property Tax & Insurance	$393,000	$1,613,000
Annual Variable Operating Cost		$11,637,000/year	$56,977,000/year
	Maintenance Material Cost	$289,000	$1,197,000
	Fuel Cell Replacement Cost	$161,000	$788,000
	Renewable Hydrogen Fuel Cost	$11,187,000	$54,992,000
Land Cost	$30.89/sq-meter	$124,000	$579,000
COE			
	2020, no curtailment	$197.06/MWh	$171.94/MWh
	2020, midpoint	$157.91/MWh	$133.76/MWh
	2020, curtailment	$118.76/MWh	$95.58/MWh
	2030, no curtailment	$150.00/MWh	$126.04/MWh
	2050, no curtailment	$136.79/MWh	$113.17/MWh

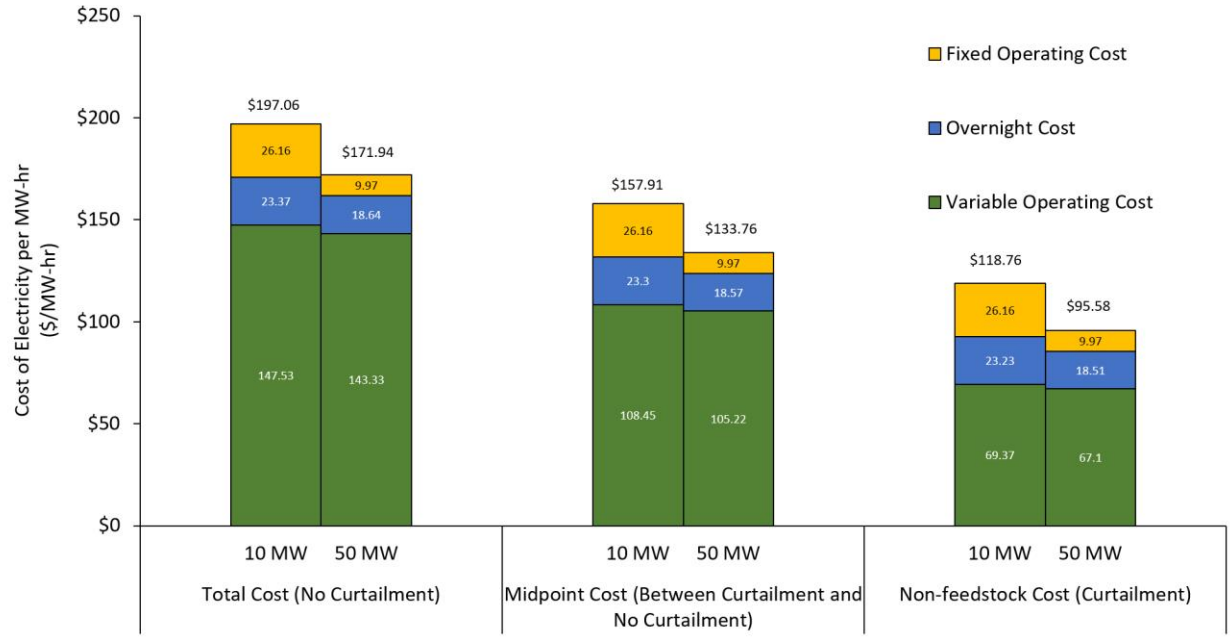

Figure 4-26: COE Comparison in 2020 for 10 MW and 50 MW RH_2-Fueled SOFC-GT Hybrid Varying Curtailment Levels

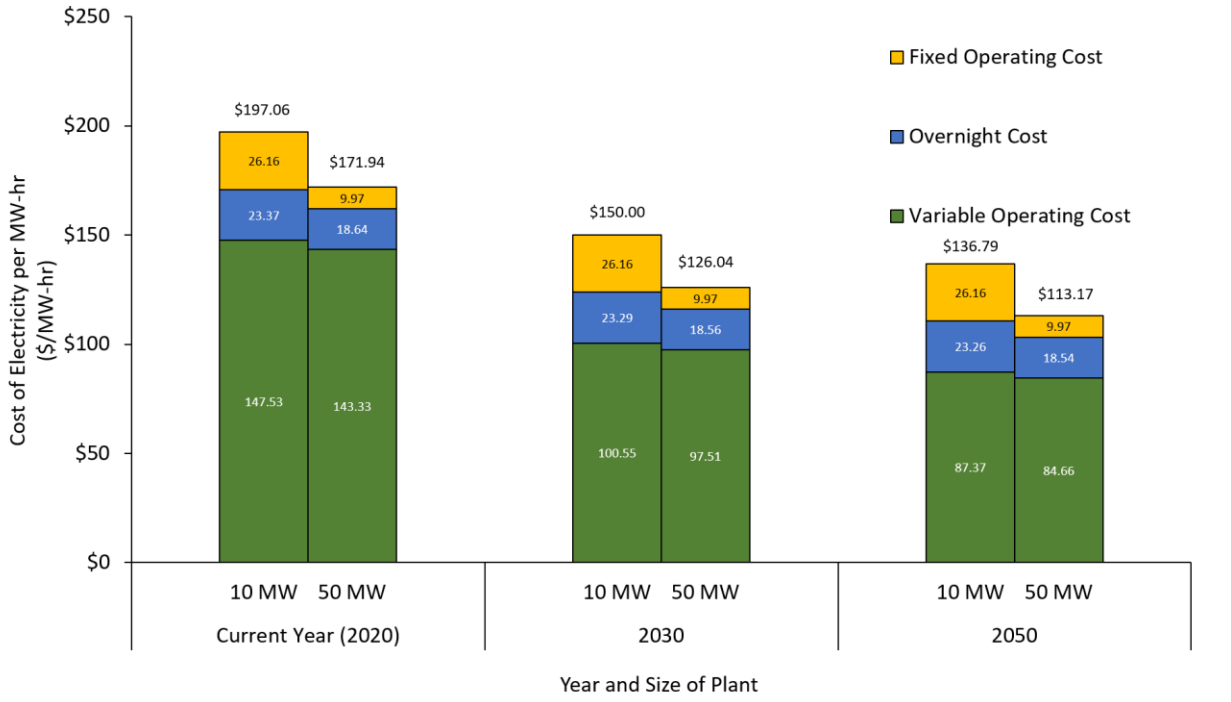

Figure 4-27: Comparison of COE for 10 MW and 50 MW RH_2-Fueled SOFC-GT Hybrid in Different Years

4.3. Development of Mobile Scale Applications

In this thesis, long-haul locomotives and tugboats are selected for analysis. For details regarding why these two applications are selected, please refer to the Mobile Applications from the Background section above.

4.3.1. 3.5 MW SOFC-GT Hybrid Systems for Long-Haul Locomotives

While the SOFC-GT hybrid technology has, in addition to a high thermal efficiency, the advantage of alleviating the environmental pollution associated with traditional diesel engines for mobile applications, the SOFC is comprised of ceramic materials and operated under high temperatures which requires, as a result, controlled ramping to avoid premature degradation. In contrast to the Proton Exchange Membrane Fuel Cell which can accommodate rapid ramp rates and on/off cycles, a SOFC is widely assumed to be best suited for operating at constant or near constant load. As a result, for the wide dynamic range associated with mobile applications, the design of a SOFC-GT power block is a major challenge. An immediate advantage of the SOFC-GT configuration (versus a standalone SOFC) is for the steady-state power to be provided by the SOFC and the transient power provided by the GT.

To maintain the natural gas in a liquid state, the LNG tank must be well insulated to minimize the transfer of heat from the surroundings to the liquid [66][67]. As heat is transferred, liquid evaporates, the vapor pressure inside the tank increases, and venting (i.e., release the vapor to the atmosphere) may be required to avoid exceeding the maximum rated pressure of the tank [68]. When vapor or liquid is extracted from the tank to fuel the SOFC/GT, the temperature (and pressure) of the mixture will decrease due to the extraction of energy from the liquid to generate vapor. To manage the pressure from falling below the minimum rated pressure of the tank, a LNG pump is typically used to convey liquid through a warming vaporizer and convey the vapor back to the tank to maintain the desired pressure [69]. For the purposes of this study, the pressure of the LNG tank was assumed to be maintained between 20 psig and 150 psig [70].

To operate the eductor, the NG needs to be introduced as a vapor and at an elevated pressure. To this end, two configurations were evaluated: (1) one consisting of vaporizing the LNG first by exchanging heat with the GT inlet air, and then to increase the pressure of the vapor using a compressor, and (2) one consisting of increasing the pressure of the LNG first by

employing a liquid pump and then vaporizing the pressurized liquid by exchanging heat with the GT inlet air. The GT exhaust heat may also be utilized to provide any additional heat required. The advantage of using the GT inlet air to supply the heat for the vaporization is to reduce the GT compression work and thus increase the overall system thermal efficiency while at the same time reducing the size of the compressor.

The analyses were conducted at three vapor pressures: 20 psig, 150 psig, and a midpoint pressure of 85 psig. The two configurations were first evaluated at 20 psig. From these results, the configuration with the higher power output/electrical efficiency was selected and the thermal performance established at the midpoint pressure of 85 psig and at the maximum pressure of 150 psig. The overall system configurations are described in more detail in the following subsections.

Configurations and Results

Fuel Compressor Configuration. Figure 4-28 shows the compressor configuration at the 20 psig LNG pressure. The GT inlet air first exchanges its heat to vaporize the LNG before it enters the GT compressor. The GT compressor discharged air is then preheated against the depleted air exhausting the SOFC cathode to the SOFC operating temperature at 700 °C. The preheated air enters the cathode side of the SOFC while the depleted air leaving the recuperator enters the combustor. The vaporized fuel is then compressed and then enters the eductor to recycle a fraction of the anode exhaust gas to the SOFC as in the previously described RH2-fueled case with anode recycle in the stationary applications. The exhaust gas from the eductor then enters the pre-reformer followed by the SOFC. In addition to increasing the overall fuel utilization as in the RH_2-fueled case, the recycled anode gas in these LNG cases provides the H_2O required for the reforming reactions and avoids carbon deposition on catalytic surfaces. The H_2 in the recycle, which is produced by reforming reactions, also converts the unsaturated and higher HC to saturated HC and CH_4 in the pre-reformer. The remaining anode exhaust gas enters the GT combustor. In this configuration, the GT exhaust flue gas emits directly without any heat recovery because it does not provide useful thermodynamic utility. Also, this simplifies the system configuration by having fewer heat exchangers and reduced system cost while maintaining a ultra-low footprint [71][72][73].

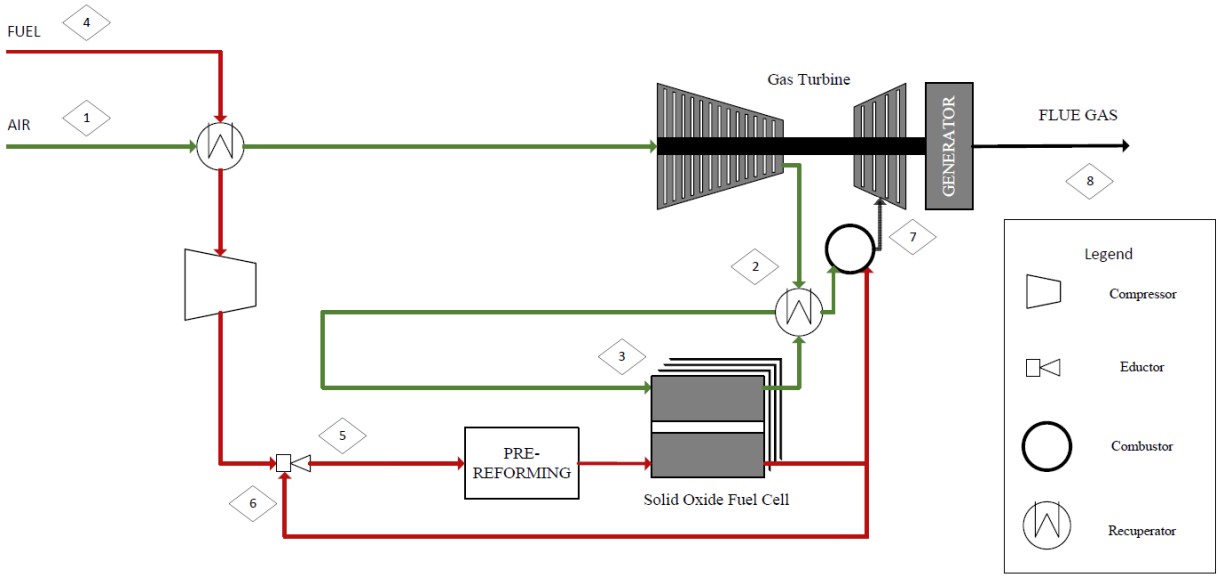

Figure 4-28: Fuel Compressor Configuration for 3.5 MW LNG-Fueled SOFC-GT Locomotive

The power output is 3.49 MW at 67.03%-LHV efficiency. Table 4-29 summarizes the overall system performance for the fuel compressor case at 20 psig LNG pressure. Note that the goal for the SOFC local thermal gradient is to keep below 15 K/cm. However, for the mobile applications at 3.5 MW power output, the SOFC local thermal gradient is slightly higher than the goal from the simulation results. On the other hand, the SOFC global thermal gradient is lower than the limit at 150 K. Therefore, overall thermal gradients are still within an acceptable range to protect the SOFC from degradation.

Table 4-29: Fuel Compressor Results for 3.5 MW LNG-Fueled SOFC-GT Locomotive

Performance		
	AC Power Output (MW_{AC})	3.49
	LHV Electrical Efficiency (%)	67.03
SOFC		
	DC Power Output (MW_{DC})	3.69
	AC Power Output (MW_{AC})	3.61
	Inverter Losses (%)	2
	Number of Stacks	102
	Fuel Flowrate (kg/hr)	397

	Operating Voltage (V)	0.82
	Operating Temperature (°C)	700
	Operating Pressure (bar)	5.00
	Overall Fuel Utilization (%)	89.36
	Single Pass Fuel Utilization (%)	81.44
	Air Utilization (%)	48.59
	Local Temperature Gradient (K/cm)	16.33
	Desired Local Temperature Gradient (K)	15.00
	Global Temperature Gradient (K)	144.70
	Maximum Global Temperature Gradient (K)	150.00
GT		
	AC Power Output (kW_{AC})	8.60
	Air Flowrate (kg/hr)	11,987
	Compressor Pressure Ratio	5.30
	Turbine Inlet Temperature (°C)	493
	Compressor Polytropic Efficiency (%)	84.85
	Compressor Mechanical Efficiency (%)	98.04
	Expander Polytropic Efficiency (%)	83.31
	Expander Mechanical Efficiency (%)	98.04
Fuel Compressor		
	AC Power Consumed (kW_{AC})	89.56
	Polytropic Efficiency (%)	66.00
	Mechanical Efficiency (%)	89.00
Heat Recuperators		
	Fuel-Preheater Effectiveness (%)	64.21
	Cathode-off Effectiveness (%)	77.45
Exhaust		
	Flue Gas Temperature (°C)	309
	Flue Gas Flowrate (kg/h)	12,346
Environmental Performance		
	NOx, ppmV dry (15% O_2 corrected) [71]	< 1

CO, ppmV dry (15% O_2 corrected) [72]	< 1
Unburnt Hydrocarbons, ppmV dry (15% O_2 corrected) [73]	< 1
CO_2 Emissions, kg/MWh	302.84

Fuel Pump Configuration. Figure 4-29 below shows the configuration of this fuel pump case. The LNG is pressurized in a pump and the majority is vaporized by a heat exchanger against the GT inlet air. There is a small amount of LNG bypasses this recuperator and combined with the vaporized fuel leaving it. The combined fuel then goes to the second recuperator against the GT exhaust where the fuel is fully vaporized. The reason to have a bypass stream is to ensure the cooled GT inlet air remains safely above 0 °C at 4 °C to avoid icing in the GT compressor inlet. The second recuperator locates in the GT exhaust is designed with an effectiveness of 90% and preheats the fuel to a temperature of around 274 °C. The preheated fuel enters the eductor to recycle a fraction of the anode exhaust gas to the SOFC as in the previously described fuel compressor case. In addition to increasing the overall fuel utilization and temperature of the anode inlet gas, the recycled anode gas provides the H_2O required for the reforming reactions and also to avoid carbon deposition on the catalytic surfaces, while the H_2 in the recycle converts the unsaturated and higher HC to saturated HC and CH_4 in the pre-reformer. The exhaust gas from the eductor then enters the pre-reformer followed by the SOFC while the remaining anode exhaust gas enters the GT combustor. The GT compressor discharges air as in the fuel compressor case is preheated against the depleted air exhausting the SOFC cathode to the SOFC operating temperature of 700 °C and then supplied to the cathode side of the SOFC, while the depleted air leaving the recuperator enters the GT combustor. In this configuration, the exhaust flue gas from the GT enters the atmosphere after providing the additional heat required for completing the fuel vaporization. Therefore, a recuperator is utilized in the GT exhaust stream.

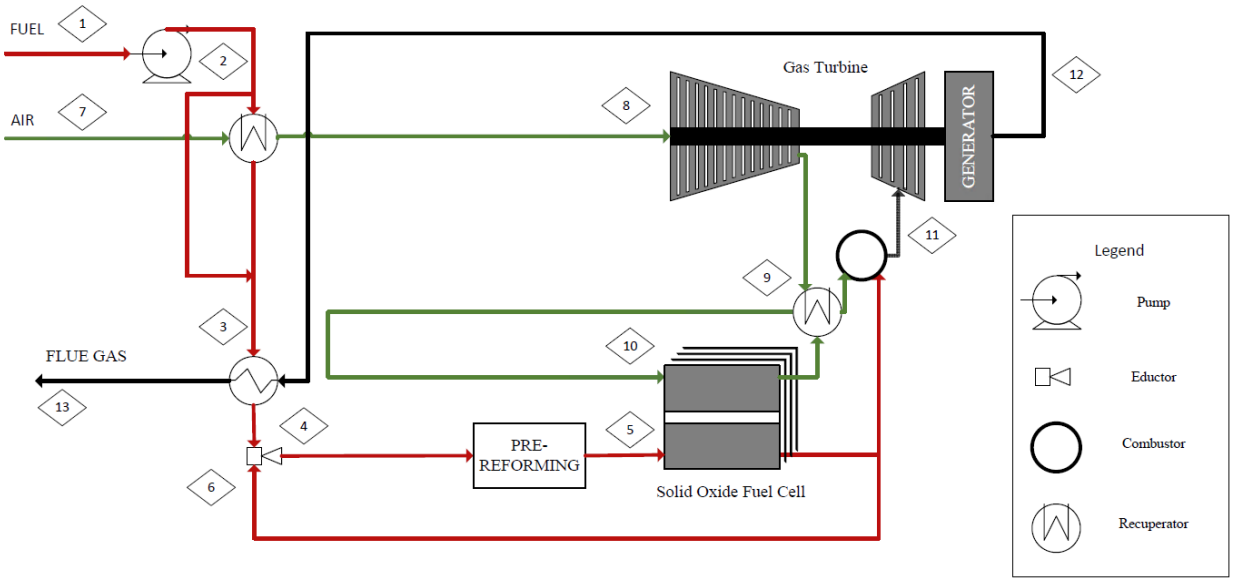

Figure 4-29: Fuel Pump Configuration for 3.5 MW LNG-Fueled SOFC-GT Locomotive

The power output is 3.50 MW at 68.65%-LHV efficiency.

Table 4-30 summarizes the overall system performance for the pump case at the 20 psig LNG pressure. Similar as the fuel compressor configuration, the SOFC local thermal gradient is slightly higher than the goal at 15 K/cm. However, the SOFC global thermal gradient is lower than the goal at 150 K which makes an overall thermal gradient still within an acceptable range to prevent it from degradation.

Table 4-30: Fuel Pump Results for 3.5 MW LNG-Fueled SOFC-GT Locomotive

Performance		
	AC Power Output (MW_{AC})	3.50
	LHV Electrical Efficiency (%)	68.65
SOFC		
	DC Power Output (MW_{DC})	3.62
	AC Power Output (MW_{AC})	3.55
	Inverter Losses (%)	2
	Number of Stacks	100

	Fuel Flowrate (kg/h)	389
	Operating Voltage (V)	0.82
	Operating Temperature (°C)	700
	Operating Pressure (bar)	5.00
	Overall Fuel Utilization (%)	89.49
	Single Pass Fuel Utilization (%)	81.69
	Air Utilization (%)	48.62
	Local Temperature Gradient (K/cm)	16.44
	Desired Local Temperature Gradient (K)	15.00
	Global Temperature Gradient (K)	144.52
	Maximum Global Temperature Gradient (K)	150.00
GT		
	AC Power Output (kW_{AC})	1.70
	Air Flowrate (kg/h)	11,726
	Compressor Pressure Ratio	5.30
	Turbine Inlet Temperature (°C)	496
	Compressor Polytropic Efficiency (%)	84.85
	Compressor Mechanical Efficiency (%)	98.04
	Expander Polytropic Efficiency (%)	83.31
	Expander Mechanical Efficiency (%)	98.04
Fuel Pump		
	AC Power Consumed (kW_{AC})	1.41
	Thermodynamic Efficiency (%)	60.00
	Mechanical Efficiency (%)	89.00
Heat Recuperators		
	GT Inlet Air-LNG Effectiveness (%)	75.93
	GT Exhaust-LNG Effectiveness (%)	90.00
	Cathode-off Effectiveness (%)	77.08
Exhaust		
	Flue Gas Temperature (°C)	285
	Flue Gas Flowrate (kg/hr)	12,115

Environmental Performance		
	NOx, ppmV dry (15% O_2 corrected) [71]	< 1
	CO, ppmV dry (15% O_2 corrected) [72]	< 1
	Unburnt Hydrocarbons, ppmV dry (15% O_2 corrected) [73]	< 1
	CO_2 Emissions, kg/MWh	295.67

Summary of Configuration and Results

Table 4-31 shows the summary of case comparisons. For the same power output, the pump case has a higher LHV efficiency compared to the compressor case because the pump requires a lower amount of power than the compressor leading to a higher overall thermal efficiency. As mentioned from Compressor and Pump in the background section, the volumetric flowrate for a gas in the compressor is much higher than that of a liquid in a pump for a given mass flowrate, which requires a much higher net work. Despite the GT inlet air in the pump case being held at a higher temperature (i.e., above the freezing temperature to avoid icing at the GT inlet), the overall system efficiency is higher for the pump case. Also, the overall system cost is expected to be lower for the pump case. Even though it has an extra heat recuperator, pumps are typically cheaper than compressors while the specific power output (i.e., net MW per unit air flowrate) is higher for the pump case making the associated equipment smaller. The resulting reduction in cost is expected to more than offset the cost of an extra recuperator used in the pump case. Based on these attributes, the pump case is selected for further analysis at the other two LNG storage pressures.

Table 4-31: Summary of 3.5 MW LNG-Fueled SOFC-GT Locomotive at 20 psig

Configuration		Compressor	Pump
	AC Power Output (MW_{AC})	3.49	3.50
	LHV Electrical Efficiency (%)	67.03	68.65
SOFC			
	DC Power (MW_{DC})	3.69	3.62
	AC Power (MW_{AC})	3.61	3.55
	Inverter Losses (%)	2	
	Number of Stacks	102	100

	Fuel Flowrate (kg/h)	397	389
	Operating Voltage (V)	0.82	
	Operating Temperature (°C)	700	
	Operating Pressure (bar)	5.00	
	Overall Fuel Utilization (%)	89.36	89.49
	Single Pass Fuel Utilization (%)	81.44	81.69
	Air Utilization (%)	48.59	48.62
	Local Temperature Gradient (K/cm)	16.33	16.44
	Desired Local Temperature Gradient (K/cm)	15.00	
	Global Temperature Gradient (K)	144.70	144.52
	Maximum Global Temperature Gradient (K)	150.00	
GT			
	AC Power (kW_{AC})	8.60	1.70
	Air Flowrate (kg/hr)	11,987	11,726
	Compressor Pressure Ratio	5.30	
	Turbine Inlet Temperature (°C)	493	496
	Compressor Polytropic Efficiency (%)	84.85	
	Compressor Mechanical Efficiency (%)	98.04	
	Expander Polytropic Efficiency (%)	83.31	
	Expander Mechanical Efficiency (%)	98.04	
Fuel Compressor/Pump			
	AC Power Consumed (kW_{AC})	89.56	1.41
	Polytropic/Pump Efficiency (%)	66.00	60.00
	Mechanical/Driver Efficiency (%)	89.00	
Heat Recuperators			
	GT Inlet Air-LNG Effectiveness (%)	64.21	75.93
	GT Exhaust-LNG Effectiveness (%)	N/A	90.00
	Cathode-off Effectiveness (%)	77.45	77.08
Exhaust			
	Flue Gas Temperature (°C)	309	285
	Flue Gas Flowrate (kg/h)	12,346	12,115

Environmental Performance		
NOx, ppmV dry (15% O_2 corrected) [71]	< 1	
CO, ppmV dry (15% O_2 corrected) [72]	< 1	
Unburnt Hydrocarbons, ppmV dry (15% O_2 corrected) [73]	< 1	
CO_2 Emissions, kg/MWh	302.84	295.67

Summary of Long-Haul Locomotives

All three cases are done in the pump configuration and inlet conditions such as the air flowrate, fuel flowrate, and the size of the SOFC are all constant across the three cases. Note that the LHV efficiency increases slightly from the minimum to maximum pressure condition. However, the local temperature gradient is slightly higher for the maximum pressure condition than the minimum pressure condition. Also, the midpoint pressure has the same LHV efficiency compared with the minimum pressure even though the midpoint pressure is higher. Therefore, it indicates that the higher efficiency is due to the difference in SOFC thermal gradient and is independent of the LNG container pressure. Table 4-32 shows the performance parameters for this long-haul locomotive application with the pump configuration.

Table 4-32: Summary of 3.5 MW LNG-Fueled SOFC-GT Locomotive

Container Condition	Minimum Pressure	Midpoint Pressure	Maximum Pressure
Container Pressure (psig)	20	85	150
AC Power Output (MW_{AC})	3.50		
LHV Electrical Efficiency (%)	68.65		68.68
Structure	Anode Recycle		
SOFC			
DC Power Output (MW_{DC})	3.62		
AC Power Output (MW_{AC})	3.55		
Inverter Loss (%)	2		
Number of Stacks	100		

Fuel Flowrate (kg/h)	389		
Operating Voltage (V)	0.82		
Operating Temperature (°C)	700		
Operating Pressure (bar)	5.00		
Overall Fuel Utilization (%)	89.49		89.55
Single Pass Fuel Utilization (%)	81.69		81.79
Air Utilization (%)	48.62		48.64
Local Temperature Gradient (K/cm)	16.44		16.50
Desired Local Temperature Gradient (K/cm)	15.00		
Global Temperature Gradient (K)	144.52		144.46
Maximum Global Temperature Gradient (K)	150.00		

GT

Condition	Custom Built Micro-GT		
AC Power Output (kW_{AC})	1.70	1.71	1.47
Air Flowrate (kg/h)	11,726		
Compressor Pressure Ratio	5.30		
Turbine Inlet Temperature (°C)	496		
Compressor Polytropic Efficiency (%)	84.85		
Compressor Mechanical Efficiency (%)	98.04		
Expander Polytropic Efficiency (%)	83.31		
Expander Mechanical Efficiency (%)	98.04		

Pump

Power Consumed (kW_{AC})	1.41	1.29	1.11
Pump Efficiency (%)	60.00		
Driver Efficiency (%)	89.00		

Heat Recuperators

Air-LNG Effectiveness (%)	75.93	72.74	50.54
GT Exhaust-LNG Effectiveness (%)	90.00		
Cathode Off Gas-Air Effectiveness (%)	77.08		77.00

Exhaust

Flue Gas Temperature (°C)	285	286	287
Flue Gas Flowrate (kg/h)	12,115		
Environmental Performance			
NOx, ppmV dry (15% O_2 corrected) [71]	<1		
CO, ppmV dry (15% O_2 corrected) [72]	<1		
Unburnt HC, ppmV dry (15% O_2 corrected) [73]	<1		
CO_2 Emissions, kg/MWh	295.67	295.69	295.53

4.3.2. 3.5 MW SOFC-GT Hybrid Systems for Tugboats

The selected configuration for a 3.5 MW LNG-fueled system for tugboats is also based on the fuel pump configuration, due to its advantages over the fuel compression configuration pointed out previously. A specialized GT air filter for marine applications which has higher pressure drop needs to be used to remove the salt content from the ambient air. Otherwise, the salt can trap in the compressor blades and reduce the aerodynamic efficiency in addition to causing corrosion. A pressure drop of 0.06 bar is selected in tugboat applications, which has twice the value of that of conventional air filter.

Configuration and Results

As depicted in Figure 4-30 below, the LNG is pressurized in a pump and a majority is vaporized by heat exchanger with the GT inlet air. The only difference from the locomotive application is preheat temperature of the second fuel heater which, for the tugboat, is 270 ℃ due to the pressure drop associated with the inlet filter.

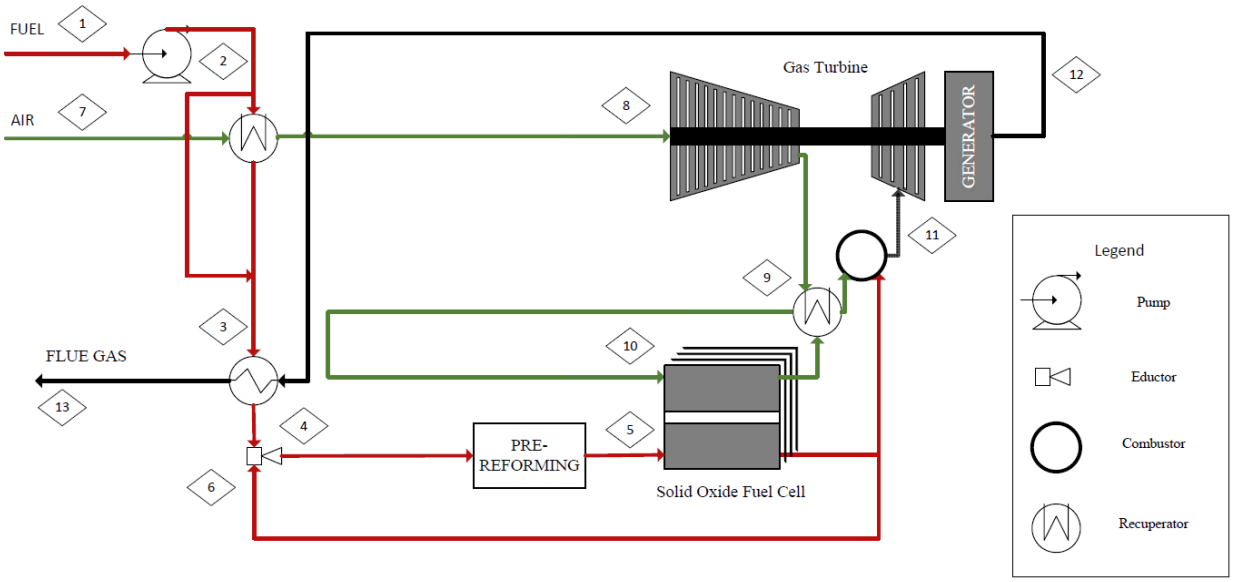

Figure 4-30: Fuel Pump Configuration for 3.5 MW LNG Hybrid Tugboat

Table 4-33 below shows the performance parameters for this tugboat application at the three LNG container pressures. Note that the power output/LHV efficiency increases slightly from the minimum to maximum pressure condition. However, as mentioned previously in the locomotive case, the local temperature gradient is slightly higher for the maximum pressure condition than the minimum pressure condition. Therefore, the difference in efficiency/power output is due to the difference in local temperature gradient and is independent of the LNG container pressure. Also note that the GT power outputs are negative, which indicates the GT consumes more power for the GT compressor than producing power from the GT expander.

Table 4-33: Summary of 3.5 MW LNG-Fueled SOFC-GT Tugboats

Container Condition	Minimum Pressure	Midpoint Pressure	Maximum Pressure
Container Pressure (psig)	20	85	150
AC Power Output (MW_{AC})	3.50		3.51
LHV Electrical Efficiency (%)	68.54	68.55	68.56
Structure	Anode Recycle		
SOFC			

DC Power Output (MW_{DC})	3.66		
AC Power Output (MW_{AC})	3.59		
Inverter Loss (%)	2		
Number of Stacks	103		
Fuel Flowrate (kg/h)	390		
Operating Voltage (V)	0.82		
Operating Temperature (°C)	700		
Operating Pressure (bar)	5.00		
Overall Fuel Utilization (%)	90.44	90.45	90.46
Single Pass Fuel Utilization (%)	83.30	83.32	83.35
Air Utilization (%)	48.16	48.17	
Local Temperature Gradient (K/cm)	16.69	16.70	16.71
Desired Local Temperature Gradient (K/cm)	15.00		
Global Temperature Gradient (K)	140.35	140.33	140.30
Maximum Global Temperature Gradient (K)	150.00		

GT

Condition	Custom Built Micro-GT		
AC Power Output (kW_{AC})	-34.36	-34.34	-34.26
Air Flowrate (kg/h)	11,973		
Compressor Pressure Ratio	5.60		
Turbine Inlet Temperature (°C)	491		
Compressor Polytropic Efficiency (%)	84.85		
Compressor Mechanical Efficiency (%)	98.04		
Expander Polytropic Efficiency (%)	83.31		
Expander Mechanical Efficiency (%)	98.04		

Pump

Power Consumed (kW_{AC})	1.40	1.27	1.09
Pump Efficiency (%)	60.00		
Driver Efficiency (%)	89.00		

Heat Recuperators

Air-LNG Effectiveness (%)	75.91	72.72	62.28
GT Exhaust-LNG Effectiveness (%)	90.00		
Cathode Off Gas-Air Effectiveness (%)	76.41	76.40	76.37
Exhaust			
Flue Gas Temperature (°C)	282	283	285
Flue Gas Flowrate (kg/h)	12,363		
Environmental Performance			
NOx, ppmV dry (15% O_2 corrected) [71]	<1		
CO, ppmV dry (15% O_2 corrected) [72]	<1		
Unburnt HC, ppmV dry (15% O_2 corrected) [73]	<1		
CO_2 Emissions, kg/MWh	296.16	296.13	296.09

4.3.3. Comparison and Summary of Mobile Scale Applications

Long-haul locomotives are selected to be the land-based mobile application while the tugboats are selected to be the marine-based mobile application. A screening analysis was first conducted in the long-haul locomotives for two configurations at the container minimum pressure at 20 psig, include fuel compressors and fuel pumps. Fuel pump configuration is determined to have a better LHV efficiency, and thus the locomotives and tugboats would be built based on this configuration except that the GT air filter in tugboat has double the pressure drop compared to land-based applications because of desalting purposes. The fuel for both land and marine applications are selected to utilize LNG, and an investigation has been done based on different LNG pressures include minimum, midpoint and maximum pressures. Same as in the stationary power applications, the mobile scale applications utilize anode recycle configuration.

Table 4-34 shows the summary of mobile applications. Although a higher pressure drop GT air filter is employed for the tugboats, the LHV efficiencies only reduce by about 0.1% compared with locomotives. This indicates that a selected pressure drop for the GT marine air filter maintains a good balance between filtering contaminants and efficiencies.

Table 4-34: Summary of 3.5 MW LNG-Fueled Mobile Applications

Applications	Locomotives			Tugboats		
Container Pressures (psig)	20	85	150	20	85	150
AC Power Output (MW_{AC})	3.50					3.51
LHV Electrical Efficiency (%)	68.65		68.68	68.54	68.55	68.56
Structure	Anode Recycle					
SOFC						
DC Power Output (MW_{DC})	3.62			3.66		
AC Power Output (MW_{AC})	3.55			3.59		
Inverter Loss (%)	2					
Number of Stacks	100			103		
Fuel Flowrate (kg/h)	389			390		
Operating Voltage (V)	0.82					
Operating Temperature (°C)	700					
Operating Pressure (bar)	5.00					
Overall Fuel Utilization (%)	89.49		89.55	90.44	90.45	90.46
Single Pass Fuel Utilization (%)	81.69		81.79	83.30	83.32	83.35
Air Utilization (%)	48.62		48.64	48.16	48.17	
Local Temperature Gradient (K/cm)	16.44		16.50	16.69	16.70	16.71
Desired Local Temperature Gradient (K/cm)	15.00					
Global Temperature Gradient (K)	144.52		144.46	140.35	140.33	140.30
Maximum Global Temperature Gradient (K)	150.00					
GT						
Condition	Custom Built Micro-GT					
AC Power Output (kW_{AC})	1.70	1.71	1.47	-34.36	-34.34	-34.26
Air Flowrate (kg/h)	11,726			11,973		
Compressor Pressure Ratio	5.30			5.60		
Turbine Inlet Temperature (°C)	496			491		

Compressor Polytropic Efficiency (%)	84.85					
Compressor Mechanical Efficiency (%)	98.04					
Expander Polytropic Efficiency (%)	83.31					
Expander Mechanical Efficiency (%)	98.04					
Pump						
Power Consumed (kW_{AC})	1.41	1.29	1.11	1.40	1.27	1.09
Pump Efficiency (%)	60.00					
Driver Efficiency (%)	89.00					
Heat Recuperators						
Air-LNG Effectiveness (%)	75.93	72.74	50.54	75.91	72.72	62.28
GT Exhaust-LNG Effectiveness (%)	90.00					
Cathode Off Gas-Air Effectiveness (%)	77.08		77.00	76.41	76.40	76.37
Exhaust						
Flue Gas Temperature (°C)	285	286	287	282	283	285
Flue Gas Flowrate (kg/h)	12,115			12,363		
Environmental Performance						
NOx, ppmV dry (15% O_2 corrected) [71]	<1					
CO, ppmV dry (15% O_2 corrected) [72]	<1					
Unburnt HC, ppmV dry (15% O_2 corrected) [73]	<1					
CO_2 Emissions, kg/MWh	295.67	295.69	295.53	296.16	296.13	296.09

5. Summary, Conclusions and Recommendations

5.1. Summary

The SOFC-GT technology is currently the best-known continuous power generation technology that can produce electric power with ultra-high efficiency and virtually zero emission of criteria pollutants. Many research papers employ natural gas for the SOFC-GT hybrid systems, and most of them focus on the reformation strategy, SOFC operating pressure, and recirculation technique. The most efficient SOFC-GT hybrid configuration operates under pressurized conditions and utilizes internal reforming with a pre-reformer.

This thesis consists of two parts. The first discusses the configurations and techno-economic analysis of 10 MW and 50 MW stationary power applications employing renewable hydrogen. The second part discusses the configurations for a 3.5 MW long-haul locomotive and a 3.5 MW tugboat employing liquefied natural gas.

For the stationary power applications, a screening analysis was first performed on the 10 MW stationary SOFC-GT hybrid using anode recirculation, and no cathode recirculation. The anode recirculation using an eductor is determined to be the best configuration for highest efficiency, and thus the 50 MW stationary hybrid employed the same configuration. The 10 MW hybrid exceeds an efficiency of 68%-LHV while on a 50 MW scale efficiency of greater than 70%-LHV is possible. Although SOFCs are modular and cost does not scale well with plant size, savings in traditional-of-plant equipment and plant operation lead to a substantial cost of electricity reduction. The COE for the 10 MW hybrid was reduced from $197.06/MWh in 2020 to $171.94/MWh when moving to a 50 MW scale. If curtailment is considered when purchasing electricity from wind and solar plants, the COE can drop 40% to $118.76/MWh for 10 MW scale and 44% to $95.58/MWh for 50 MW scale in 2020. With advancement in technology and support in government policies, the COE for the 10 MW hybrid is expected to reduce to $150/MWh in 2030 and $126.04/MWh when moving to a 50 MW scale. The COE is expected to further reduce to $136.79/MWh in 2050 for a 10 MW scale and to $113.17/MWh for a 50 MW scale.

For the mobile power applications, a screening analysis is first performed on the 3.5 MW long-haul locomotive SOFC-GT hybrid using fuel pump and a fuel compressor. A fuel pump is determined to be the best configuration and thus is applied for both the locomotive and tugboat

applications for three different LNG container pressures, namely minimum, midpoint and maximum tank pressures at 20, 85 and 150 psig, respectively. The efficiencies are independent of the container pressures and are greater than 68%-LHV for both the 3.5 MW long-haul locomotive and the 3.5 MW tugboat. These efficiencies are very close to the 10 MW stationary application due to the advantage of using the low temperature heat sink associated with the evaporation of the LNG prior to its use in the SOFC, which is expected to greatly increase the overall efficiency.

5.2. Conclusions

For stationary applications:

- The 50 MW stationary application has only 1.72% higher LHV efficiency but 12.7% lower COE in 2020 compared to the 10 MW stationary application.

  Both the 10 MW and 50 MW stationary applications use the same configuration but some of the components including the fuel compressors and GT are slightly more efficient in the 50 MW scale than those of the 10 MW scale. This results into a 50 MW scale efficiency of 70.22%, which is 1.72% higher than the 10 MW scale efficiency of 68.50%. However, this is not so significant compared to its reduction of COE in 2020, which is around a 12.7% reduction from a 10 MW at $197.06/MWh to a 50 MW at $171.94/MWh.

- The COE in 2020 for a 10 MW scale can possibly be reduced by 40% and for a 50 MW scale be reduced by 44% assuming the feedstock cost is near zero during curtailments from wind and solar plants.

  If the cost for purchasing electricity can be near zero during curtailment from wind and solar plants, the COE in 2020 can possibly be reduced by about 40% to $118.76/MWh for a 10 MW scale and by about 44% to $95.58/MWh for a 50 MW scale.

- The COE for a 10 MW plant is expected to decrease by 24% in 2030 and by 31% in 2050. For a 50 MW plant, it is expected to decrease by 27% in 2030 and by 34% in 2050.

  With technological advancement and more deployments for renewable infrastructure, the cost of renewable hydrogen is expected to decrease drastically. For a 10 MW scale, the COE is expected to decrease by 24% from $197.06/MWh to $150.00/MWh in 2030 and by 31% to $136.79/MWh in 2050. Similarly, for a 50 MW

scale, the COE is expected to decrease by 27% from $171.94/MWh to $126.04/MWh and by 34% to $113.17/MWh in 2050.

For mobile applications:

- The use of a low temperature heat sink associated with the evaporation of LNG significantly increases the overall efficiency.

  LNG stored at cryogenic temperatures needs to be in vapor form and at a pressure high enough to operate the eductor. The advantage of using the GT inlet air to supply the heat for the LNG vaporization is that it reduces the GT compression work and thus the overall system thermal efficiency while at the same time reducing the size of the compressor. In addition, GT exhaust heat may also be utilized to provide any additional heat required for vaporization, thus reducing the amount of heat rejection and thus improving the system efficiency. It is shown that a 3.5 MW hybrid utilizing LNG in this configuration can reach about the same LHV efficiencies compared with the 10 MW RH_2 stationary hybrid.

- Utilizing a fuel pump is more efficient than utilizing a fuel compressor when applicable.

  From a thermodynamic perspective, putting in work for a gas result in a heat addition, and gas temperature increases with pressure increases. On the other hand, putting in work for a liquid result in a change of volume, but temperature stays constant with pressure increases. However, the specific volume is much higher in a gas than in a liquid because the volumetric flowrate for a gas is much higher than that of a liquid for a given mass flowrate. Therefore, using a compressor requires significantly higher amount of work input and thus using a pump is always more efficient.

- The LHV efficiencies are independent of the LNG container pressures.

  The LHV efficiencies are almost the same among different container pressures. The small differences in efficiencies are due to the SOFC local thermal gradients, and not directly relate to the change in container pressures.

- Tugboats have almost the same LHV efficiencies compared to the long-haul locomotives even though a higher GT compressor work due to higher pressure drop from marine air filter.

  Although a higher pressure drop GT air filter is employed for the tugboats, the LHV efficiencies only reduce by about 0.1% compared with locomotives. This indicates

that a selected pressure drop for the GT marine air filter maintains a good balance between filtering contaminants and efficiencies.

For both applications:

- Anode recirculation is the most efficient recirculation technique for SOFC-GT hybrid.

  The higher the efficiency, the lower is the amount of heat rejected to the atmosphere. In this case study, heat is primarily carried away with the flue gas. Out of the three cases (anode recirculation, cathode circulation and no recirculation), the anode recirculation had the lowest amount of exhaust flue gas flowrate and temperature while maintaining the lowest air flowrate. Recirculation helps to cool the SOFC and thus less excess air is required for cooling. Therefore, a lower air flowrate to the GT translates to a higher power output/efficiency. Although the exhaust temperature for the anode recirculation is higher than that for the no recirculation, its lower flow rate more than offsets the higher temperature.

5.3. Recommendations

- The results reveal promise for economically viable implementation.

  The ultra-high efficiencies and the reasonable COE of the stationary hybrids portend a promising future market opportunity.

- Stationary applications are more ready for commercialization than mobile.

  The stationary application of a fuel cell for distributed power generation has a relatively less demanding duty cycle than the application for mobile applications. Consequently, station applications are expected to be first commercialized with a 1 MW example by Mitsubishi already emerging.

- Operating SOFC-GT hybrids with anode recirculation.

  Among anode, cathode, and no recirculation, anode recirculation yields the highest power output/electrical efficiency.

- The utilization of LNG in mobile applications is beneficial.

  For mobile applications with near continuous duty such as locomotives and tugboats, LNG provides a higher stored power and energy density while improving the LHV-efficiency given its higher energy density compared to CNG and its cryogenic nature as a heat sink.

- A reduction in renewable H_2 cost is required to enable H_2 as a fuel for distributed generation.

  While the TPC for a renewable H_2-fueled SOFC-GT is acceptable, the current cost for renewable H_2 results in a relatively expensive COE due to the price of electricity to power electrolyzers from solar and wind. If this price in the future is discounted (e.g., by purchasing and utilizing excess electricity that might be otherwise curtailed to power electrolyzers), the H_2-fueled hybrid COE will be proportionally reduced.

  An electric grid techno-economic analysis will identify technology portfolio mixes and tariff options to monetize renewable H2 at competitive levels and thereby inform policy makers of steps that can be taken to enable the market for zero-carbon hydrogen.

Note that the results presented are from computer simulations and therefore the next step is to establish a controlled laboratory capability at a scale (e.g., 500 kW to 1 MW) selected to utilize commercial or near commercial SOFC and GT components for verification. The laboratory would serve as a vehicle for developing, testing, and optimizing both the hardware and control for both stationary and mobile applications, and an informational source for enabling the market. Given that the stationary application of a fuel for distributed power generation has a relatively less demanding duty cycle than the application for mobile applications, stationary applications are expected to be first commercialized with a 1 MW example by Mitsubishi already emerging. The deployment of a unit at a location where the performance can be judiciously monitored, and the unit can be operated with a portfolio of distributed power generation scenarios would serve as a major step to enable the market.

6. Bibliography

[1] "Electricity in the U.S. - U.S. Energy Information Administration (EIA)." [Online]. Available: https://www.eia.gov/energyexplained/electricity/electricity-in-the-us.php. [Accessed: 15-Feb-2020].

[2] F. Rosner, "UC Irvine UC Irvine Electronic Theses and Dissertations Techno-Economic Analysis of IGCCs Employing Novel Warm Gas Carbon Dioxide Separation and Carbon Capture Enhancements for High-Methane Syngas," University of California, Irvine, 2018.

[3] Ashok D. Rao, Ed., *Combined cycle systems for near-zero emission power generation*. Cambridge: Woodhead Publishing, 2012.

[4] "Fuel Cell Handbook," Morgantown, 2004.

[5] G. C. Karvountzi, C. M. Price, and P. F. Duby, "Comparison of molten carbonate and solid oxide fuel cells for integration in a hybrid system for cogeneration or tri-generation," *Am. Soc. Mech. Eng. Adv. Energy Syst. Div. AES*, vol. 44, pp. 139–150, 2004.

[6] RYAN O'HAYRE, SUK-WON CHA, WHITNEY G. COLELLA, and FRITZ B. PRINZ, *FUEL CELL FUNDAMENTALS*, 3rd ed. Hoboken: John Wiley & Sons, Inc., 2016.

[7] A. Buonomano, F. Calise, M. D. d'Accadia, A. Palombo, and M. Vicidomini, "Hybrid solid oxide fuel cells-gas turbine systems for combined heat and power: A review," *Applied Energy*. 2015.

[8] F. Zabihian and A. Fung, "A Review on Modeling of Hybrid Solid Oxide Fuel Cell Systems," *Int. J. Eng.*, no. 3, pp. 85–119.

[9] A. A. Ponomareva, A. G. Ivanova, O. A. Shilova, and I. Y. Kruchinina, "Current state and prospects of manufacturing and operation of methane-based fuel cells (review)," *Glas. Phys. Chem.*, vol. 42, no. 1, pp. 1–19, 2016.

[10] X. Zhang, S. H. Chan, G. Li, H. K. Ho, J. Li, and Z. Feng, "A review of integration strategies for solid oxide fuel cells," *Journal of Power Sources*. 2010.

[11] S. J. McPhail, A. Aarva, H. Devianto, R. Bove, and A. Moreno, "SOFC and MCFC: Commonalities and opportunities for integrated research," *Int. J. Hydrogen Energy*, vol. 36, no. 16, pp. 10337–10345, 2011.

[12] F. Calise, A. Palombo, and L. Vanoli, "Design and partial load exergy analysis of hybrid SOFC-GT power plant," *J. Power Sources*, vol. 158, no. 1, pp. 225–244, 2006.

[13] F. Calise, A. Palombo, and L. Vanoli, "A finite-volume model of a parabolic trough photovoltaic/thermal collector: Energetic and exergetic analyses," *Energy*, vol. 46, no. 1, pp. 283–294, 2012.

[14] S. H. Chan, H. K. Ho, and Y. Tian, "Modelling of simple hybrid solid oxide fuel cell and gas turbine power plant," *J. Power Sources*, 2002.

[15] F. Calise, G. Ferruzzi, and L. Vanoli, "Parametric exergy analysis of a tubular Solid Oxide Fuel Cell (SOFC) stack through finite-volume model," *Appl. Energy*, vol. 86, no. 11, pp. 2401–2410, 2009.

[16] D. Cocco and V. Tola, "Externally reformed solid oxide fuel cell-micro-gas turbine (SOFC-MGT) hybrid systems fueled by methanol and di-methyl-ether (DME)," *Energy*,

vol. 34, no. 12, pp. 2124–2130, 2009.

[17] F. Ishak, I. Dincer, and C. Zamfirescu, "Energy and exergy analyses of direct ammonia solid oxide fuel cell integrated with gas turbine power cycle," *J. Power Sources*, vol. 212, pp. 73–85, 2012.

[18] M. J. Moran, H. N. Shapiro, D. D. Boettner;, and M. B. Bailey, *Fundamentals of Engineering Thermodynamics*, 8th ed. Wiley, 2014.

[19] "3 Types of Air Compressors (Plus Benefits and Comparison)." [Online]. Available: https://www.homestratosphere.com/types-of-air-compressors/. [Accessed: 28-Oct-2020].

[20] B. J. Huang, J. M. Chang, C. P. Wang, and V. A. Petrenko, "1-D analysis of ejector performance," *Int. J. Refrig.*, vol. 22, no. 5, pp. 354–364, 1999.

[21] K. Huang and S. C. Singhal, "Cathode-supported tubular solid oxide fuel cell technology: A critical review," *J. Power Sources*, vol. 237, pp. 84–97, 2013.

[22] F. Calise, M. Dentice d' Accadia, L. Vanoli, and M. R. von Spakovsky, "Single-level optimization of a hybrid SOFC-GT power plant," *J. Power Sources*, vol. 159, no. 2, pp. 1169–1185, 2006.

[23] T. W. Song, J. L. Sohn, J. H. Kim, T. S. Kim, S. T. Ro, and K. Suzuki, "Performance analysis of a tubular solid oxide fuel cell/micro gas turbine hybrid power system based on a quasi-two dimensional model," *J. Power Sources*, vol. 142, no. 1–2, pp. 30–42, 2005.

[24] J. Larminie and A. Dicks, *Fuel Cell Systems Explained*. 2003.

[25] D. F. Cheddie, "Integration of a solid oxide fuel cell into a 10 MW gas turbine power plant," *Energies*, vol. 3, no. 4, pp. 754–769, 2010.

[26] W. J. Yang, S. K. Park, T. S. Kim, J. H. Kim, J. L. Sohn, and S. T. Ro, "Design performance analysis of pressurized solid oxide fuel cell/gas turbine hybrid systems considering temperature constraints," *J. Power Sources*, vol. 160, no. 1, pp. 462–473, 2006.

[27] D. F. Cheddie, "Thermo-economic optimization of an indirectly coupled solid oxide fuel cell/gas turbine hybrid power plant," *Int. J. Hydrogen Energy*, vol. 36, no. 2, pp. 1702–1709, 2011.

[28] X. Zhang, S. Su, J. Chen, Y. Zhao, and N. Brandon, "A new analytical approach to evaluate and optimize the performance of an irreversible solid oxide fuel cell-gas turbine hybrid system," *Int. J. Hydrogen Energy*, vol. 36, no. 23, pp. 15304–15312, 2011.

[29] B. Nag and K. G. Murty, "Diesel locomotive fueling problem (LFP) in railroad operations," *Opsearch*, vol. 49, no. 4, pp. 315–333, 2012.

[30] L. Caretto, S. Fritz, J. Hedrick, M. Iden, and L. Schmid, "An Evaluation of Natural Gas-fueled Locomotives," San Francisco, 2007.

[31] "Counties Designated 'Nonattainment' for Clean Air Act's National Ambient Air Quality Standards (NAAQS)," *Environmental Protection Agency*, 2020. [Online]. Available: https://www3.epa.gov/airquality/greenbook/map/mapnpoll.pdf. [Accessed: 20-Oct-2020].

[32] Air Resources Board, "Technology Assessment: Freight Locomotives," no. November, 2016.

[33] “California requires ships, trucks to eliminate tons of pollution | CalMatters.” [Online]. Available: https://calmatters.org/environment/2020/08/california-ships-trucks-pollution-ports/. [Accessed: 20-Oct-2020].

[34] “Liquefied natural gas - U.S. Energy Information Administration (EIA).” [Online]. Available: https://www.eia.gov/energyexplained/natural-gas/liquefied-natural-gas.php. [Accessed: 24-Jun-2020].

[35] “Price of Liquefied U.S. Natural Gas Exports (Dollars per Thousand Cubic Feet).” [Online]. Available: https://www.eia.gov/dnav/ng/hist/n9133us3m.htm. [Accessed: 30-Oct-2020].

[36] A. S. Martinez, J. Brouwer, and G. S. Samuelsen, “Feasibility study for SOFC-GT hybrid locomotive power: Part I. Development of a dynamic 3.5 MW SOFC-GT FORTRAN model,” *J. Power Sources*, vol. 213, no. x, pp. 203–217, 2012.

[37] A. S. Martinez, “Simulation of Dynamic Operation and Coke-Based Degradation for SOFC-GT- Powered Medium and Long Haul Locomotives,” University of California, Irvine, 2011.

[38] Mohammad Ali Azizi, “Solid Oxide Fuel Cell-Gas Turbine Hybrid Power Systems: Energy Analysis, Control Assessments, Fluid Dynamics Analysis and Dynamic Modeling for Stationary and Transportation Applications,” University of California, Irvine, 2018.

[39] P. Ahrend, A. Azizi, J. Brouwer, and G. S. Samuelsen, “A Solid Oxide Fuel Cell-Gas Turbine Hybrid System for a Freight Rail Application,” in *13th International Conference on Energy Sustainability*, 2019, pp. 1–5.

[40] “WTUG 5801 LNG HT.” WARTSILA, 2017.

[41] P. T. McGuigan, “Salt in the marine environment and the creation of a standard input for gas turbine air intake filtration systems,” *Proc. ASME Turbo Expo 2004*, vol. 7, pp. 767–775, 2004.

[42] L. P. Lingaitis and L. Liudvinavičius, “Electric drives of traction rolling stocks with AC motors,” *Transport*, vol. 21, no. 3, pp. 223–229, 2006.

[43] J. L. Kirtley, A. Banerjee, and S. Englebretson, “Motors for Ship Propulsion,” *Proc. IEEE*, vol. 103, no. 12, pp. 2320–2332, 2015.

[44] J. P. Kopasz, “Fuel cells and odorants for hydrogen,” *Int. J. Hydrogen Energy*, vol. 32, no. 13, pp. 2527–2531, 2007.

[45] M. M. Foss, “Introduction to LNG: An overview on liquefied natural gas (LNG), its properties , the LNG industry , and safety considerations,” no. June, pp. 1–36, 2012.

[46] L. O’Conner, “Building natural gas locomotives,” *ASHRAE J. (American Soc. Heating, Refrig. Air-Conditioning Eng. (United States)*, vol. 36:4, 1994.

[47] R. Perret, “Solar Thermochemical Hydrogen Production Research (STCH) Thermochemical Cycle Selection and Investment Priority,” *Sandia Rep.*, no. May, pp. 1–117, 2011.

[48] R. M. Privette, T. A. Flynn, M. A. Perna, and R. Holland, “2.5 MW PEM fuel cell system for navy ship service power,” 2009.

[49] U.S. Department of Energy/NETL, “Cost and Performance Baseline for Fossil Energy

Plants Volume 3a: Low Rank Coal to Electricity: IGCC Cases," *Doe/Netl-2010/1399*, vol. 3, no. May, 2011.

[50] DOE/NETL, "Techno-Economic Analysis of integrated gasification fuel cell Systems," 2014.

[51] U.S. Department of Energy, "Analysis of Natural Gas Fuel Cell Plant Configurations," *Doe/Netl-2011/1486*, p. 125, 2011.

[52] F. Rosner, A. Rao, and S. Samuelsen, "Economics of cell design and thermal management in solid oxide fuel cells under SOFC-GT hybrid operating conditions," *Energy Convers. Manag.*, vol. 220, no. March, p. 112952, 2020.

[53] "Manufacturing Cost Analysis of 100 and 250 kW Fuel Cell Systems for Primary Power and Combined Heat and Power Applications," Columbus, OH 43201, 2016.

[54] F. Rosner, D. Yang, A. Rao, and S. Samuelsen, "Gas Turbine Price Projection for n-th Plant Equipment Cost," *Eng. Econ. (In Rev.*, 2020.

[55] J. Reed *et al.*, "Roadmap for the Deployment and Buildout of Renewable Hydrogen Production Plants in California," 2020.

[56] "Electricity From Wind Energy Statistics and Data." [Online]. Available: https://ww2.energy.ca.gov/almanac/renewables_data/wind/index_cms.php. [Accessed: 15-Oct-2020].

[57] "California Solar Energy Statistics and Data." [Online]. Available: https://ww2.energy.ca.gov/almanac/renewables_data/solar/index_cms.php. [Accessed: 15-Oct-2020].

[58] "Analysis: California wind power could increase by 21GW by 2030 - updated | Windpower Monthly." [Online]. Available: https://www.windpowermonthly.com/article/1366920/analysis-california-wind-power-increase-21gw-2030-updated. [Accessed: 15-Oct-2020].

[59] "California to add 25GW of renewables by 2030 under new roadmap | PV Tech." [Online]. Available: https://www.pv-tech.org/news/california-to-add-25gw-of-renewables-by-2030-under-new-roadmap. [Accessed: 15-Oct-2020].

[60] "Stanford study shows how to power California with wind, water and sun." [Online]. Available: https://news.stanford.edu/news/2014/july/clean-energy-california-072414.html. [Accessed: 15-Oct-2020].

[61] J. Reed, "Interview with Industrial Expert," 2020.

[62] "California ISO - Managing Oversupply." [Online]. Available: http://www.caiso.com/informed/Pages/ManagingOversupply.aspx#dailyCurtailment. [Accessed: 21-Oct-2020].

[63] "Fuel Cell Energy Company Update," *FuelCellEnergy*, no. September. pp. 1–26, 2018.

[64] S. Kaplan, "Power plant characteristics and costs," 2010.

[65] Andrew Van Dam, "Detailed data show the value of land under homes across the country," *The Washington Post*, 2019.

[66] "Natural Gas Locomotives and Natural Gas Fuel Tenders - Energy Conversions, Inc."

[Online]. Available: https://www.energyconversions.com/tender.htm. [Accessed: 04-Jan-2021].

[67] M. E. Iden, “LIQUEFIED NATURAL GAS (LNG) AS A FREIGHT RAILROAD FUEL: PERSPECTIVE FROM A WESTERN U.S. RAILROAD,” in *ASME 2012 Rail Transportation Division Fall Technical Conference*, 2012, pp. 1–9.

[68] Q. S. Chen, J. Wegrzyn, and V. Prasad, “Analysis of temperature and pressure changes in liquefied natural gas (LNG) cryogenic tanks,” *Cryogenics (Guildf).*, vol. 44, no. 10, pp. 701–709, 2004.

[69] R. Larson, S. Nason, and C. Industries, “LNG on the Rails--Precursor to LH2 on the Rails?,” 2019.

[70] National Renewable Energy Laboratory, “Using LNG as a Fuel in Heavy-Duty Tractors,” Golden, Colorado, 1999.

[71] W. L. Lundberg *et al.*, “Pressurized Solid Oxide Fuel Cell/ Gas Turbine Power System,” p. 156, 2000.

[72] P. J. J. Welfens *et al.*, “Design Optimiation of a Hybrid Solid Oxide Fuel Cell & Gas Turbine Power Generation System,” *Energy Policies Eur. Union*, pp. 1–7, 2001.

[73] M. Gandiglio, F. De Sario, A. Lanzini, S. Bobba, M. Santarelli, and G. A. Blengini, “Life cycle assessment of a biogas-fed solid oxide fuel cell (SOFC) integrated in awastewater treatment plant,” *Energies*, vol. 12, no. 9, 2019.